The multifaceted role of eosinophils in adipose tissue: from metabolism to allergy

By

William Reid Bolus

Dissertation

Submitted to the Faculty of the

Graduate School of Vanderbilt University

in partial fulfillment of the requirements

for the degree of

DOCTOR of PHILOSOPHY

In

Molecular Physiology and Biophysics

December 16th, 2017

Nashville, Tennessee

Approved:

Richard O'Brien, Ph.D.

David Harrison, M.D.

Timothy Blackwell, M.D.

John Stafford, Ph.D., M.D.

ACKNOWLEDGEMENTS

First and foremost, I would like to express my deep gratitude for the opportunity to work under the mentorship of Dr. Alyssa Hasty. Dr. Hasty has taught me a great deal about the scientific process, from grant writing, manuscript composition, and experimental design, to speaking at conferences and lab management. I feel privileged to have gained this experience in such a positive work environment, into which Dr. Hasty has invested so much time and energy. Dr. Hasty has displayed exceptional leadership, finding ways to specialize my PhD training to ensure the greatest success possible. I look forward to seeking her expertise for years to come as I develop my scientific career in future endeavors.

I would next like to acknowledge the wealth of guidance and knowledge that my dissertation committee has provided. I have great respect and admiration for Drs. Richard O'Brien, David Harrison, Timothy Blackwell, and John Stafford. This team of scientists has challenged me to produce my best work, thoughtfully critiquing my studies from conception to completion. I believe my PhD training has been greatly enhanced under the direction of my dissertation committee and for that I will be forever thankful.

I would be remiss not to thank the wonderful members of the Hasty lab, both past and present. It has been a joy to work with these individuals, and develop relationships that will last long after I leave the Hasty lab. My lab mates have greatly helped me in troubleshooting experiments, thinking through unexpected data sets, collaborating on projects, and maintaining a positive

outlook when lab-life is most trying. I am eager to see how each member of the Hasty lab continues to grow and achieve their goals.

I would like to extend a wide-reaching thank you to the Molecular Physiology and Biophysics Department here at Vanderbilt University. There is no shortage of experts from a range of scientific disciplines to consult for advice. The faculty members are bold in their pursuit of scientific understanding, the students are eager to learn and contribute to their fields, and the staff keeps the department running flawlessly.

Support for this dissertation research was provided by a Career Development Award from the American Diabetes Association (ADA) (1-07-CD-10), an Innovation Award from the ADA (1-17-IBS-140), an American Heart Association (AHA) Established Investigator Award (12EIA827), a Scholarship from Vanderbilt Digestive Disease Research Center (DK058404), a Veterans Affairs Merit Award (5I01BX002195), a Molecular Endocrinology Training Program pre-doctoral fellowship (DK07563), and an AHA pre-doctoral fellowship (15PRE25560126).

TABLE OF CONTENTS

Page

LIST OF FIGURES AND TABLES

Figure **Page**

LIST OF ABREVIATIONS

aPKC = atypical protein kinase C

AT = adipose tissue

AUC = area of the curve

BMI = body mass index

BSA = bovine serum albumin

CCR2 = C-C chemokine receptor type 2

CDC = center for disease control

CISR = cell imaging shared resource

CLS = crown-like structure

DHSR = digital histology shared resource

eAT = epididymal adipose tissue

EL = epithelial layer

FACS = fluorescence activated cell sorting

FCSR = flow cytometry shared resource

FFA = free fatty acid

H&E = hematoxylin and eosin

HFD = high fat diet

IFN-γ = interferon-gamma

ILC2 = type 2 innate lymphoid cell

IL1β = interleukin 1 beta

IRS = insulin receptor substrate

InsR = insulin receptor

IP = intraperitoneal

LP = lamina propria

LPS = lipopolysaccharide

mAT = mesenteric adipose tissue

MCP1 = monocyte chemoattractant protein 1

MMPC = mouse metabolic phenotyping center

NKT = natural killer T cells

OVA = ovalbumin

pAT = perirenal adipose tissue

PDK1 = 3-phosphoinositide-dependent protein kinase 1

PIP_3 = phosphatidylinositol (2,4,5)-triphosphate

PIP_2 = phosphatidylinositol 4,5-bisphophate

PI3K = phosphatidylinositol 3-kinase

rIL5 = recombinant interleukin 5

RT = room temperature

sAT = subcutaneous adipose tissue

SCF = stem cell factor

TG = Triglycerides

TH = tyrosine hydroxylase

TNF-α = tumor necrosis factor alpha

T1D = type 1 diabetes

T2D = type 2 diabetes

WHO = world health organization

CHAPTER I

INTRODUCTION

The obesity crisis

Obesity has reached epidemic proportions worldwide, with some of the greatest severity in the United States. As of 2016, not a single state in the U.S. had an obesity rate less than 20% (1). The most recent data reports ~70% of the American population is overweight (body mass index (BMI) ≥ 25 kg/m^2) and ~35% obese (BMI ≥30 kg/m^2) (2, 3). Obesity is a metabolic disorder leading to increased risk for cardiovascular disease, type 2 diabetes, asthma, certain cancers, and various other diseases (4). A report compiled of 57 prospective analyses of nearly a million adults, showed that obesity can decrease a person's life span up to 10 years (5). The economic burden of obesity has also reached astonishing numbers, with an estimated annual medical cost of $147 billion in the U.S, ~10% of all medical spending (6). It is therefore of the utmost importance to understand the mechanisms by which obesity contributes to an array of debilitating and life-threatening diseases.

Diabetes: type 1 and type 2

Diabetes

It is estimated that 9.4% of the U.S. population has diabetes, which is the 7th leading cause of death in the U.S. (7). The American Diabetes Association defines diabetes by one or more parameters: an A1C $\geq$ 6.5%, fasting plasma glucose $\geq$ 126 mg/dl, and/or a 2-hr oral glucose tolerance test reading $\geq$ 200 mg/dl (8). Despite the definition of diabetes being largely fixated on glucose levels, decades of study have revealed many of the underlying complexities of the disease, including its multiple etiologies.

Type 1 diabetes

In type 1 diabetes (T1D), there is autoimmune destruction of the body's insulin producing β-cells that results in a lack of sufficient insulin to maintain proper glucose levels. While the exact trigger of the autoimmune cascade is not known, it has been shown that certain genes (e.g. HLA, INS, PTPN22, IL2RA, and CTLA4) can confer susceptibility (9). Viral infections and intestinal bacterial disturbances have also been shown in some subsets to associate with the onset of β-cell autoimmunity (9); however, this data has yielded mixed results and thus the degree to which viral infections and bacterial disturbances contribute to T1D is still an area of much debate. Once autoimmunity has been established, autoantibodies against the β-cell-containing islets can be detected. The presence of autoantibodies precedes clinical onset of T1D, in part due to the ability of the islets to lose at least 40% of β-cell mass before compromising glucose levels; in some cases, up to 90% of β-cell mass can be depleted before the onset of T1D

(10). After substantial loss of β-cell mass, exogenous insulin is required to maintain glucose homeostasis, albeit with less fine-tuned regulation than the body's endogenous mechanisms.

Type 2 diabetes

A major consequence of obesity is the increased risk for developing type 2 diabetes (T2D) (4). One of the most debilitating complications of T2D is cardiovascular disease, including macrovascular complications such as atherosclerosis and amputation as well as microvascular complications such as retinopathy, nephropathy, and neuropathy (11). T2D is a disease in which the body cannot effectively maintain blood glucose homeostasis. Similar to T1D, compromised glucose homeostasis in T2D arises from a loss of functional β-cells, but with a different etiology. In a healthy state, insulin is secreted by β-cells of the pancreas in response to elevated blood glucose, which then orchestrates the uptake of glucose into a variety of tissues for energy or storage (Fig. 1.1), adapted from Stumvoll *et al.* (12). Upon weight gain, inflammatory signaling in metabolic tissues interferes with insulin signaling pathways, which can lead to insulin resistance (IR) (molecular signaling discussed in detail below) (13, 14). As IR is established and progresses, β-cell mass must expand and produce more insulin to elicit the body's uptake of glucose. Eventually, nutrient excess and the demand on β-cells cause β-cell failure (i.e. diminished insulin secretion, decreased insulin gene expression, and eventually apoptosis) via lipotoxicity, reactive oxygen species, and/or endoplasmic reticulum stress (15); at this point

there is not sufficient insulin to maintain glucose homeostasis, leading to the onset of T2D.

It is important to mention that there are multiple other forms of diabetes, such as, gestational diabetes, neonatal diabetes mellitus, maturity onset diabetes of the young, and latent autoimmune diabetes in adults, which have their own specific etiologies but are not discussed in detail within this body of work.

GWAS of type 2 diabetes

Genome-wide association studies (GWAS) have been a powerful tool to identify new genes underlying complex diseases like T2D and obesity. GWAS analysis of T2D has emphasized the importance of proper β-cell function and has explained about 10% of disease heritability (16). These studies have identified over 75 loci associated with T2D susceptibility (17). Among them SNPs in *G6PC2* and *MTNRIB* were discovered to be associated with fasting blood glucose levels (16). *G6PC2* plays a role in insulin secretion by dephosphorylating glucose-6-phosphate produced by the β-cell glucose-sensing enzyme, glucokinase. The *MTNRIB* gene encodes the melatonin receptor MT2. The ligand for MT2 is melatonin, a hormone that regulates circadian rhythm and can influence insulin secretion and glucose levels (18-20). Multiple SNPs in the genes *G6PC2* and *MTNRIB* were found in subsequent independent studies (21, 22). As summarized by Billings *et al.*, most loci discovered in GWAS analysis of T2D point to primary defects in the β-cell (16). However, only ~10% of T2D heritability is currently explained by genetic variants, and as such, larger data sets across a greater span of the T2D population may be needed. Given that β-cells are so crucial to

the regulation of glucose homeostasis, it is not surprising that loci implicated in β-cell function have appeared so strongly in GWAS analysis of T2D. As the remaining loci responsible for T2D heritability are discovered, it may be found that loci variation in organs and tissues that contribute to T2D in less straight-forward ways, such as AT, are found to also contribute to susceptibility.

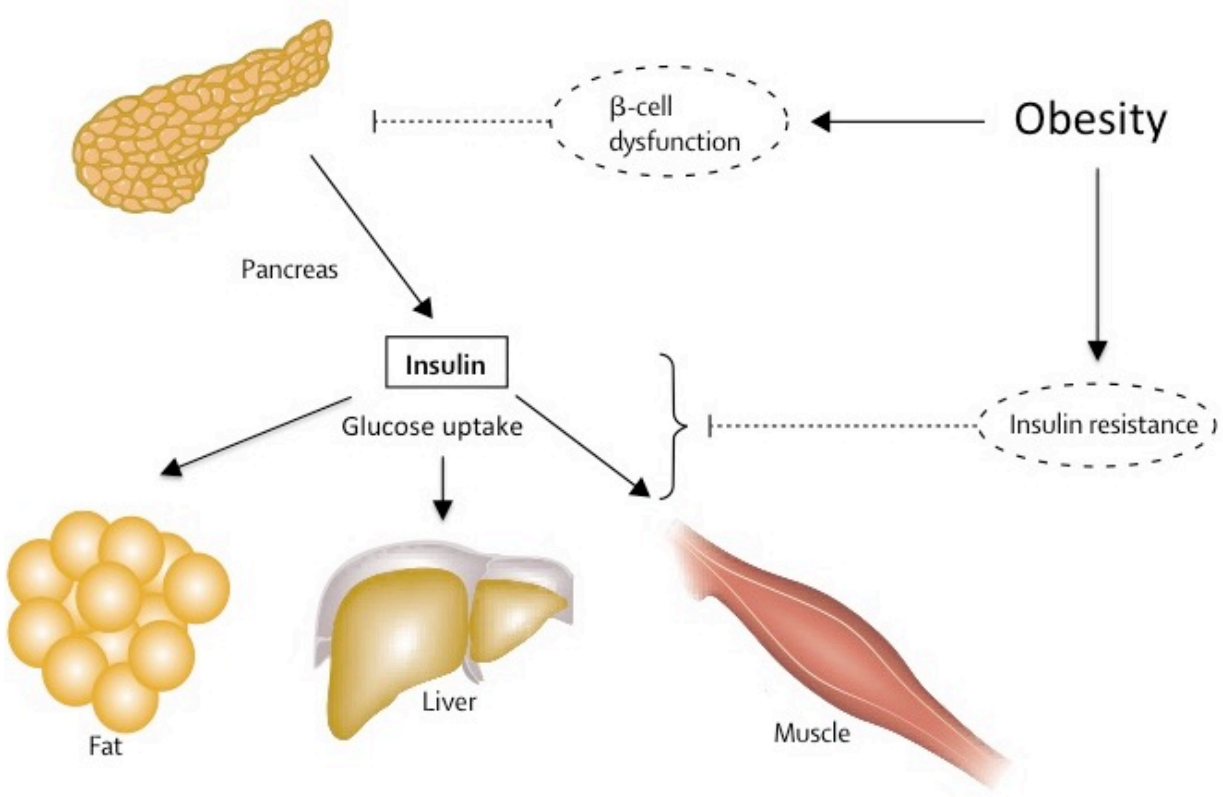

Figure 1.1 Effect of obesity on glucose tolerance.
Obesity can lead to insulin resistance and β-cell dysfunction, which in turn reduces glucose uptake in the fat, liver, and muscle. Adapted from Stumvoll et al., 2005.

Insulin signaling

In healthy individuals, digestion of a meal leads to glucose absorption into the blood, which in turn stimulates insulin release from β-cells. Upon insulin binding to the insulin receptor (InsR), a cascade of signaling events triggers glucose uptake in the muscle, liver, and adipose tissue (AT), as well as inhibition of lipolysis in AT. More specifically, insulin initiates InsR autophosphorylation of its tyrosine residues. The now activated InsR phosphorylates tyrosine on insulin receptor substrate (IRS) proteins. With IRS-1/2 phosphorylated, phosphatidylinositol 3-kinase (PI3K) is recruited to the plasma membrane and generates the lipid second messenger phosphatidylinositol (2,4,5)-triphosphate (PIP_3) from phosphatidylinositol 4,5-bisphophate (PIP_2). Membrane-bound PIP_3 allows 3-phosphoinositide-dependent protein kinase 1 (PDK1) to bind and subsequently phosphorylate the serine/threonine kinases, protein kinase B/AKT and atypical protein kinase C (aPKC). AKT and aPKC stimulate translocation of the glucose transporter, GLUT4, from intracellular vesicles to the cellular membrane, allowing glucose to enter the cell (Figure 1.2, panel A (23)).

Nutrient excess during obesity induces an inflammatory state in adipocytes via a variety of mechanisms. For example, excess circulating free fatty acids (FFA) can activate toll-like receptors (TLR) or become inflammatory lipid mediators such as diacylglyceride (DAG) leading to activation of cellular stress pathways. Secondly, adipocytes expand in size leading to hypoxia. Additionally, hyperactive metabolism can lead to the generation of reactive oxygen species (ROS). This combination of inflammatory stimuli lead to

transcription of inflammatory cytokines such as TNF-α and monocyte chemoattractant protein 1 (MCP1), as well as enzymatic proteins such as IRF-3, NFκB, HIF-1, and AP-1. This also leads to activation of the NLRP3 inflammasome, which allows for secretion of proinflammatory cytokine IL-1β (Figure 1.2, panel B (23)). This cocktail of proinflammatory cytokines and FFAs hinder insulin signaling by activating the stress kinases, IKK and JNK. IKK and JNK then phosphorylate inhibitory sites on IRS-1/2 (24). Ultimately, this inflammatory-mediated state of IR reduces uptake of peripheral glucose by reducing GLUT4 translocation to the plasma membrane and inhibiting proper downregulation of hepatic glucose output, leading to hyperglycemia (Figure 1.2, panel C (23, 25)). Additionally, adipocytes begin to indiscriminately release FFA, which then can be ectopically stored in tissues like the muscle and liver, further antagonizing the IR.

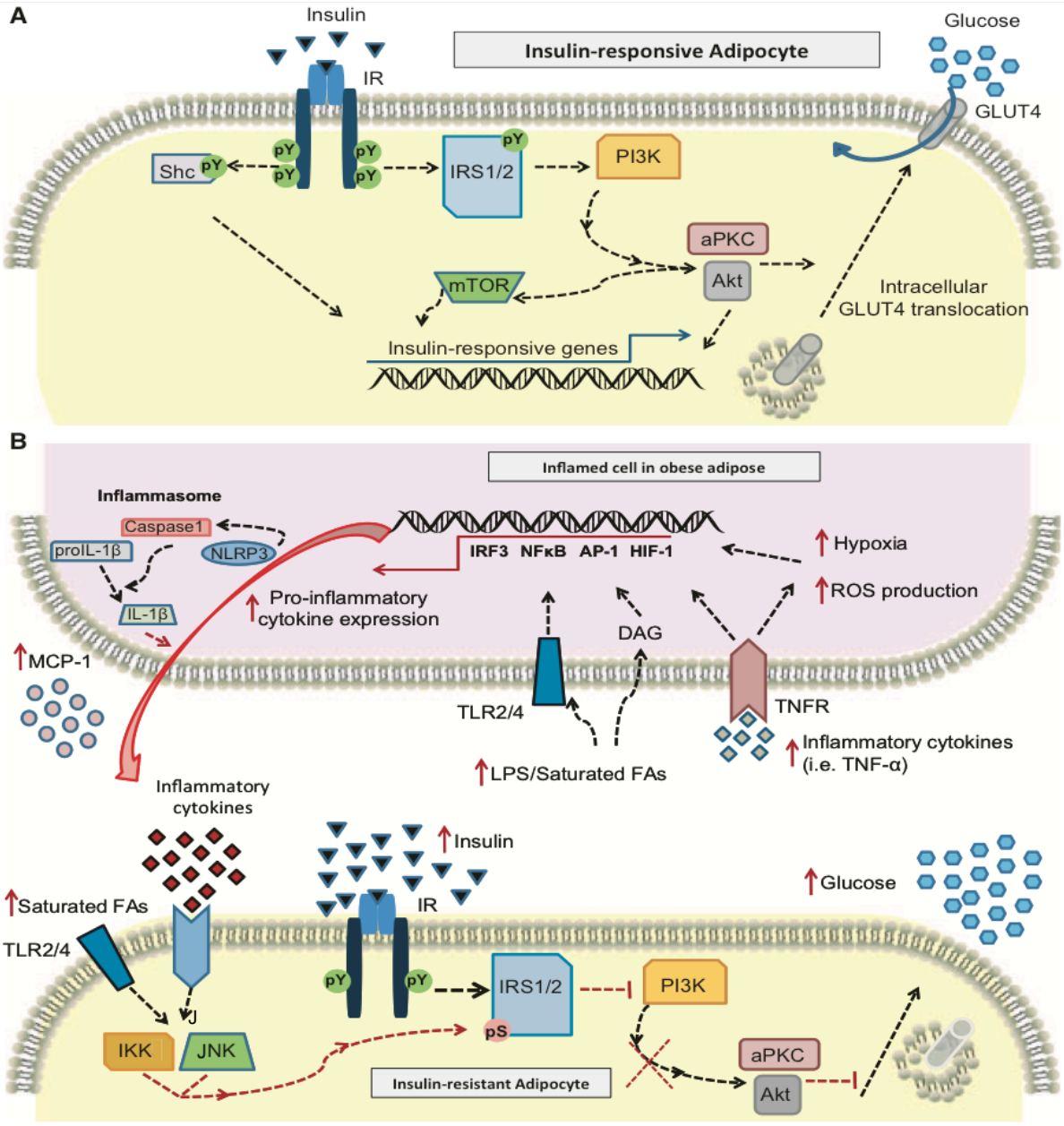

Figure 1.2 Illustration of how inflammation disrupts functional insulin-mediated glucose uptake in an adipocyte.
Insulin acts through the insulin receptor and various signaling molecules to induce GLUT4 translocation to the plasma membrane for glucose uptake. Obesity stimuli can cause inflammation that acts back on the adipocyte to impair proper insulin signaling, preventing glucose from entering the cell. From Johnson *et al.,* 2012.

Adipose tissue homeostasis

AT serves the vital function of regulating energy stores on a daily and long-term basis. AT has a remarkable ability to expand and contract, remodeling itself to the needs of the body (Fig. 1.3) (26). In times of excess calories, AT will store lipids as triglyceride. When calories are scarce, AT can release FFA through lipolysis as an energy source for tissues throughout the body such as the liver and muscle. Expansion occurs in a healthy way when hypertrophy and hyperplasia are accompanied by appropriate angiogenesis and extracellular matrix remodeling. However there is a limit to how much lipid adipocytes can store while still maintaining functionality. When expansion supersedes this limit, AT homeostasis is lost, marked by an increase in plasma FFA and TG, inflammatory immune cells, poor vasculature, hypoxia, fibrosis, inflammation, and adipocyte cell death (Fig. 1.3) (26). This dysfunctional state coincides with the onset of IR and is thought to contribute to obesity-associated diseases (26).

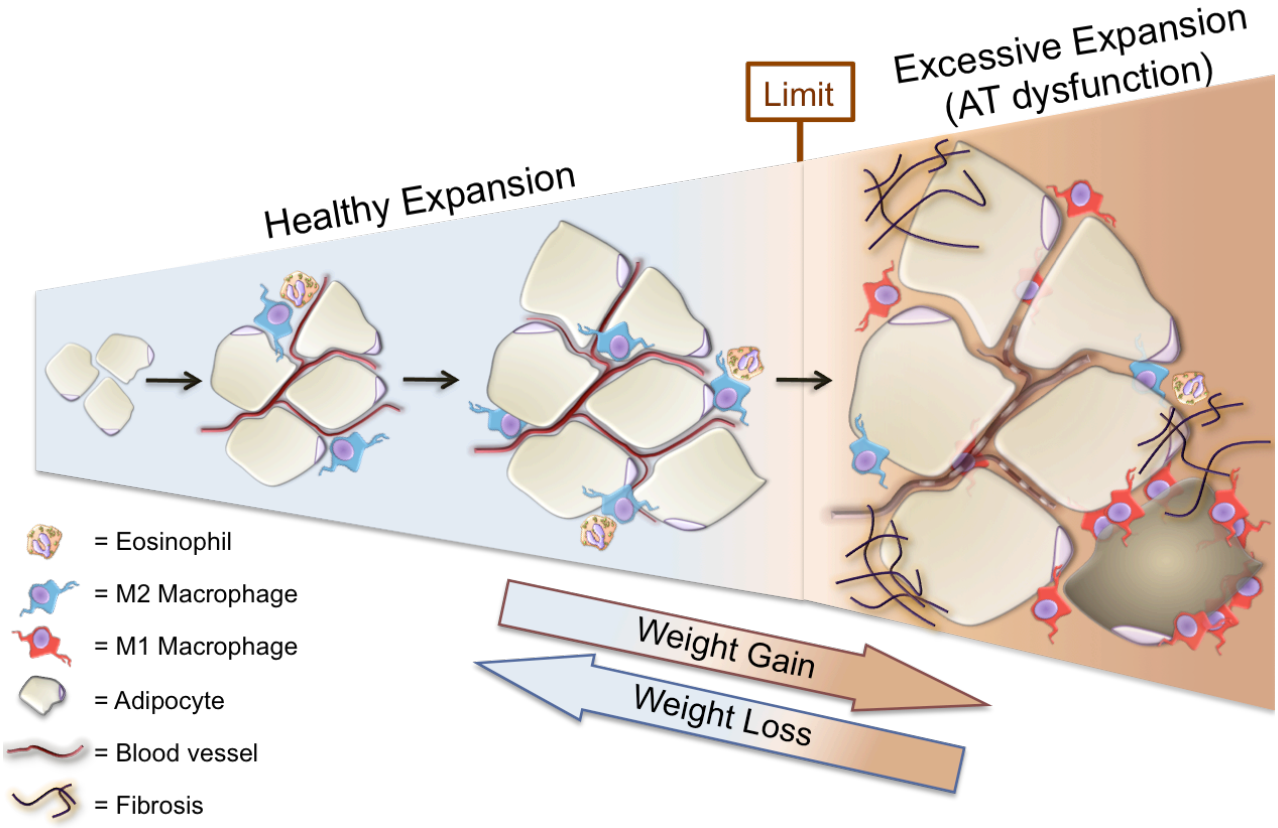

Figure 1.3 Adipose tissue expansion.
Adipose tissue expands in a healthy way to store extra energy in the form of lipids. After a limit of expansion, adipose dysfunction occurs characterized by increases in proinflammatory immune cells, poor vascularization, fibrosis, and adipocyte cell death.

Immune cells of adipose tissue

One of the hallmarks of obesity is an increase in AT inflammation. For example, there is a dramatic increase in proinflammatory cytokine, TNF-α during obesity in AT of both mice (27) and humans (28). Furthermore, removing TNF-α by antibody depletion in obese mice was shown to improve insulin sensitivity (29). The next inquiry was what cell type is responsible for the TNF-α in adipose tissue. Though it has been shown that adipocytes themselves can express TNF-α, the vast majority of TNF-α was found to be produced by macrophages (30, 31).

Indeed, macrophages are found in significant quantities in lean AT, but accumulate to even higher numbers in obese AT (31). Macrophages are highly plastic and can switch between pro- and anti-inflammatory phenotypes depending on environmental cues, in what has been termed macrophage polarization. M1-like macrophages are more proinflammatory, expressing markers such as TNF-α and interleukin 1 beta (IL1β), can be stimulated by lipopolysaccharide (LPS) and interferon-gamma (IFN-γ), and are associated with clearing bacterial pathogens. M2-like macrophages are more anti-inflammatory, expressing markers such as transforming growth factor beta (TGF-β) and interleukin 10 (IL10), can be stimulated by interleukin 4 (IL4) and interleukin 13 (IL13) and are associated with wound healing and tissue homeostasis. Anti-inflammatory M2-like macrophages are the predominant cells in lean AT, while pro-inflammatory M1-like macrophages greatly outnumber M2s in the obese state (Fig. 1.4, (32)). Likewise there are many other immune cells that contribute

to AT homeostasis, often through regulation of M2- vs. M1-like macrophage polarization. In the obese state there are more Th1 T cells, CD8 cytotoxic T cells, and Natural Killer cells, while lean adipose tissue is populated by Tregs, Th2 T cells, and eosinophils (32). The particular combination of AT immune cells during the lean or obese state gives rise to a unique milieu of cytokines that can influence local AT function as well as circulate systemically to act on other tissues of the body.

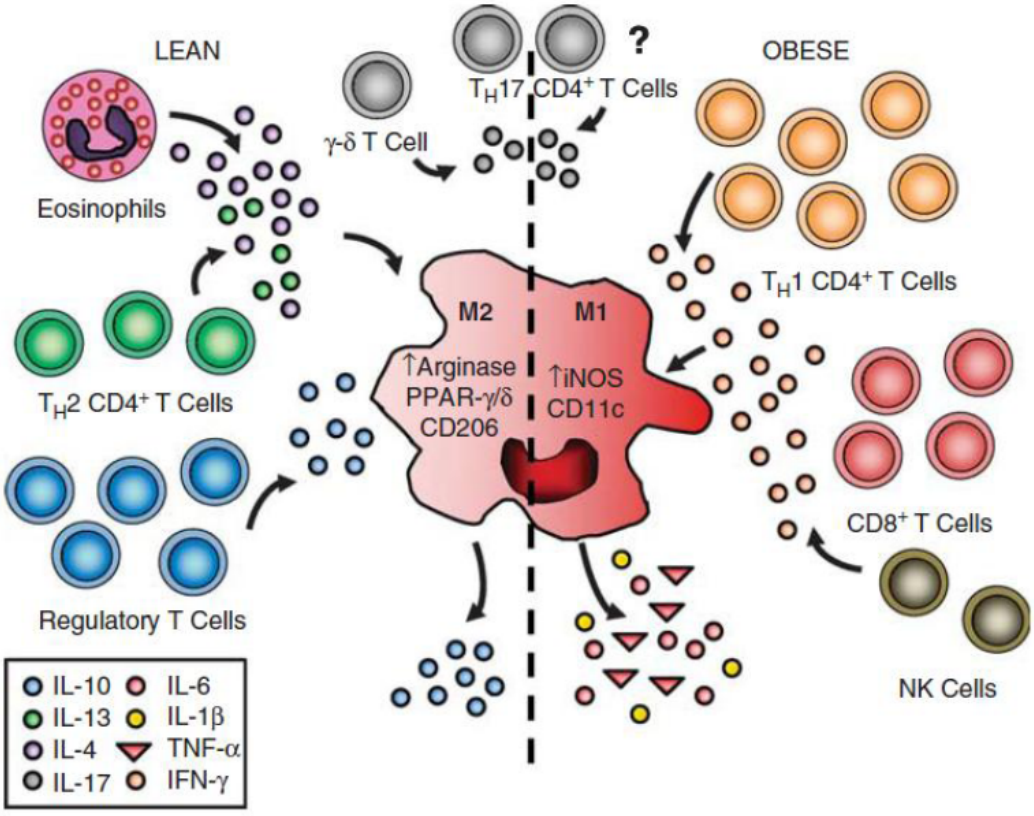

Figure 1.4 Immune cell milieu of adipose tissue.
In lean AT, there is an abundance of eosinophils Th2 CD4+ T cells, and regulatory T cells, all of which contribute to the M2-like polarization of the AT macrophages through cytokine production of IL-10, IL-13, and IL-4. In contrast, obese AT accumulates Th1 CD4+ T cells, CD8+ T cells, and NK cells, that polarize M1-like macrophages by secreting IFN-γ. From Winer *et al*., 2012.

The macrophage: a key player in adipose inflammation

Macrophages were only discovered to be a central player in AT homeostasis in the last few decades. Localization of macrophages to AT was reported as early as 1988, but the difference in lean vs. obese macrophage populations was not appreciated until 2003 when Weisberg *et al.* (31) and Xu *et al*. (30) showed a more inflammatory profile of obese AT macrophages. These studies showed that AT macrophage accumulation and their inflammatory markers positively correlated with weight gain and adipocyte size. Furthermore, AT macrophage accumulation occurred both in genetic models of obesity as well as diet-induced obesity. Furthermore, the increase in AT macrophages during obesity was also seen in humans. These studies showed that during obesity, AT macrophage inflammatory gene expression preceded rising circulating insulin levels and that treatment with a known insulin-sensitizing agent (rosiglitazone) reduced macrophage markers (i.e. MAC-1, F4/80, CD68) in AT (30). Many studies have built upon this seminal work, replicating these findings and expanding the field's knowledge of how macrophages influence both AT and whole-body insulin sensitivity. This established that exploiting mechanisms that regulate macrophage number or inflammatory state could be of great value in treating obesity and T2D.

Adipose macrophage recruitment by CCL2, and its receptor CCR2

In humans and mice, there is elevated expression of many different chemokines and chemokine receptors in obese compared to lean AT (30, 31, 33). One such chemokine is MCP1/CCL2 and its receptor C-C chemokine receptor type 2 (CCR2). CCR2 is expressed in many leukocytes, including monocytes, dendritic cells, T cells, NKT cells, and eosinophils (34, 35). The axis of ligand, CCL2, and its receptor, CCR2, is one of the most potent for monocyte recruitment in inflammatory settings. Further support for a potential role of CCL2/CCR2 in ATM recruitment stems from the fact that AT gene expression of CCR2 and its ligands (CCL2, CCL7, and CCL8) is increased 2-7 fold in obese compared to lean mice (36). Thus, several groups have assessed CCL2 and CCR2 deficient mice to determine whether ATM recruitment is reduced.

Kanda *et al.* showed increased levels of CCL2 both in AT and plasma of obese mice corresponding with increased AT macrophage content (37), and identified adipocytes as one source of CCL2. Transgenic AT-specific overexpression of CCL2 increases AT macrophage infiltration, insulin resistance, fasting blood glucose, serum FFA, and hepatic steatosis, even in the lean state. From the other end of the spectrum, $CCL2^{-/-}$ mice in their studies had reduced HFD-induced ATM accumulation, associated with decreased insulin resistance, serum FFA, and hepatic steatosis. In stark contrast to this, studies by Inouye *et al.* (38) and Kirk *et al.* (39) saw no reduction in ATM accumulation in $CCL2^{-/-}$ mice challenged with short-term or long-term HFD. In both of these studies, the $CCL2^{-/-}$ mice gained more weight and had slightly worsened insulin resistance

compared to controls (38, 39). Thus, because the published literature is mixed, it is difficult to declare a definitive role for CCL2 in macrophage recruitment to AT.

Because CCR2 is a receptor for several chemokines in addition to CCL2, and CCR2 deficiency results in a near absence of circulating monocytes (40), it is plausible that CCR2 deficiency could have a greater impact than CCL2 deficiency on macrophage recruitment to AT. Weisberg *et al*. compared weight-matched $CCR2^{-/-}$ and wild type mice and found that $CCR2^{-/-}$ mice fed HFD for 24 weeks display reduced ATMs concomitant with lower fasting blood glucose and insulin levels as well as higher plasma adiponectin (36). This finding was reproduced by Sullivan *et al.* in mice fed HFD for 20 weeks (41) and by Lumeng *et al.* who detected in $CCR2^{-/-}$ mice reduced recruitment of ATMs to dead/dying adipocytes, also known as crown-like structures (CLS) (42). We performed a time course study of HFD-feeding in $CCR2^{-/-}$ mice, and were only able to detect a reduction in ATMs after 20 weeks (43). Thus, the age of mice and time on HFD is important in detecting effects of CCR2 deficiency. We also found that $CCR2^{-/-}$ mice have increased eosinophils in their AT early after HFD-feeding (43, 44). The contribution of these unique CCR2 deficiency-related eosinophils to AT inflammation was not previously known, but is explored in detail in Chapter 3 of this dissertation.

The eosinophil

Eosinophils are multifunctional leukocytes that can be histologically identified by the presence of a multi-lobular nucleus and a cytoplasm dense with granules. They develop in the bone marrow, migrate into the blood, and infiltrate tissues in response to various cytokines and chemokines: IL-5; GM-CSF; Eotaxins 1, 2, and 3: RANTES: etc. (45). Their granules are composed of 4 primary constituents: major basic protein, eosinophil cationic protein, eosinophil-derived neurotoxin, and eosinophil peroxidase (45). Eosinophils also produce an assortment of cytokines, chemokines, and lipid mediators (Fig. 1.5, (45). These agents can regulate tissue damage (46, 47), wound healing (48), the onset of estrus (49), mammary gland development (50), GI tract remodeling (51), and T-

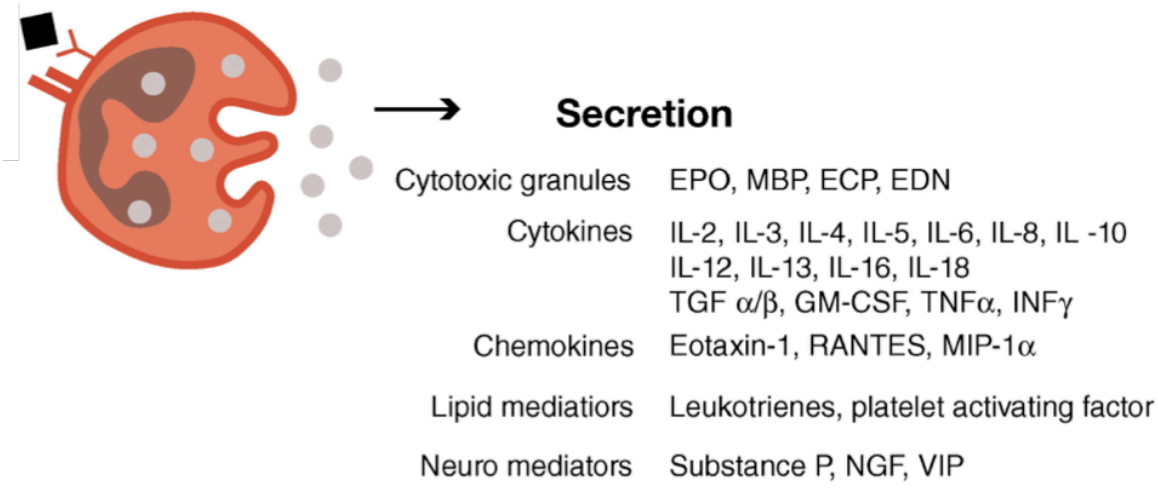

cell proliferation, polarization, and apoptosis (52, 53).

Figure 1.5 Eosinophil products.
Eosinophil granules are composed of 4 primary constituents: EPO, MBP, ECP, and EDN. They also produce an assortment of cytokines that can be secreted or stored in the granules for secretion at a later time. Eosinophils produce lipid products, such as leukotrienes and platelet activating factor, that can act as signaling molecules to other cells. Eosinophils even have neuro-modulatory capabilities through their expression of Substance P, NGF, and VIP. Adapted from Rothenberg *et al.,* 2006.

Classic understanding of eosinophils in disease

Parasitic infections

Eosinophils are classically associated with parasitic infections and allergic diseases like asthma, and are often thought of as “cytotoxic effector cells” (45). Eosinophils are considered protective against parasitic infections, such as helminth. Eosinophils migrate to the site of infection where they degranulate or otherwise assist in the destruction of parasites. They’ve been shown *in vitro* to indirectly support cellular-mediated (antibody response) destruction (54-56) or by direct granule release damage (57, 58). Eosinophils can even act as antigen presenting cells by presenting parasitic antigens to mount an immune response (59). Studies modulating eosinophil numbers during parasitic infection have returned mixed results based on the type of parasite used as well as the model system (i.e. under/over production of eosinophils by genetic means or antibody depletion) (60). The general conclusion is that there is some selectivity in the parasites that eosinophils protect against, with some of the strongest effects against *N. brasiliensis* and *Angiostrongylus cantonensis* (60).

Allergy and Asthma

In contrast to parasitic infections, eosinophils are considered pathogenic in allergy and asthmatic conditions (61). It has been shown in models of allergic airway disease and intestinal allergy, that exposure to antigen causes eosinophils to traffic to endotracheal lymph nodes and Peyer’s patches (52, 62-64). There are mixed views on whether recruitment of eosinophils to sites of allergy is more dependent on chemotactic eotaxins and their receptor CCR3 or

the IL5/IL5R pathway; inhibition of either pathway has shown at least partial efficacy to reduce airway hyperreactivity and lung damage under asthmatic conditions as well as reducing allergic skin inflammation (65-70).

Eosinophils as metabolic regulators: a role in tissue homeostasis

Significant populations of eosinophils are found in the GI tract, uterus, bone marrow, thymus, and AT under *healthy* conditions. It is interesting to point out that these are sites of high cell turnover and tissue remodeling. Rosenberg *et al.* published a Nature review titled *Eosinophils: changing perspectives in health and disease*, illuminating "the contributions of eosinophils to the maintenance of health, and how dysregulated eosinophil function promotes various disease states (71)." Novel theories like the LIAR hypothesis suggest: "eosinophils are actually regulators of *Local Immunity And/or Remodeling/R*epair in both health and disease…(and)...accumulation occurs as part of a strategy(ies) to maintain tissue homeostasis (72)." It is becoming increasing clear that eosinophils are much more than simple effector cells.

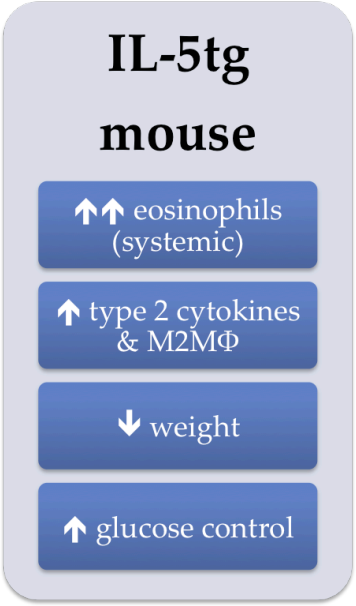

Figure 1.6 Summary of the first model of hypereosinophilic AT.
Systemic eosinophils, including AT eosinophils, are dramatically increased in the IL5tg mouse line. Eosinophilia is achieved by driving expression of an IL5 gene construct under the CD3 promoter and enhancer within T cells, leading to highly elevated levels of IL5. In turn, eosinophil proliferation, activation, and chemotaxis are upregulated, while apoptosis is downregulated. Systemic eosinophilia is associated with increased type 2 cytokines (i.e. IL4/IL13) and increased M2-like macrophage polarization in AT, as well as decreased weight gain and improved glucose tolerance on a HFD.

Though only recently observed in AT, seminal studies have shown eosinophils were associated with lean healthy AT compared to obese, and that they promoted M2-like polarization of AT macrophages (73-75). Studies by Wu *et al.* were the first to show AT eosinophils decline with weight gain in association with increased AT M1-like macrophages and metabolic impairments (Fig. 1.6 and 1.7, (73)). Interestingly, mouse models with systemically increased eosinophils were impervious to high fat diet induced obesity and insulin resistance, while eosinophil-deficient mice were more vulnerable to the onset of insulin resistance (73). Molofsky *et al.* further elucidated that AT eosinophil numbers are maintained by IL5 that is largely secreted by local type 2 innate lymphoid (ILC2) cells (Fig. 1.7 (74). Building upon these initial findings, Hams *et al.* showed that body weight and glucose control are impacted by ILC2 and natural killer T cells (NKT) cells in a model of HFD-fed obesity, attributed to the accumulation of eosinophils and M2-like macrophages in visceral AT (Fig. 1.7 (75). Necessary for maintaining an anti-inflammatory state of AT, resident eosinophils were shown to

express IL-4 and ILC2s to express IL-13 (73, 74). These studies culminated in an understanding that eosinophils influence body weight and systemic glucose control through the regulation of AT inflammation and insulin resistance by facilitating a network of immune cell interactions (Fig. 1.7). In the simplest terms, AT eosinophils positively correlate with metabolic fitness.

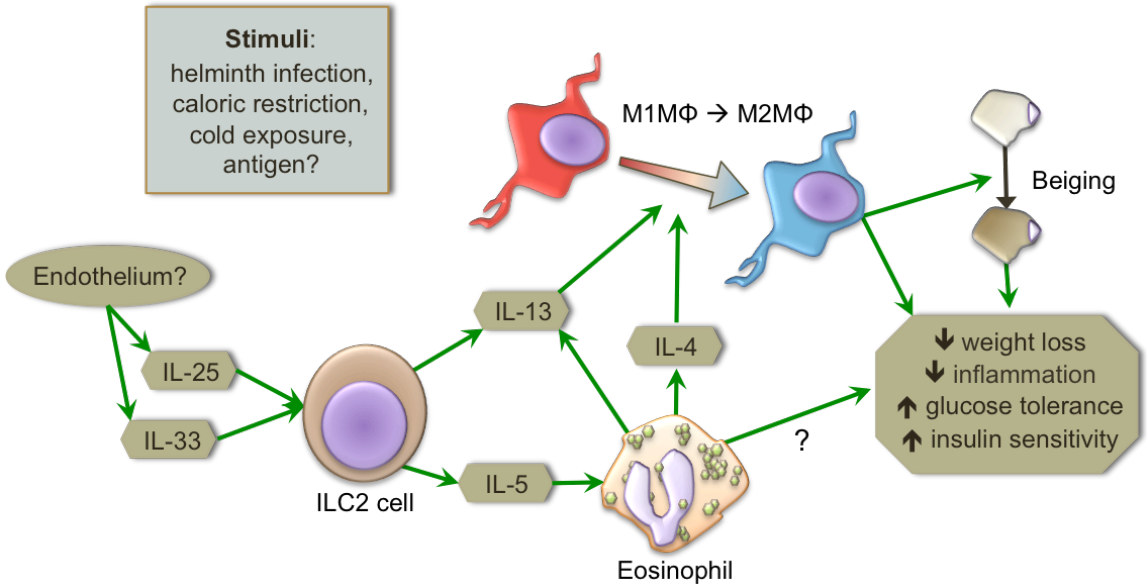

Figure 1.7 Current understanding of the role of eosinophils in AT based on immunometabolism literature.
An undefined source of IL33/IL25 can activate ILC2 cells in AT which then produce IL13 and IL5. Eosinophils accumulate in AT in response to the IL5, and produce IL4 and IL13. IL4/IL13 polarize macrophages from an M1- to an M2-like state, which has been shown to induce weight loss, decrease inflammation, and improve glucose tolerance and insulin sensitivity.

The presence of eosinophils in lean AT and the reduction of eosinophils in obesity when inflammation occurs, suggests eosinophils may serve to maintain healthy AT. In addition to inflammatory cytokines, eosinophils also secrete an assortment of resolving and remodeling mediators: TGF-β, protectin D1, IL-4, IL-8, IL-10, IL-13, VEGF, and stem cell factor (45, 76). Eosinophils are poised to inflict cytotoxic tissue damage as well as restorative tissue repair. Such a cell type could be critical to an environment such as AT where extensive expansion and contraction must occur on a daily basis to account for energy demands and surplus.

Significance

Obesity has reached epidemic proportions worldwide, with some of the greatest severity in the United States. The most recent data reports ~70% of the American population is overweight (BMI ≥ 25 kg/m^2) and ~35% obese (BMI ≥30 kg/m^2) (2, 3). Obesity is a metabolic disorder leading to increased risk for cardiovascular disease, type 2 diabetes, asthma, certain cancers, and various other diseases (4). A hallmark of obesity is AT inflammation and associated AT dysfunction. It is important to understand how immune cells accumulate in AT and regulate inflammation. We used CCR2$^{-/-}$ mice to study macrophage chemotaxis to AT, and also discovered that CCR2 regulates the chemotactic factors (i.e. *Il5* and *Ccl11*) that upregulate AT eosinophil accumulation. Studies prior to our work suggested that directly manipulating eosinophils (particularly in AT) could impart beneficial effects in obese subjects. Thus we developed an

interventional treatment model of restoring obese AT eosinophils to higher levels of lean AT by injection of rIL5. AT eosinophils were successfully increased with rIL5, but there was no reduction in obesity and its comorbidities. Lastly, we discovered that repeated exposure to a foreign substance such as bovine serum albumin (BSA) could greatly increase AT eosinophil numbers. While there were no metabolic improvements in mice chronically exposed to BSA, we have evidence to believe AT is capable of mounting a type 2 allergic response to antigens similar to the lung of an asthmatic, resulting in this large increase in AT eosinophils. Future studies will determine whether the massive AT eosinophilia following BSA exposure feeds back to modulate lung function, increasing both incidence and severity of asthmatic symptoms such as increased mucus production and airway hyperresponsiveness. Such studies may help in explaining the clinical link between obesity and allergic conditions such as asthma. In conclusion, we have found that restoring AT eosinophils to either physiological levels or super-physiological levels during obesity is not able to improve metabolic fitness (e.g. weight gain, glucose intolerance). Furthermore, we may have discovered a novel site of allergy that could offer insights and serve as a therapeutic target for obese subjects that have increased difficulty with allergic disease.

CHAPTER II

MATERIALS AND METHODS

Animal models

All animal procedures were carried out with prior approval from Vanderbilt's Institutional Animal Care and Usage Committee. Body composition was measured to obtain lean mass and fat mass by nuclear magnetic resonance using at Bruker Minispec instrument (Woodlands, TX) in Vanderbilt's Mouse Metabolic Phenotyping Center (MMPC). Isoflurane overdose was used to euthanize mice, immediately followed by cervical dislocation. Circulating blood was removed by perfusing the left ventricle of the heart with ~10-15 mL PBS. Individual tissues were then removed, weighed, and either snap-frozen in liquid nitrogen, fixed in 10% formalin, fixed in 1% PFA, or processed to isolate immune cells, in preparation for later analysis.

Chapter III:

Male WT and CCR2$^{-/-}$ mice on a C57BL/6 background were purchased from Jackson Laboratory (Bar Harbor, Maine) and maintained in the Vanderbilt animal facility. At 8 weeks of age, mice were fed a chow diet or 60% kcal from fat HFD (Research Diets, New Brunswick, NJ) *ad libitum* for 6-8 weeks and had free access to water. Given the primary goal of inducing dietary obesity, a diet with a high caloric composition derived from fat (60% from total kcal) was used; however, other micronutrients were not matched between diets.

Chapter IV:

C57BL/6J male wild type mice were purchased from the Jackson Laboratory (Bar Harbor, Maine) at 7 weeks of age and housed in the animal facility at Vanderbilt University for 1 week to acclimate. At 8 weeks of age, mice either remained on chow diet or were given *ad libitum* access to 60% kcal from fat HFD (Research Diets, New Brunswick, NJ) for 8 weeks. Mice received either 50 ng recombinant IL5 (rIL5; R&D Systems, Minneapolis, MN) protein (in 0.001% BSA as carrier protein) by intraperitoneal (IP) injection twice per week to elevate eosinophils, 0.001% BSA vehicle control, or PBS control (Fig. 4.1A). Not all mice respond to the 50 ng dose of rIL5 with increased eosinophils. With our goal of studying mice with elevated eosinophils compared to normal, only rIL5-treated mice that had AT eosinophils greater than 1 standard deviation above the mean of saline controls were used for analysis.

Chapter V:

C57BL/6J male wild type mice were purchased from the Jackson Laboratory (Bar Harbor, Maine) at 7 weeks of age and housed in the animal facility at Vanderbilt University for 1 week to acclimate. BALB/cJ mice and IL33 KO mice (on BALB/cJ background) were kindly provided by Dr. Stokes Peebles and transferred between animal faculties at Vanderbilt. At 8 weeks of age, mice either remained on chow diet or were given *ad libitum* access to 60% kcal from fat HFD (Research Diets, New Brunswick, NJ) for 4 or 8 weeks. Mice received either

saline, 0.001% BSA, 0.01% BSA, or 0.1% BSA by IP for the duration of diet to test antigen response.

Immune cell isolation and flow cytometry

AT stromal vascular fraction cell isolation:

AT was excised and minced into fine pieces in a 1% FBS PBS solution. Minced AT was digested with 2 mg/mL type II collagenase for 40 min at 37^{o}C at 200 rpm rotation. PBS with 1 % FBS solution was added to neutralize the digestion and solution was passed through a 100 μm filter. After centrifugation to remove floating adipocytes, the cell pellet was treated with ACK lysis buffer to remove red blood cells. Reaction was neutralized by dilution with 1% FBS PBS, centrifuged, and decanted; cell pellet was resuspended and used for further analysis.

Liver non-parenchymal cell isolation:

Liver was excised and minced in 1 mg/ml type II collagenase in 3% FBS PBS solution. Minced liver was incubated at 37°C for 30 min at 200 rpm rotation. Cell suspension was filtered through a 100 μm filter and centrifuged at 300 RPM for 3 min. Supernatant was collected and centrifuged at 1500 RPM for 10 min. Pellet was resuspended in 40% Percoll and overlaid on top of 60% Percoll. Percoll gradient was centrifuged at 2000 RPM for 20 min. The two middle layers of the Percoll gradient were collected in 3% FBS in RPMI and centrifuged at 1500 RPM for 10 min. Supernatant was discarded; cell pellet was resuspended and stained for flow cytometry.

Peritoneal immune cell isolation:

Peritoneal immune cells were collected by flushing the peritoneal cavity with 10 mL of DMEM. Cells were washed 2x and then used for flow cytometry as described below.

Small intestine immune cell isolation:

Intestine between stomach and cecum was excised and cleaned of fat and Payer's patches. Fecal matter was removed by flushing with PBS. Intestine was cut longitudinally and mucus gently scraped away with forceps. Intestine was cut into 1 cm pieces, cleaned of remaining mucus by vigorous shaking with PBS in a 50 mL conical tube. Pieces were incubated in dissociation media [1x HBSS (Ca/Mg-free), 5 mM EDTA, and 10mM HEPES] for 20 min at 37^{o}C at 200 rpm rotation to separate lamina propria (LP) from epithelial layer (EL). Mixture was vortexed vigorously and passed through 100 μm filter. Supernatant was collected as EL fraction, while remaining tissue in filter was collected and finely minced for LP fraction. LP fraction was incubated in digestion solution [10% FBS, 2 mg/mL (250 U/mL) type IV collagenase, DMEM) for 20 min at 37^{o}C at 200 rpm rotation; then supernatant passed through a 100 micron filter. LP fraction tissue was digested, filtered a second time, and LP supernatants were combined. EL and LP fractions were pelleted, resuspended in a 40% Percoll solution, centrifuged, and decanted; cell pellet was resuspended and used for further analysis.

Bone marrow cell isolation:

Hind-leg was removed from mouse at hip joint and bone was cleaned of tissue. Ends of bone were cut from both tibia and femur and bones were flushed with RPMI. Collected marrow was passed through a 27-gauge needle several times slowly to create a single cell suspension. After centrifugation and decantation, the cell pellet was treated with ACK lysis buffer to remove red blood cells. Reaction was neutralized by dilution with 1% FBS PBS, centrifuged, and decanted; cell pellet was resuspended and used for further analysis.

Blood cell isolation:

Approximately 200 µL blood was collected retro-orbitally in heparinized capillary tube while under anesthesia, but prior to euthanasia. Blood was diluted with 2 mL deionized water in a 15 mL conical tube, and mixed by inverting for 15 seconds to lyse red blood cells. Reaction was neutralized by dilution with 10 mL 1% FBS PBS, centrifuged, and decanted; cell pellet was resuspended and used for further analysis.

Flow cytometric analysis and Fluorescence Activated Cell sorting (FACS):

Isolated immune cells were first incubated with Fc Block (BD Biosciences, San Jose, CA) for ≥5 min on ice. Cells were stained for 30 min at 4^{o}C, while protected from light, with a combination of fluorophore-conjugated antibodies: F4/80: APC - (eBiosciences, Waltman, MA), CD11b: FITC/APC-Cy7/APC (BD Biosciences), SiglecF: PE/BV450 (BD Biosciences), CD45: PE-Cy7(BD), APC-Cy7/BV605

(Biolegend), CD3: FITC (BD Biosciences), TCRβ: APC-Cy7 (BD Biosciences), CD4: A700 (BD biosciences), CD8: FITC/V500 (BD Biosciences), CD19: APC-Cy7 (BD Biosciences), Ly6C: FITC (BD Biosciences), Ly6G: PE (BD Biosciences), MHCII: FITC (BD Biosciences). Cells were washed several times, counting beads added, and stained with viability dye, [1 μg/mL 4',6-diamidino-2-phenylindole (DAPI) or propidium iodide (PI)], just before flow cytometric analysis. Cells were analyzed on a 4-laser BD LSR Fortessa (BD Biosciences) or a FACSAria III cell sorter (BD Biosciences). FACS selected cells were sorted based on gating schemes in Fig. 4.1B, centrifuged, supernatant removed, and snap frozen in liquid nitrogen for later processing. Results were analyzed using FlowJo software. Flow Cytometry experiments were performed in the Vanderbilt Flow Cytometry Shared Resource (FCSR).

RNA isolation, cDNA synthesis, and real-time RT-PCR

Chapter III:

RNA was isolated by the guanidine isothiocyanate-phenol-chloroform method using TRIzol (BD Biosciences) according to the manufacturer's protocol. Potentially contaminating DNA was digested using DNase1 (Life Technologies). RNA was reverse transcribed into cDNA using iScript RT (Bio-Rad, Hercules, CA). Relative gene expression between samples was assessed using the FAM-conjugated TaqMan Gene Expression Assay (Life Technologies), normalized to glyceraldehyde-3-phosphate dehydrogenase, and statistically analyzed by the Pfaffl method (77).

Chapter IV & V:

The Qiagen RNeasy Mini Kit was used to isolate RNA according to the manufacturer's instructions, after tissues were initially homogenized in TRIzol (BD Biosciences). Purified RNA was reverse transcribed via iScript RT (Bio-Rad, Hercules, CA) into cDNA. Differences in relative gene expression were quantified using FAM-conjugated TaqMan Gene Expression Assay (Life Technologies). Data were normalized to the housekeeping gene, 18s, and analyzed by the Pfaffl method (77).

Cell and tissue imaging

All images were captured on either an 1) Axiophot widefield light microscope available through the Vanderbilt Cell Imaging Shared Resource (CISR), 2) Olympus FV-1000 confocal inverted microscope (CISR), or 3) Leica SCN400 Slide Scanner microscope at the Digital Histology Shared Resource (DHSR). The only modification to images was removal of background discoloration.

Eosinophil and macrophage detection in whole AT:

Intact AT pieces of ~3 mm^3 in size were fixed in 1% PFA for 1 h with agitation. Samples were washed in PBS and blocked in goat serum at a 1:5 dilution in PBS for 1 h at room temperature (RT) with agitation. Rat anti-mouse SiglecF-*PE* (BD Biosciences) and anti-mouse F4/80-Allophycocyanin (eBiosciences) were applied at a 1:50 dilution in goat serum overnight at 4 ^{o}C. Samples were washed and then stained with 1 μg/mL DAPI (BD Biosciences) for 3 min at RT with

agitation. Samples were mounted on No. 1.0 coverglass bottom culture dishes in 90% buffered glycerol solution for imaging on an Olympus FV-1000 confocal inverted microscope. Approximately 4-5 images were captured from multiple stained pieces of AT for each mouse. There were 4 mice per group for a total of ~15-20 images per experimental group. Cell number was quantified from each image using ImageJ software and averaged for a representative count. Multiple confocal slices spanning ~30-50 microns were reconstructed into a 3D rendering using ICY software (Bio Image Analysis, Paris, France) or Imaris software.

Hematoxylin and eosin (H&E) stain:

Chapter III: Cytospins were performed with 8,000-40,000 cells spun for 5 min at 600-1000 rpm and stained with Hemacolor (LABSCO, Louisville, KY) according to manufacturer's instructions.

Chapter IV: Tissue was first fixed in 10% formalin and embedded in paraffin. H&E staining was performed on 7 micron sections of AT via traditional methods. Briefly, sections were placed in xylene to remove paraffin, hydrated, stained with hematoxylin, rinsed with tap water, stained with eosin, dehydrated, placed in xylene, mounted with Permount, and coverslipped.

Fast Green/ Neutral Red Stain:

FACS sorted cells were cytospun for 5 min at 600 rpm. Slides were fixed for 10 min in ice cold 100% methanol for 10 min, immersed in Fast Green FCF (Sigma-Aldrich) for 24 h at RT, and immersed in Neutral Red (Sigma-Aldrich) for 48-72 h at RT.

Major Basic Protein detection by HRP:

FACS sorted cells were cytospun for 5 min at 600 rpm. Slides were fixed for 10 min in ice cold 100% methanol for 10 min, incubated in 3% H_2O_2 for 15 min at RT to remove endogenous peroxidase activity, non-specific binding blocked with 5% normal goat serum for 1h at RT, incubated with primary rat anti-mouse major basic protein antibody (kindly provided by the laboratories of Drs. Nancy and Jamie Lee, Mayo Clinic Arizona) overnight at 4 ^{o}C, incubated in secondary HRP goat anti-rat antibody (Santa Cruz Biotechnology, Dallas, TX) for 1 h at RT, DAB reaction was carried out according to the manufacturer's instructions (Life Technologies), and counter stained with Hemacolor nuclear stain #3 (LABSCO).

Bone marrow derived eosinophil differentiation

Bone marrow was extracted from femurs and tibias of lean WT and CCR2$^{-/-}$ mice and were differentiated as adapted from Dyer *et al.* (78). Briefly, red blood cells were removed by suspension in ACK Lysing Buffer. Remaining cells were cultured for 4 d at 37^{o}C at 1 x 10^{6} cells/mL in RPMI supplemented with 20% FBS, 100 IU/ml penicillin, 10 µg/mL streptomycin, 2 mM glutamine, 25 mM HEPES, 1x

nonessential amino acids, 1 mM sodium pyruvate, and 50 μM 2-ME. During days 0-4, 100 ng/mL stem cell factor (SCF) and 100 ng/mL FLT3 Ligand (PeproTech, Rocky Hill, NJ) were added. During days 5-12, SCF and FLT3 were replaced with IL-5 (R&D Systems, Minneapolis, MN). Fresh media was applied on days 4, 8, and 10. Cell aliquots were collected for RNA isolation on days 0, 4, 8, 10, and 12. Cytospins were performed on days 4 and 10. Eosinophil differentiation was confirmed on day 10 by flow cytometry. Eosinophils were identified as $F4/80^{lo}$, $CD11b^{lo}$, and $SiglecF^{+}$.

Glucose tolerance test

Mice were fasted for 6 hours during the light cycle. Fasting blood glucose levels were read using an ACCU-CHEK Aviva Plus glucometer (Roche, Basel, Switzerland) via the tail vein after a small tail clip. A 20% glucose solution was administered IP at 2 mg/kg lean mass, followed by blood glucose readings at times 15, 30, 45, 60, 90, and 120 post glucose dose.

Triglyceride tolerance test

Mice were fasted overnight for 16 h to deplete liver glycogen stores and induce lipolysis. Blood was collected via the tail vein after a small tail clip to measure fasting TGs, FFAs, glucose, and cholesterol. Mice received an oral gavage of olive oil at 200 μL/mouse, and additional blood was collected for analysis at times 1, 2, 3, 4, 5 h after gavage.

Ad libitum mixed-meal tolerance test

Mice were fasted overnight for 16 h. Blood was collected via the tail vein after a small tail clip to measure fasting glucose, insulin, triglycerides (TG), FFA, and cholesterol. Mice were re-fed up to 1.5 g high fat diet *ad libitum* and additional blood was collected for analysis at times 0.5, 1, 2, 3, 4 h after refeeding.

Plasma insulin

Insulin was measured by the Vanderbilt Hormone Assay and Analytical Services Core (HA&ASC) via radioimmunoassay using a double antibody procedure. Final analysis was accomplished by quantifying bound radioactive counts with a Packard Gamma counter connected to a computerized data reduction station.

Plasma lipids

FFAs were measured from mouse serum using a Cell Biolabs FFA Assay Kit via the manufacturer's instructions (Cell Biolabs, San Diego, CA). TGs were measured from mouse serum using an Infinity TG Assay Kit via the manufacturer's instructions (Thermo Fisher Scientific, Middletown, VA). Cholesterol was measured from mouse serum using an Infinity Cholesterol Assay Kit via the manufacturer's instructions (Thermo Fisher Scientific).

Energy expenditure and cold challenge

Mice were placed in metabolic cages at Vanderbilt's MMPC for 2 days at 21^{o}C room temperature (RT) followed by 2 days at 4^{o}C. The temperature flux took approximately 1 h to reach 4^{o}C. Body weight, food & water consumption, oxygen & carbon dioxide levels, and movement were all measured continuously throughout the duration of the 4-day study.

Statistics

Chapter III:

GraphPad Prism 5.0 software was used for all statistical analyses. Statistical tests include: student's t-test, one-way ANOVA followed by a post-hoc Student's *t*-test if the ANOVA was significant. A two-way ANOVA was used to compare measurements with two different variables. Outliers were excluded from the data for each individual parameter if outside the range of the mean ± 2 SD. A *P* value of ≤0.05 was considered significant.

Chapter IV & V:

GraphPad Prism 7.0 software was used for all statistical analyses. Statistical tests include: student's *t*-test, one-way ANOVA with a Holm-Sidak *post-hoc* test for multiple comparisons, and two-way ANOVA with a Holm-Sidak *post-hoc* test for multiple comparisons. Outliers were removed by the ROUT method, with Q = 5%. Significance was defined by a *P* value of ≤0.05.

CHAPTER III

CCR2 DEFICIENCY LEADS TO INCREASED EOSINOPHILS, ALTERNATIVE MACROPHAGE ACTIVATION, AND TYPE 2 CYTOKINE EXPRESSION IN ADIPOSE TISSUE

(Adapted from Bolus, *et al.* 2015. *J Leukoc Biol*. 2015 Oct;98(4):467-77.)

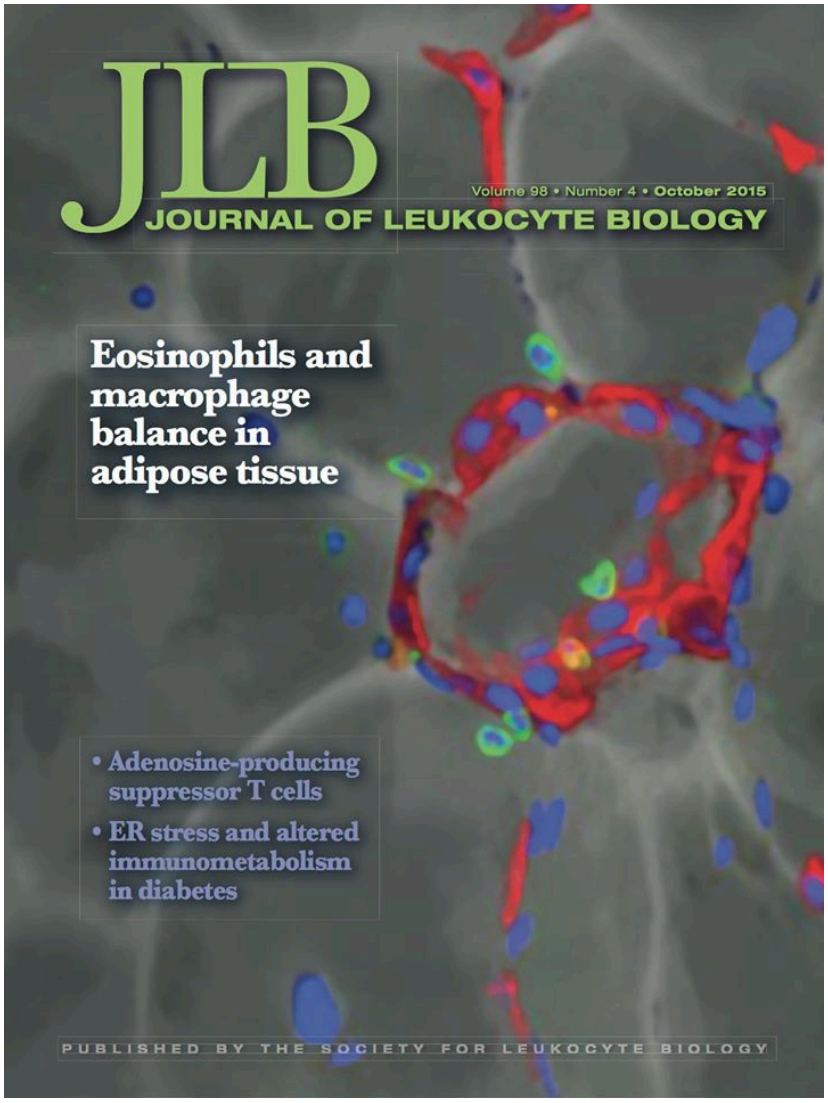

Introduction

CCR2 is a member of the CC-chemokine family of receptors that is primarily known for its ability to bind CCL2, leading to chemotaxis of leukocytes (79, 80). CCR2 is also known to be a receptor for additional chemokines, including CCL7, CCL8, CCL13, and CCL16 [reviewed in (81)]. CCR2 is expressed on the surface of leukocytes from multiple lineages including monocytes, macrophages, lymphocytes and granulocytes, and its expression is tightly regulated, differing from one cell type to another (82). Leukocytes from mice with a gene-targeted deficiency of CCR2 ($CCR2^{-/-}$) show no differences in rolling velocity but do have reduced adhesion to the endothelium and decreased extravasation into inflamed tissues in response to CCL2 (83). Furthermore, $CCR2^{-/-}$ mice have a severe reduction in the number of circulating $Ly6C^{hi}$ inflammatory monocytes due to impaired egress from the bone marrow (40). The loss of circulating inflammatory monocytes in $CCR2^{-/-}$ mice decreases macrophage accumulation at sites of acute inflammation, such as thioglycollate-induced peritonitis (43, 84). Given the potent role of CCR2 in monocyte chemotaxis, $CCR2^{-/-}$ mice have previously been used to study the role of macrophages in chronic inflammatory diseases such as atherosclerosis and obesity (36, 40).

It is established that obesity leads to immune-system driven chronic inflammation that promotes insulin resistance and type 2 diabetes in rodents and humans [reviewed in (85)]. This inflammation is characterized by an influx of inflammatory immune cells into metabolic tissues such as AT (30, 31). The role of CCR2 in leukocyte accumulation during chronic inflammation such as obesity is not yet clear. Based upon the near absence of circulating Ly6C^{hi} monocytes in CCR2$^{-/-}$ mice (40), it was anticipated that AT macrophage accumulation would be severely blunted. However, we (43) and others (36) have shown AT macrophage accumulation in obese CCR2$^{-/-}$ mice is only mildly decreased, and this reduction is only apparent after long periods of high fat diet (HFD) feeding. No effects of CCR2 deficiency on macrophage accumulation have been reported at earlier periods of HFD feeding when initiation of macrophage recruitment occurs. Moreover, tissues of CCR2$^{-/-}$ mice display diminished type-1 (84) and increased type-2 immune responses (86). Increased expression of IL-4 and "M2" macrophage markers, arginase (*Arg1*) and Ym1 (*Chil3*), characterize the enhanced type-2 response (43, 86). Additionally, we previously found that hematopoietic CCR2 deficiency leads to aberrant accumulation of a unique myeloid cell population in AT of obese mice (43). In the current report, we identify these cells as eosinophils and further characterize their contribution to AT inflammation in the lean and obese state.

Eosinophils were only recently discovered in AT and have already been found to play an important function in sustaining alternative activation of AT macrophages (73-75). AT eosinophils were shown to decrease in obesity, concomitant with M1-like polarization of the AT macrophages. Additionally, mice with systemically elevated eosinophils were protected against developing obesity-related insulin resistance, while mice with eosinophil deficiency were more prone to developing insulin resistance (73). Accumulation of AT eosinophils is mediated by IL-5 secreted predominantly by resident ILC2 cells (74). The studies summarized above demonstrate that eosinophils can protect against metabolic defects associated with obesity-induced inflammation.

In the current report we show that CCR2 deficiency leads to increased eosinophil number in AT, with no differences in bone marrow, blood, or spleen. Increased AT eosinophil number was positively correlated with AT *Il5* expression, suggesting that local eosinophil recruitment, proliferation, and/or decreased apoptosis may account for the increased numbers in CCR2$^{-/-}$ mice. Similar to previous reports (73) increased AT eosinophils occurred concomitantly with M2-like macrophage activation and increased AT expression of type-2 cytokines *Il4, Il5,* and *Il13*. The tissue localization of macrophages in AT is known to be an indicator of their function, with cells located in CLSs showing greater inflammatory potential (87). While eosinophils are confined to interstitial spaces in AT of obese wild type (WT) mice, we found that eosinophils localize to both CLSs and interstitial spaces in AT of obese CCR2$^{-/-}$ mice. To our knowledge this is the first report associating CCR2 deficiency with increases in AT eosinophils,

implicating that this receptor plays an important role in eosinophil migration to, or cell turnover in, AT. Furthermore we found that CCR2$^{-/-}$ bone marrow cultures differentiate *in vitro* with higher expression of genes critical to the eosinophil lineage compared to WT bone marrow. This study provides a unique setting in which local AT eosinophil accumulation can be studied and contrasted to that of systemically elevated eosinophils observed in the IL-5 transgenic mouse model (73). In addition, this mouse model provides a platform for identifying novel mechanisms of AT eosinophil and type 2 immunity regulation by CCR2.

Results

CCR2 deficiency leads to an increased percent and total number of eosinophils in adipose tissue.

To determine the role of CCR2 signaling on AT immune cell composition, WT and CCR2$^{-/-}$ mice were placed on a chow diet or HFD for 6-8 weeks to induce obesity. At the start of the study, there were no differences between the genotypes in body weight (data not shown). All mice fed a HFD became obese, but there were no genotype effects on body weight or metabolic phenotype, as we have previously reported (43). To elaborate, we previously found no difference in glucose tolerance between WT and CCR2$^{-/-}$ mice at 6 and 12 weeks of HFD, yet there was a modest improvement in these parameters in CCR2$^{-/-}$ mice after an extended 20 weeks of HFD feeding (43). There were no differences in insulin tolerance, weight gain, percent adiposity, or epididymal AT weight between genotypes at 6, 12, or 20 weeks on HFD.

Immune cell content of the epididymal AT (eAT) from WT (Fig. 3.1A-B) and CCR2$^{-/-}$ (Fig. 3.1C-D) mice was analyzed by flow cytometry. Based on previous work by our group and others (43, 73, 74), eosinophils were identified as CD11b^{lo}, F4/80^{lo}, SiglecF^{+} cells (Fig. 3.1A & C). Identification of eosinophils was further confirmed by the presence of characteristic green granules with a Fast Green/ Neutral Red stain (Fig. 3.1E & G) and by staining of major basic protein via HRP (Fig. 3.1I & K), both of which were absent in the macrophage population identified as CD11b^{hi}, F4/80^{hi}, and SiglecF^{-} cells (Fig. 3.1B, D, F, H, J & L). In addition, cytospins of sorted CD11b^{lo}, F4/80^{lo}, SiglecF^{+} cells

demonstrated multilobular (Fig. 3.1E, G, & K) or donut shaped nuclei (Fig. 3.1I) characteristic of eosinophils. This is in striking contrast to sorted macrophages that exhibited round nuclei with higher cytoplasmic volume (Fig. 3.1F, H, J & L).

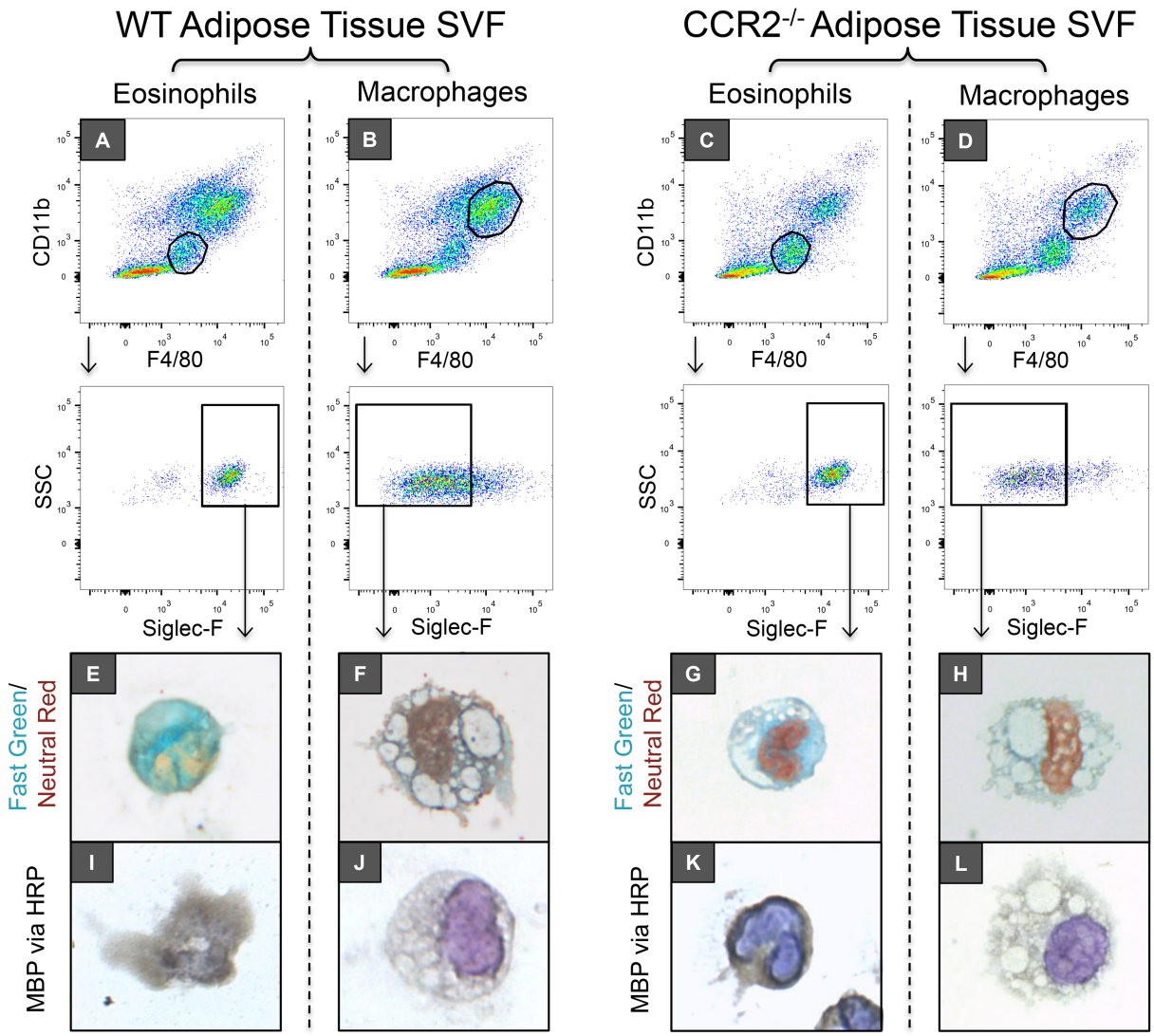

Figure 3.1 Identification of eosinophils by flow cytometry, Fast Green/ Neutral Red, and Major Basic Protein.
Epididymal AT from lean WT and CCR2$^{-/-}$ mice was collected, the SVF isolated, and cells sorted by FACS. FACS sorted A, C) eosinophils [CD11b^{lo}, F4/80^{lo}, SiglecF^{+}] and B, D) macrophages [CD11b^{hi}, F4/80^{hi}, SiglecF^{-}] from the SVF of AT of WT (left) and CCR2$^{-/-}$ (right) mice. E-H) Fast Green/ Neutral Red staining and I-L) major basic protein detection by HRP were performed on eosinophils (E, I, G, K) and macrophages (F, J, H, L). Images are representative of n=2-3 mice per group. The only modification to images was removal of background discoloration and neutralizing to a white background for even comparison.

With the validated gating strategy described above, we next evaluated the relative difference in percent AT eosinophils from WT and CCR2$^{-/-}$ mice when in the lean versus obese state. Replicating published data (73), the percent eosinophils of live stromal vascular cells decreased in eAT from WT mice with obesity (Fig. 3.2A). In contrast, we show for the first time that eAT eosinophil percentages were 3.72-fold higher in obese CCR2$^{-/-}$ mice compared to obese WT mice (Fig. 3.2A; $P<0.0001$). A similar increase in eosinophils of obese CCR2$^{-/-}$ compared to WT mice was observed in other AT depots analyzed: perirenal (pAT; Fig. 3.2B; $P<0.005$), mesenteric (Fig. 3.2C; $P<0.05$) and subcutaneous (Fig. 3.2D; $P<0.005$). Although the percentage of eosinophils in other fat pads was lower than eAT, the fold change between genotypes was 2 to 4-fold higher in all white fat pads of obese CCR2$^{-/-}$ mice examined.

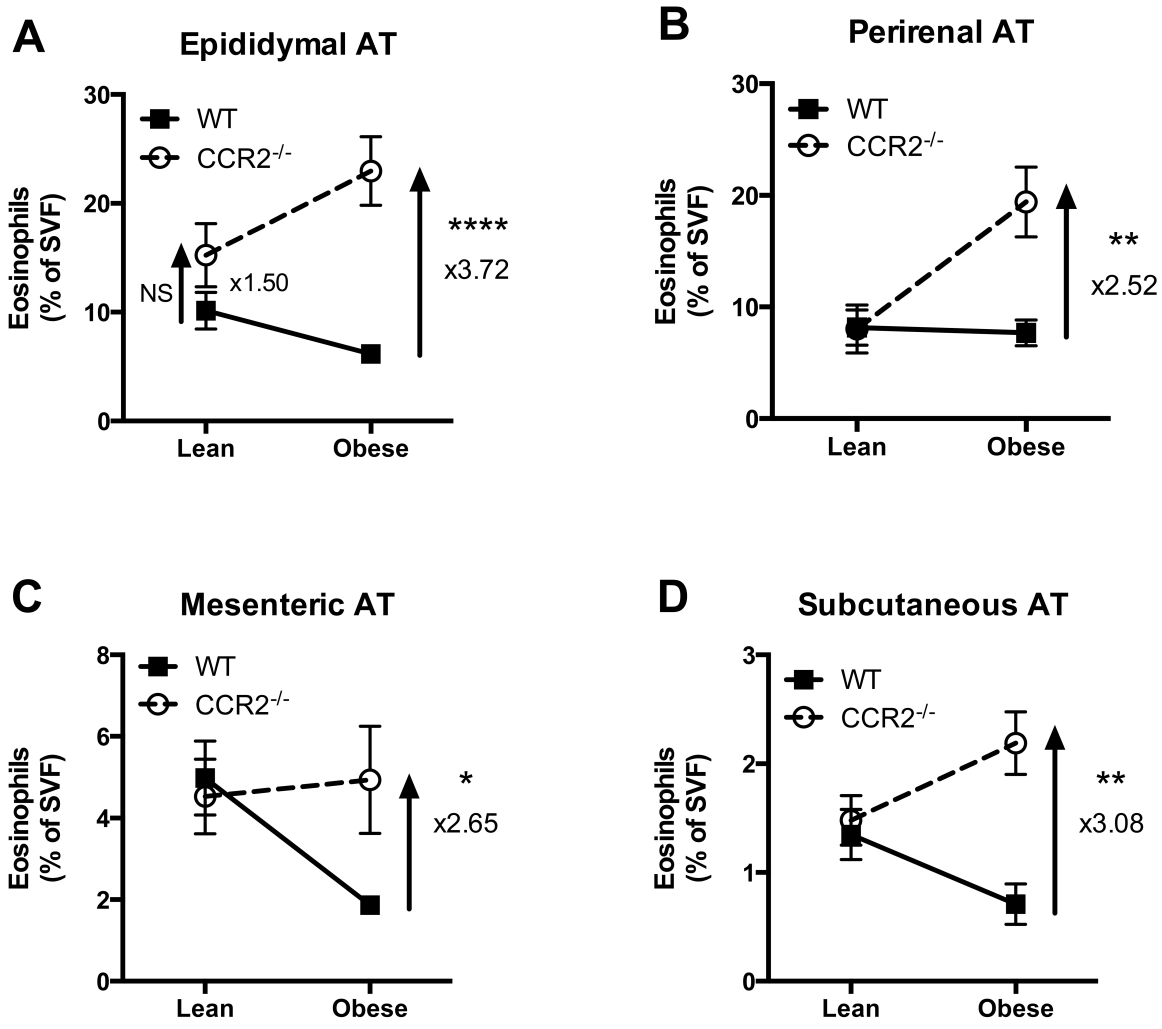

Figure 3.2 High fat diet induced obesity in CCR2$^{-/-}$ mice leads to increased eosinophils in white adipose tissue.

White AT from lean and obese WT and CCR2$^{-/-}$ mice was collected, the SVF isolated, and the percentage of eosinophils quantified by flow cytometry. A) epididymal, B) perirenal, C) mesenteric, and D) subcutaneous. Data are presented as mean ± SEM representing the difference in percent eosinophils between lean and obese for each genotype; n=5-10 mice per group.

*P<0.05 Difference between genotypes of mice on the same diet.

**P<0.005 Difference between genotypes of mice on the same diet.

****P<0.0001 Difference between genotypes of mice on the same diet.

Though the following results detail AT macrophage and eosinophil composition, the results should be interpreted with the understanding that AT is composed of a variety of other cell types including but not limited to the adipocytes themselves, preadipocytes, mesenchymal stem cells, endothelial progenitor cells, T cells, and B cells, as well as the vascular and neuronal network. Furthermore, AT is often discussed in terms of interstitially spaced regions and CLSs, due to the inflammatory variation of immune cells in such regions. It has been established that macrophages in CLSs possess a proinflammatory phenotype (87); however, the localization of eosinophils to CLSs has not been reported. To examine AT macrophage and eosinophil localization in obese CCR2$^{-/-}$ mice and obese WT mice, we used confocal immunofluorescence microscopy to construct a 3D rendering of images spanning ~50 microns. The 3D constructs allowed us to distinguish macrophages by F4/80 staining and eosinophils both by SiglecF staining and by visualization of the multi-lobular and donut-shaped nuclei, which are not discernible in traditional Z-stack analysis. In lean mice of both genotypes, eAT macrophages and eosinophils localized interstitially, though CCR2$^{-/-}$ mice had a significantly higher percentage of interstitial eosinophils than WT (Fig. 3.3A & D; Fig. 3.4A & C). During obesity, a surge of macrophages accumulated in eAT of WT mice and macrophages were >2.5-fold more likely to localize to CLSs than interstitial spaces (Fig. 3.3B-C; Fig. 3.4B) as has been reported by numerous groups (30, 31, 87, 88). This surge of CLS macrophage accumulation during obesity was blunted in eAT of CCR2$^{-/-}$ mice (Fig. 3.3F; Fig. 3.4B). CLSs were frequently found in both obese genotypes.

However in contrast to obese WT mice, in which eosinophils were confined to interstitial spaces (Fig. 3.3B-C; Fig. 3.4D), eosinophils in obese CCR2$^{-/-}$ mice were often found in CLSs (Fig. 3.3E-F; Fig. 3.4D. This is the first time eosinophils have been shown to localize to CLS in any mouse model. It is interesting to observe that these relatively subtle fluxes in eosinophil number correlate with more drastic alterations in macrophage content (see scale bar of Fig. 3.4B & D). An example of an F4/80^{+} macrophage and SiglecF^{+} eosinophil in close proximity in eAT is shown in Fig. 3.3, Panel G. Magnified images of eAT eosinophils with the classical multilobular and donut-shaped nuclei are shown in Fig. 3.3H & I.

Because the total eosinophil percentage was also relatively high in pAT (Fig. 3.2B), we performed confocal immunofluorescence to determine the localization of eosinophils in this fat pad (Fig. 3.5 & 3.6). Macrophages were selectively found in interstitial spaces of pAT from lean WT mice, but were equally distributed between interstitial spaces and CLSs within pAT of lean CCR2$^{-/-}$ mice. Similar to eAT, eosinophils were detected more frequently in pAT of CCR2$^{-/-}$ mice compared to WT. Likewise, pAT eosinophils of CCR2$^{-/-}$ mice localized to interstitial spaces and CLSs in a similar pattern to eAT eosinophils both in lean and obese mice.

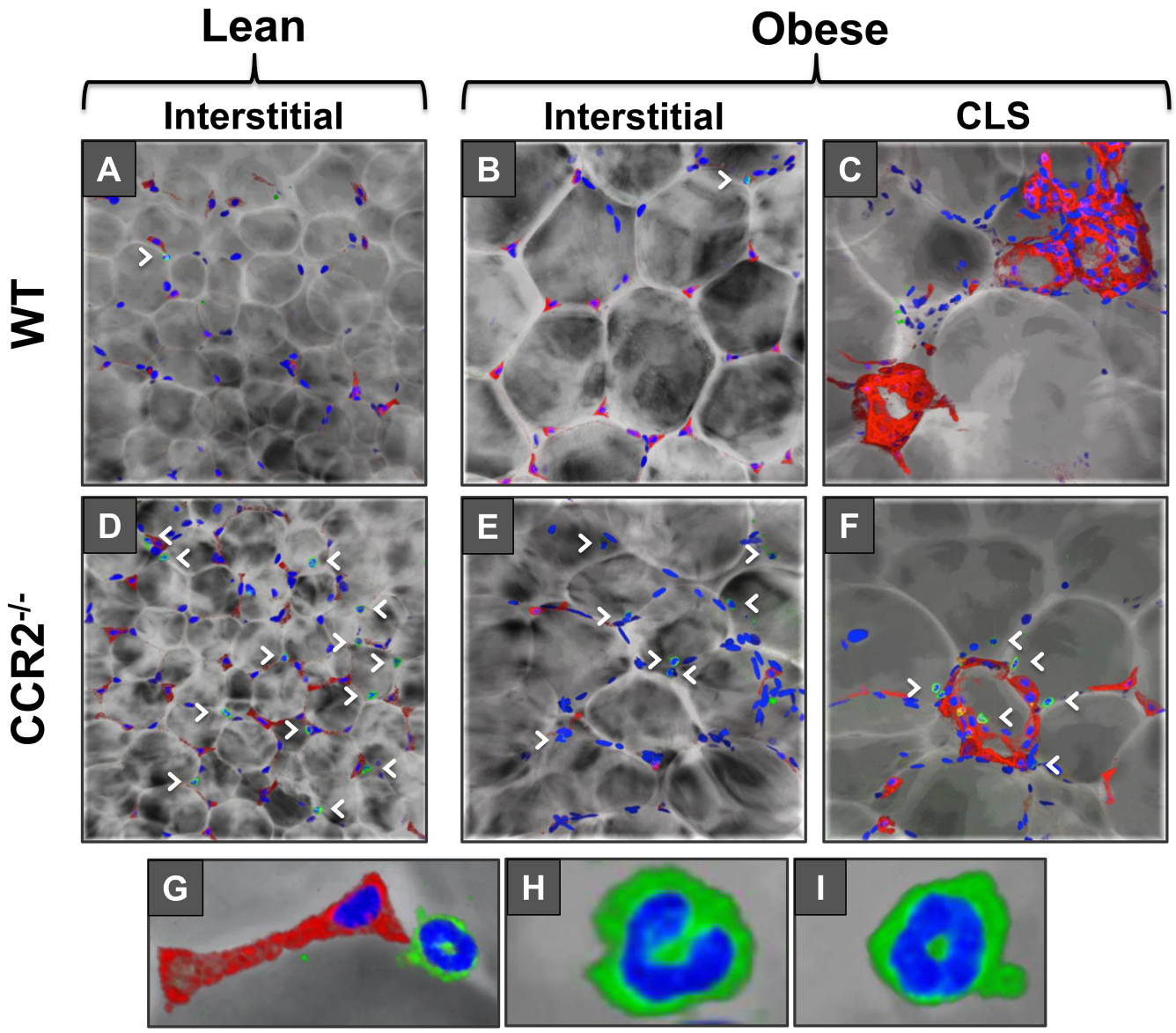

Figure 3.3 Localization of eosinophils and macrophages to interstitial spaces or CLSs in epididymal adipose tissue.
Epididymal AT was collected from lean and obese WT and CCR2$^{-/-}$ mice. AT was stained with SiglecF (green) for eosinophils, F4/80 (red) for macrophages, and DAPI (blue) for nuclei and imaged by confocal immunofluorescence microscopy; visualized as a computer generated 3D rendering. Interstitially spaced macrophages and eosinophils from lean A) WT and D) CCR2$^{-/-}$ mice and from obese B) WT and E) CCR2$^{-/-}$ mice. Crown-like-structure (CLS) localized macrophages and eosinophils from obese C) WT and F) CCR2$^{-/-}$ mice. G) Magnified image of juxtaposed macrophage and eosinophil for comparison. H-I) High-magnification images of CCR2$^{-/-}$ AT eosinophils exhibiting prototypical multi-lobular or donut-shaped nuclei. Arrowheads demonstrate some of the eosinophils visible in each image. Images are representative of 3 images per mouse with n=4 mice per group.

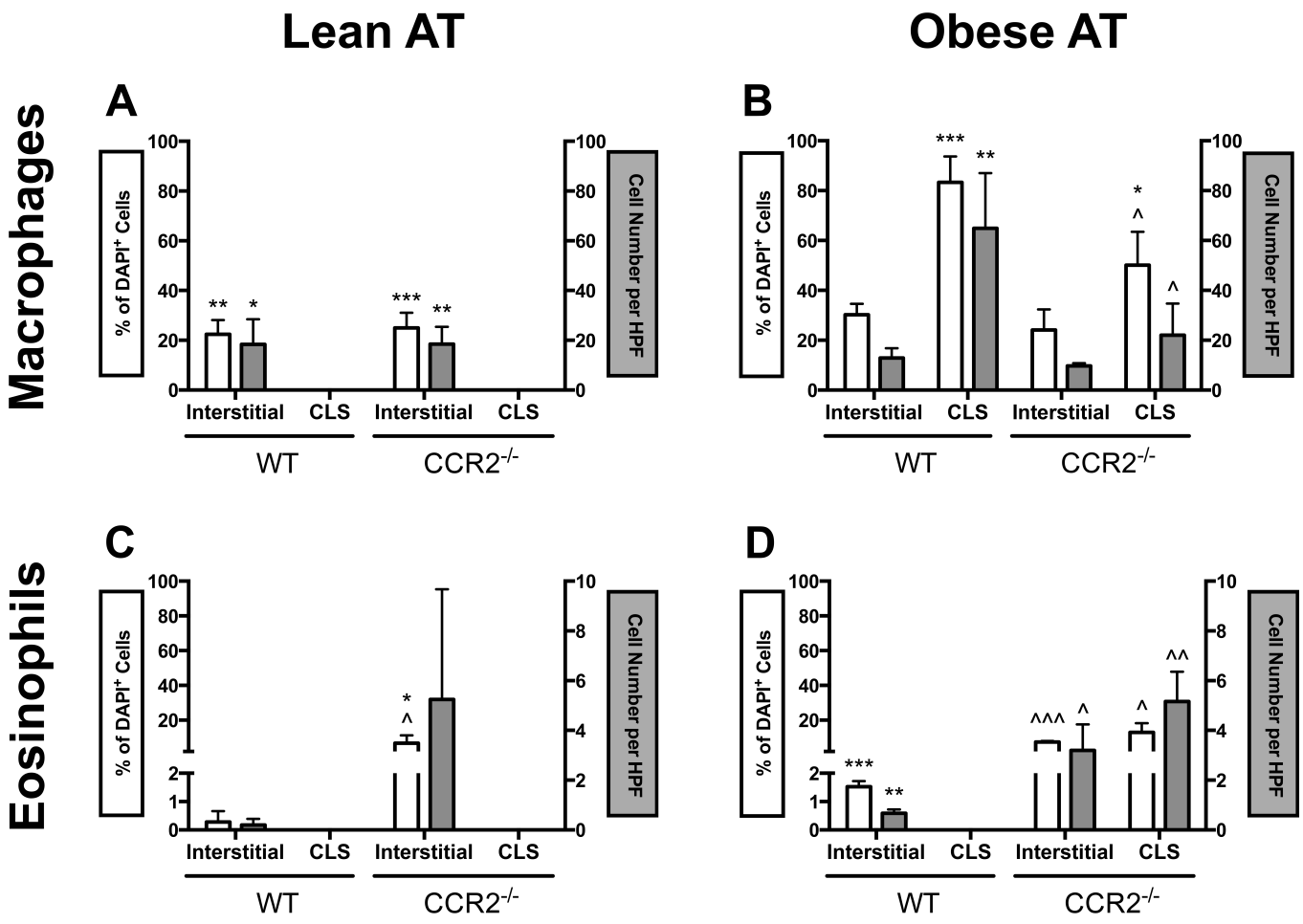

Figure 3.4 Quantification of macrophages and eosinophils in CLS or interstitially spaced regions of epididymal adipose tissue.
Immune cell localization from images in Figure 3 was quantified by percent of DAPI$^+$ cells (white bars) and absolute cell number per high power field (grey bars). A) Macrophages in eAT of lean mice; B) Macrophages in eAT of obese mice; C) Eosinophils in eAT of lean mice; D) Eosinophils in eAT of obese mice. Data are shown as the mean ± SEM with n=3-4 mice per group.
*P<0.05 Difference between locations within the same genotype.
**P<0.005 Difference between locations within the same genotype.
***P<0.0005 Difference between locations within the same genotype.
^ P<0.05 Difference between genotypes within the same location.
^^P<0.005 Difference between genotypes within the same location.

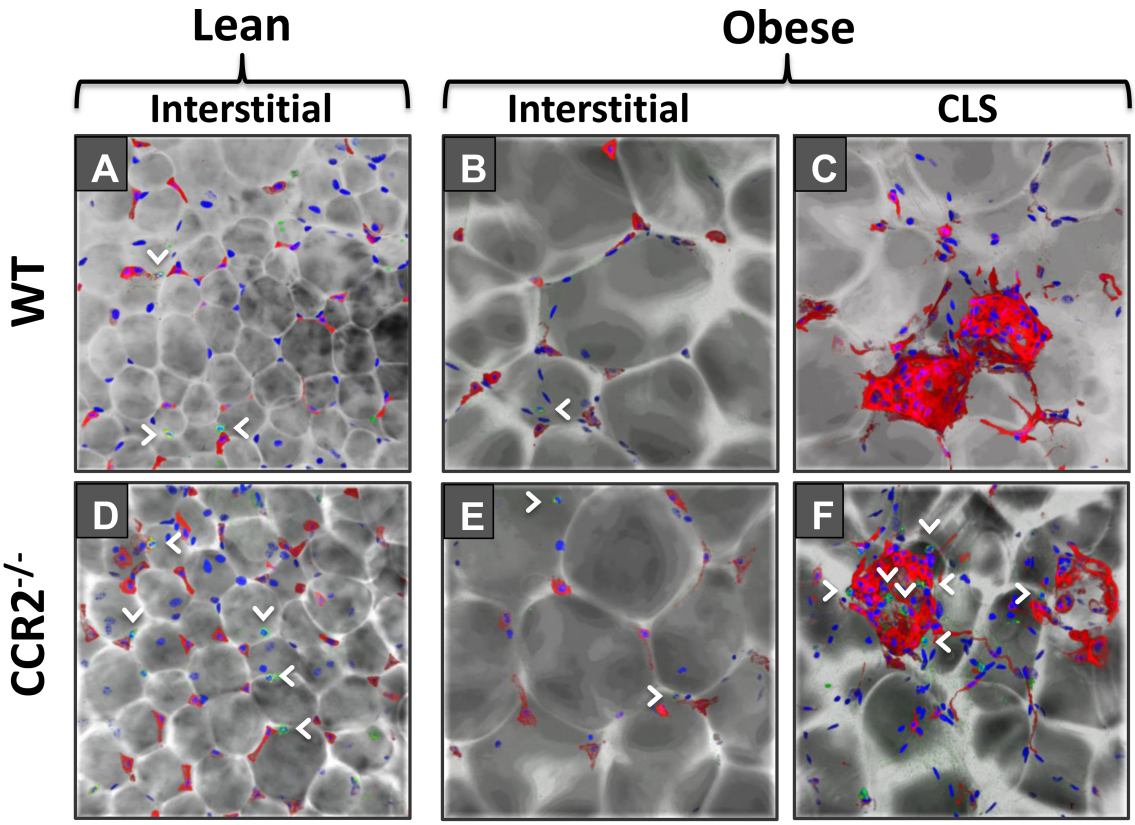

Figure 3.5 Localization of eosinophils and macrophages to CLS or ISS regions of perirenal AT. Perirenal adipose tissue pieces from WT and CCR2$^{-/-}$ mice fed chow or high fat diet (HFD) for 6-8 weeks were stained with SiglecF (green) for eosinophils, F4/80 (red) for macrophages, and DAPI (blue) for nuclei and imaged by confocal immunofluorescence microscopy; visualized as a computer generated 3D rendering. Interstitially spaced (ISS) macrophages and eosinophils from chow-fed A) WT and D) CCR2$^{-/-}$ mice and from HFD-fed B) WT and E) CCR2$^{-/-}$ mice. Crown-like-structure (CLS) localized macrophages and eosinophils from HFD-fed C) WT and F) CCR2$^{-/-}$ mice. Arrowheads demonstrate some of the eosinophils visible in each image. Images are representative of 3 images per mouse with n=4 mice per group.

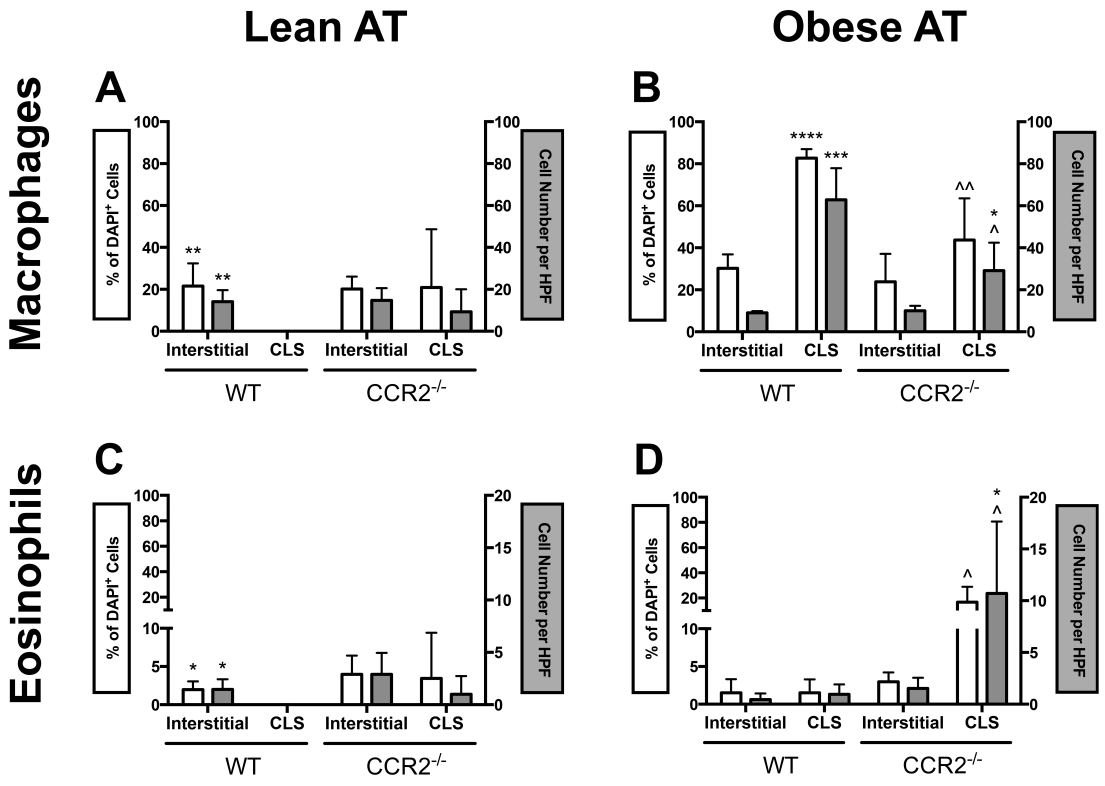

Figure 3.6 Quantification of eosinophils and macrophages in CLS or ISS regions of perirenal AT. Perirenal adipose tissue pieces from WT and CCR2$^{-/-}$ mice fed chow or high fat diet (HFD) for 6-8 weeks were stained with SiglecF (green) for eosinophils, F4/80 (red) for macrophages, and DAPI (blue) for nuclei and imaged by confocal immunofluorescence microscopy; visualized as a computer generated 3D rendering. A) Macrophages in chow-fed mice; B) Macrophages in HFD-fed mice; C) Eosinophils in chow-fed mice; D) Eosinophils in HFD-fed mice. Data are shown as the mean ± SEM, with n=4 mice per group.
*P<0.05 Between locations within the same genotype.
***P<0.001 Between locations within the same genotype.
^ P<0.05 Between genotypes within the same location.
^^P<0.01 Between genotypes within the same location.

In addition to adipose tissue, eosinophils accumulate in the peritoneal cavity of CCR2$^{-/-}$ mice.

The number of eosinophils in bone marrow, blood, spleen, and liver were quantified. While eosinophils in livers of lean WT mice were higher than all other groups, no differences in other tissues were detected (Fig. 3.7A-D). In contrast, quantification of non-elicited peritoneal cavity cells revealed a greater than 5-fold increase in peritoneal eosinophils in CCR2$^{-/-}$ mice compared to WT mice (Fig. 3.7E; P<0.05).

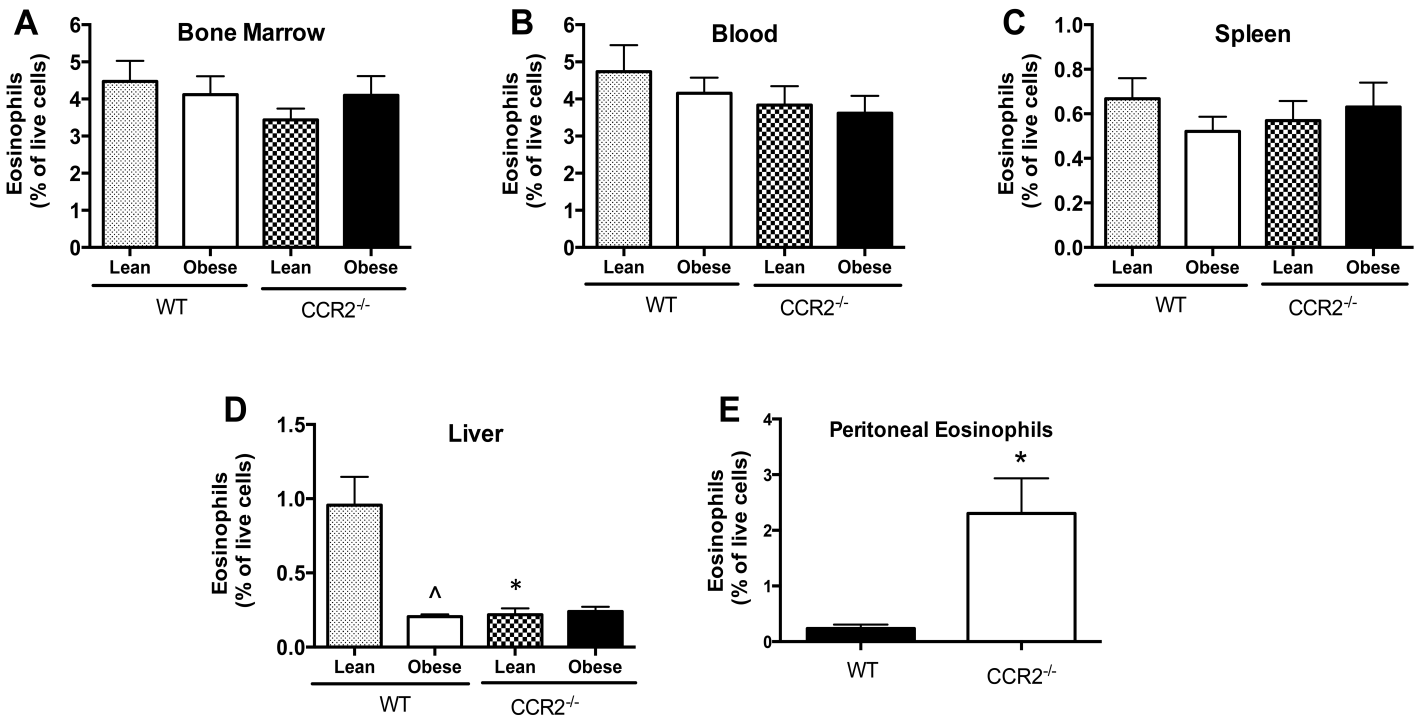

Figure 3.7 Besides adipose tissue, the peritoneal cavity is the only other site of eosinophil accumulation detected in CCR2$^{-/-}$ mice. WT and CCR2$^{-/-}$ mice were fed chow or high fat diet (HFD) for 6-8 weeks. Quantification of the percentage of eosinophils of all live cells by flow cytometry. A) Bone Marrow, B) Blood, C) Spleen, D) Liver and E) Naïve (non-stimulated) peritoneal cavity. Data are presented as mean ± SEM, n=5-6 per group for tissues; n=3 per group for peritoneal cavity.
*P<0.05 Difference between genotypes of mice on the same diet.
^P<0.05 Difference between diets of mice on the same diet.

Bone marrow derived CCR2$^{-/-}$ eosinophils display increased expression of key eosinophil genes during differentiation in vitro, but present the same numerical yield as WT.

To determine a potential mechanism for AT eosinophil accumulation in CCR2$^{-/-}$ mice, we tested whether bone marrow cells from CCR2$^{-/-}$ mice have an altered potential to differentiate into eosinophils. Bone marrow cells were isolated from the femurs and tibias of lean WT and CCR2$^{-/-}$ mice and differentiated into eosinophils as previously described (78) and detailed in the Materials and Methods section. Upon differentiation with IL-5 over a time course of 0, 4, 8, 10, and 12 days, we observed an increase (up to 300-fold) in many eosinophil-associated genes. These included: 1) eosinophil granule proteins: eosinophil peroxidase and major basic protein; 2) eosinophil receptors: IL-5 receptor α and chemokine C-C motif receptor 3; 3) eosinophil transcription factor: GATA binding protein 1; and 4) eosinophil cytokines: interleukin 4, and interleukin 6 (gene names: *Epx, Prg2, Il5ra, Ccr3, Gata1, Il4,* & *Il6* respectively). These data indicate that the bone marrow cells had differentiated into eosinophils in both genotypes (Fig. 3.8A-G). Interestingly, *Epx, Prg2,* and *IL5ra* were significantly elevated in CCR2$^{-/-}$ bone marrow derived eosinophils when compared to WT eosinophils; however, other eosinophil-associated genes i.e. *Ccr3*, *Gata1*, *Il4* and *Il6* were not differentially expressed between genotypes. *Mpo*, a neutrophil-specific marker, was reduced in both genotypes, confirming the specificity of the differentiation process (Fig. 3.8H). To further confirm the purity of eosinophil cultures, cells were cytospun after 10 days of differentiation and analyzed by Hemacolor

staining. Fig. 3.8I & K show the characteristic multi-lobular nuclei and granularity of differentiated eosinophils in WT and CCR2$^{-/-}$ cultures. At Day 10 of differentiation, ~84% of cells were eosinophils in both WT and CCR2$^{-/-}$ cultures (Fig. 3.8J & L). Likewise the growth curves of WT and CCR2$^{-/-}$ cultures were statistically indistinguishable from each other (Fig. 3.8M). These data show that although CCR2 deficiency alters expression of some genes in bone marrow derived eosinophils, it does not alter the numerical yield. Thus, eosinophil differentiation is unlikely to directly account for the observed increase in eosinophil number in AT of CCR2$^{-/-}$ mice.

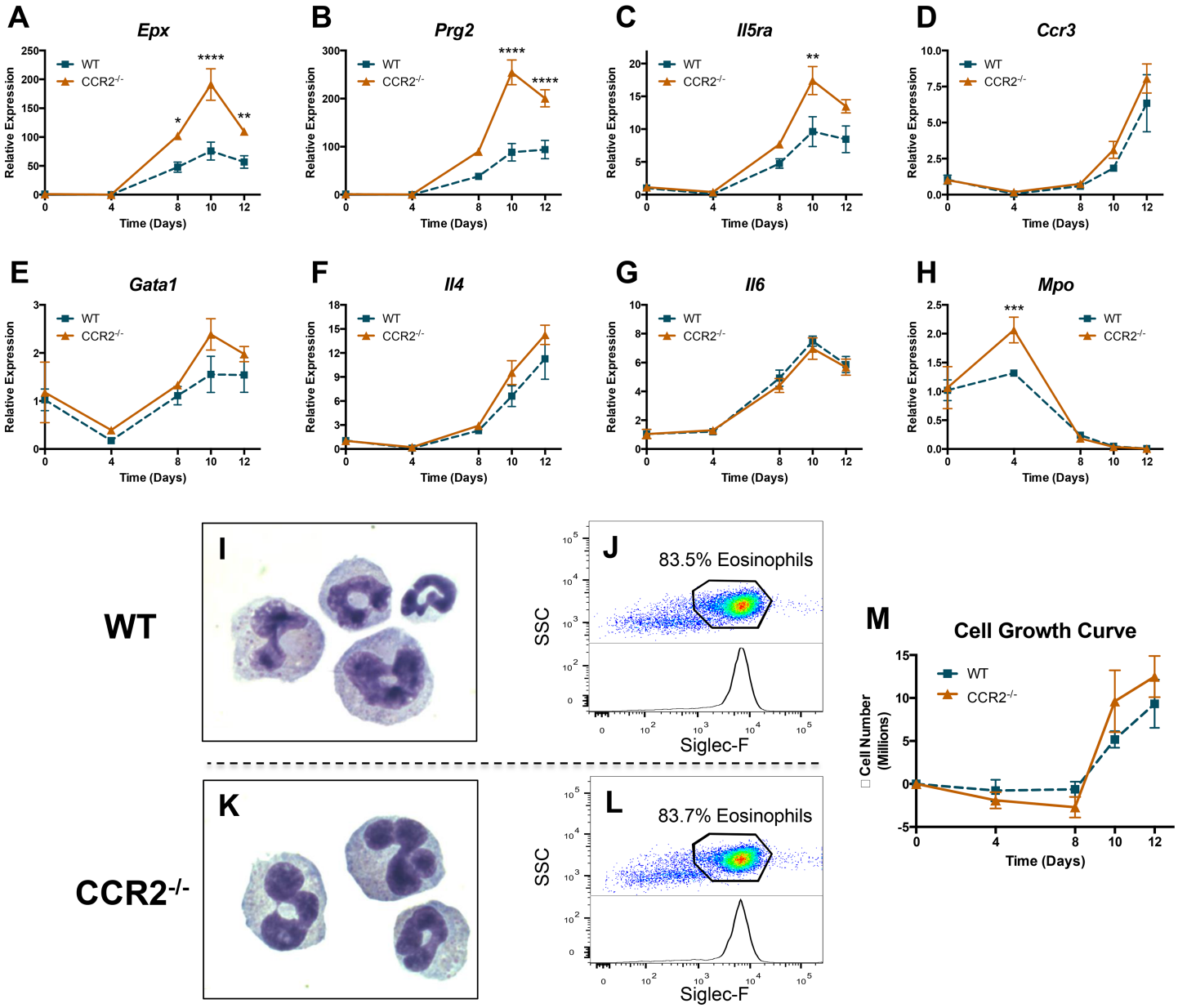

Figure 3.8 Bone marrow derived CCR2$^{-/-}$ eosinophils display increased expression of key eosinophil genes during differentiation *in vitro*.

Bone marrow cells were collected from lean WT and CCR2$^{-/-}$ mice and differentiated into eosinophils *in vitro* according to the Methods section. Briefly, cells were cultured with stem cell factor and FLT3 ligand for 4 days and subsequently cultured with IL-5 for 8 days. Expression of eosinophil specific genes A) *Epx,* B) *Prg2,* C) *Il5ra,* D) *Ccr3,* E) *Gata1*, eosinophil secreted cytokines F) *Il4* and G) *Il6* and non-eosinophil specific genes H) *Mpo* throughout differentiation. Cytospin Hemacolor® images of bone marrow derived eosinophils at 10 days of differentiation from I) WT and K) CCR2$^{-/-}$ mice. Percent purity of eosinophils from J) WT and L) CCR2$^{-/-}$ at 10 days of differentiation. M) Total cell growth rate throughout differentiation. Data are normalized to Day 0 for each genotype and are presented as mean ± SEM with n=2 for Day 0 and n=4 for Days 4-12.

*P<0.05 Difference between genotypes

**P<0.01 Difference between genotypes

****P<0.0001 Difference between genotypes

Increased eosinophils in adipose tissue correlate with increased expression of local Il5.

We next looked for AT-specific mechanisms to explain the local increase in eosinophil number, namely the expression of the eosinophil growth factor, IL-5, as well as eosinophil chemokines CCL11, CCL24, CCL3 and CCL5. IL-5 is strongly linked with eosinophil function as it regulates cellular differentiation, proliferation/apoptosis, activation, and accumulation (89, 90) and was recently shown to contribute to eosinophil accumulation in AT (74). We found that eAT of obese CCR2$^{-/-}$ mice had significantly higher *Il5* expression than that of WT counterparts (Fig. 3.9A), strongly correlating with the high number of eosinophils in CCR2$^{-/-}$ eAT (Fig. 3.2).

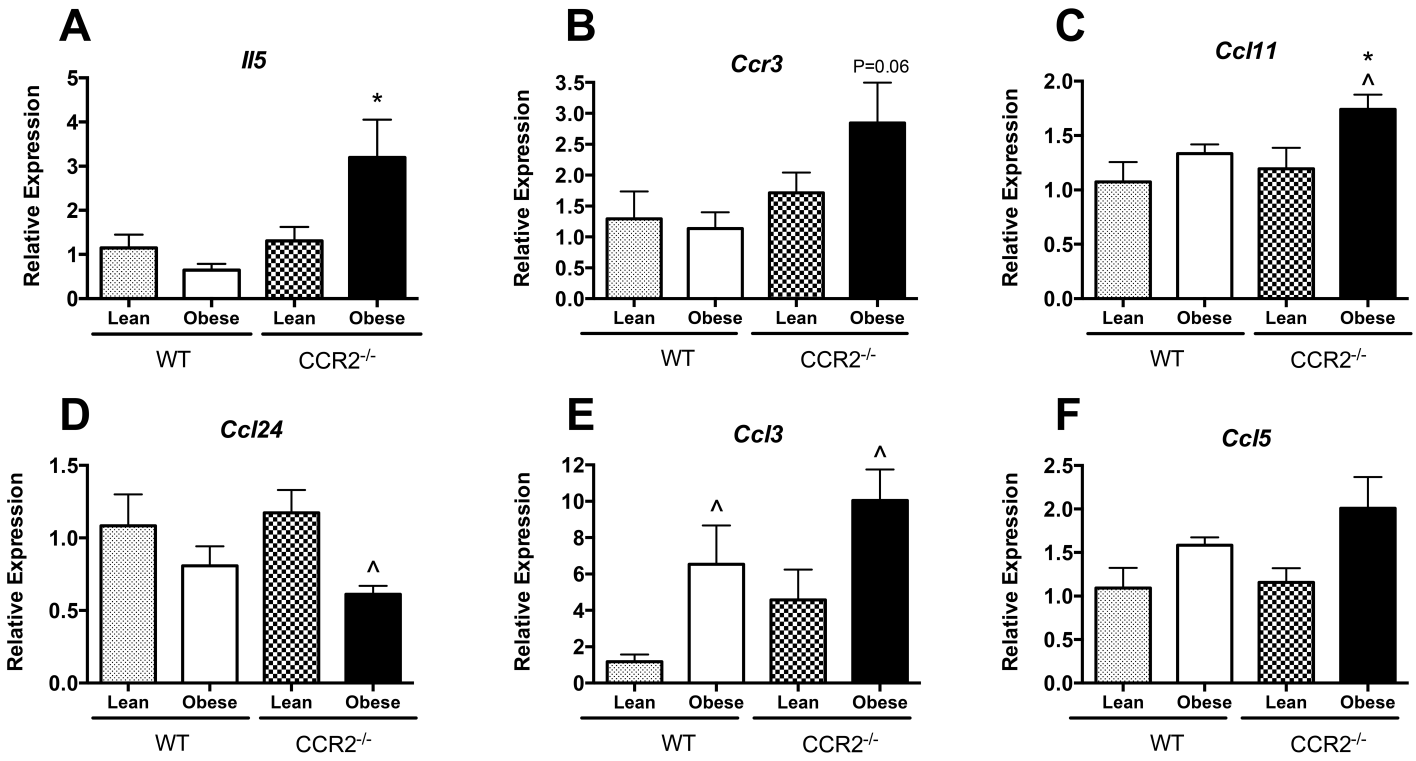

Figure 3.9 Eosinophil-chemoattractant expression in adipose tissue.
Total RNA was isolated from eAT of lean and obese WT and CCR2$^{-/-}$ mice and used for real-time RT-PCR analysis. Relative expression of A) *Il5,* B) *Ccr3*, C) *Ccl11*, D) *Ccl24*, E) *Ccl3*, and F) *Ccl5.* Data are normalized to lean WT control and presented as mean ± SEM with n=5-7 mice per group.
*P<0.05 Difference between genotypes of mice on the same diet.
^P<0.05 Difference between diets in mice of the same genotype.

Tissue expression of the chemokine receptor CCR3 is associated with eosinophil recruitment (91). *Ccr3* expression trended toward an increase in eAT of CCR2$^{-/-}$ mice during obesity, positively correlating with increased eosinophils in the tissue (Fig. 3.9B; P=0.06). A subset of chemokines known as eotaxins bind CCR3 to promote eosinophil chemotaxis. There are 2 known eotaxins in mice: eotaxin 1 (CCL11) and eotaxin 2 (CCL24), both of which have been shown to be important in eosinophil chemotaxis under different inflammatory conditions [reviewed in (45, 91)]. Expression of *Ccl11* was upregulated in obese CCR2$^{-/-}$

mice in comparison to obese WT mice (Fig. 3.9C; $P<0.05$) as well as in comparison to their own lean controls ($P<0.05$). The expression of *Ccl24* was decreased in obese CCR2$^{-/-}$ mice ($P<0.05$) compared to their respective lean controls but was not different between genotypes (Fig. 3.9D). The chemokines CCL3 and CCL5 also promote eosinophil chemotaxis via binding to CCR1 (91). Obesity significantly increased the expression of *Ccl3* (Fig. 3.9E) in both genotypes compared to lean controls, but there was no difference between genotypes. Expression of *Ccl5* was modestly increased by obesity in both genotypes (Fig. 3.9F).

We analyzed all chemokine data with respect to eosinophil number and found that expression of *Il5* in eAT had a strong positive correlation ($r^2=0.9210$, $P<0.05$) to the mean number of eAT eosinophils in the four groups of mice. This is in contrast to the absence of correlation of *Ccl11* ($r^2=0.4582$, $P=0.32$), *Ccl24* ($r^2=0.1432$, $P=0.62$), *Ccl3* ($r^2=0.2899$, $P=0.46$) and *Ccl5* ($r^2=0.2573$, $P=0.49$) expression with eAT eosinophil number. These data implicate IL-5 as the putative local modulator of AT-specific eosinophil cell turnover (i.e. recruitment, proliferation, and/or apoptosis).

CCR2$^{-/-}$ mice manifest increased M2-like macrophages and type-2 cytokine expression in epididymal adipose tissue.

To investigate the inflammatory state of immune cells in AT, expression of M2 macrophage polarizing cytokines, *Il4* and *Il13*, were first assessed in RNA isolated from whole eAT. Expression of eAT *Il4* was significantly increased in lean ($P<0.05$) and obese ($P<0.05$) CCR2$^{-/-}$ mice, compared to their WT counterparts (Fig. 3.10A). Likewise, although eAT *Il13* expression was increased in both genotypes during obesity ($P<0.01$), CCR2$^{-/-}$ eAT had significantly higher *Il13* mRNA levels ($P<0.05$; Fig. 3.10B). We determined that eAT *Il4* was expressed mainly in the SVF fraction of obese WT mice (data not shown), indicating that adipocytes were not the source of IL-4. Interestingly, eAT *Il13* expression was higher in adipocytes compared to the SVF of obese WT mice (data not shown). In addition to eosinophils, T regulatory cells (T_{regs}) have been found to play an important role in sustaining an anti-inflammatory environment in AT (92). FOXP3 is a transcription factor critical for the differentiation and function of T_{regs} and it is exclusively expressed by these cells in AT (93, 94). Expression of *Foxp3* in eAT was significantly higher in lean ($P<0.01$) and obese ($P<0.05$) CCR2$^{-/-}$ mice compared to respective WT controls (Fig. 3.10C).

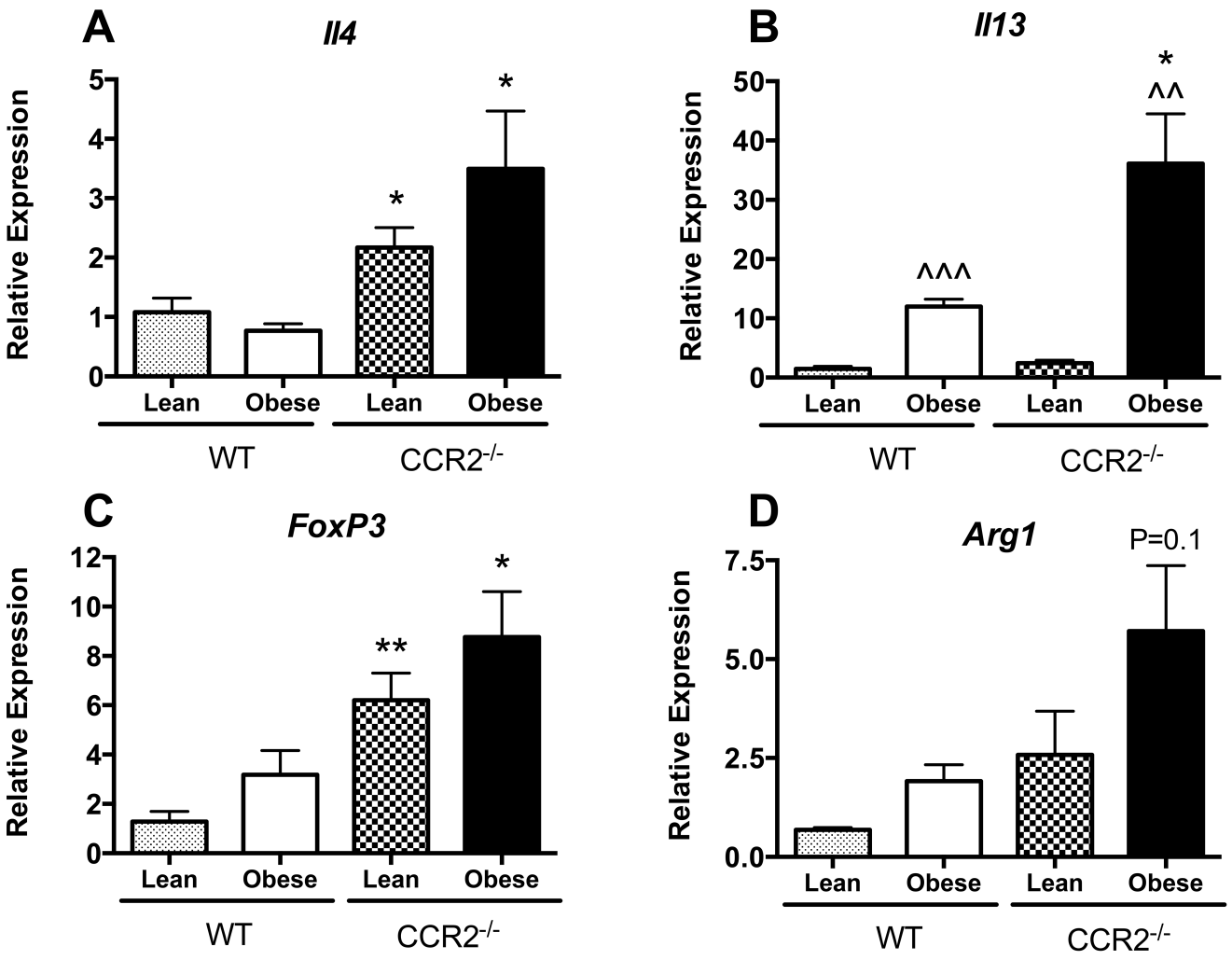

Figure 3.10 Adipose tissue eosinophil accumulation is associated with type-2 cytokine expression.
Total RNA was isolated from eAT of lean and obese WT and CCR2$^{-/-}$ mice and used for real-time RT-PCR analysis. Relative expression of A) *Il4*, B) *Il13*, C) *Foxp3*, D) *Arg1*. Data are presented as mean ± SEM with n=5-7 mice per group.
*P<0.05 Difference between genotypes of mice on the same diet.
**P<0.01 Difference between genotypes of mice on the same diet.
^^P<0.01 Difference between diets in mice of the same genotype.
^^^P<0.001 Difference between diets in mice of the same genotype.

We previously showed an increase in *Arg1* expression in AT of CCR2$^{-/-}$ mice (43). In the current study, we were able to recapitulate increased *Arg1* expression in total eAT (Fig. 3.10D), indicating a predominant M2-like macrophage polarization in the CCR2$^{-/-}$ mice. To specifically determine macrophage polarization, eAT macrophages from both WT and CCR2$^{-/-}$ mice were isolated by FACS and expression of various M1 and M2 markers were assessed. The gene for CD11c (*Itgax)*, the classical M1-like protein identified in AT (87)*,* was increased in eAT macrophages from obese WT mice as expected. However, *Itgax* was maintained at lower levels in macrophages from eAT of obese CCR2$^{-/-}$ mice (Fig. 3.11A). With regards to M2 markers, the gene for Fizz1 protein, *Retnla,* was reduced in eAT macrophages from obese WT mice but levels of this M2 marker were preserved in eAT macrophages from obese CCR2$^{-/-}$ mice (Fig. 3.11B). Furthermore, while M2 genes for arginase and Ym1, (*Arg1* and *Chil3,* respectively) were unchanged in eAT macrophages during obesity in WT mice, they were upregulated in eAT macrophages of CCR2$^{-/-}$ mice (Fig. 3.11C & D); albeit with the caveat that *Chil3* started at a lower value in CCR2$^{-/-}$ eAT macrophages compared to WT. In line with the field's understanding that *in vivo* macrophages are rarely entirely polarized to either M1 or M2, we found that some genes were not changed by obesity in either genotype (*Clec10a, Nos2, Tnfα;* data not shown). Nevertheless, overall these changes demonstrated a general pattern of alternative activation of macrophages in the eAT of CCR2$^{-/-}$ mice.

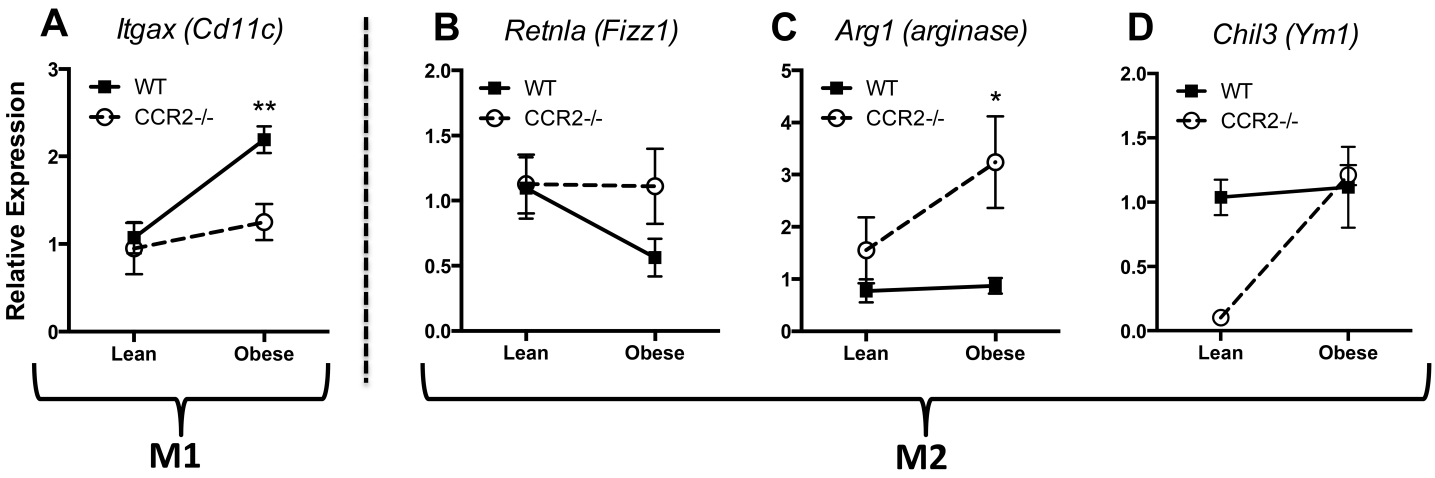

Figure 3.11 CCR2$^{-/-}$ counteracts typical adipose tissue M1 macrophage polarization associated with obesity. F4/80^{hi};CD11b^{hi};SiglecF- macrophages were sorted from the eAT SVF of lean and obese WT and CCR2$^{-/-}$ mice and used for real-time RT-PCR analysis. Relative expression of A) *Itgax* (CD11c), B) *Retnla* (Fizz1), C) *Arg1* (arginase), and D) *Chil3* (Ym1). Data are normalized to lean WT control and presented as mean ± SEM with n=4-5 mice per group.
*P<0.05 Difference between genotypes of mice on the same diet.
**P<0.01 Difference between genotypes of mice on the same diet.

Discussion

In addition to defense against foreign pathogens, immune cells are involved in the normal physiology of metabolic organs and in the pathogenesis of metabolic disorders. In AT, several cells have been identified as promoters of insulin resistance - among them “M1” polarized macrophages (31), B cells (30), $CD4^+$ T_H1 cells, and $CD8^+$ T cells (31, 95); while other immune cells have been identified as insulin sensitizers - as is the case for “M2” polarized macrophages (87), $CD4^+$ T_H2 cells, T regulatory cells (92), and eosinophils (73-75). Recent studies by Wu *et al.* demonstrated that eosinophils sustain alternative activation of AT macrophages and contribute to improved glucose tolerance and insulin sensitivity in mice (73). These findings demonstrated that the inflammatory, insulin resistant AT in obese mice has a reduction in eosinophils, suggesting that eosinophils help maintain AT homeostasis. Additionally, IL-5 transgenic mice, with global elevations in eosinophils, are protected from HFD-induced obesity and insulin resistance. In subsequent work, Molofsky *et al.* demonstrated that ILC2 cells are responsible for producing IL-5, which recruits and sustains the eosinophils in the AT (74). Such findings encouraged further study by Hams *et al.*, who showed that ILC2 and NKT cells influence glucose homeostasis and body weight in HFD-fed mice by inducing and maintaining eosinophils and M2-like macrophages in visceral AT (75). Furthermore, AT eosinophils produce IL-4 and ILC2 cells produce IL-13 (73, 74). Thus, in AT, eosinophils and ILC2 cells are thought to coordinate a homeostatic type-2 immune environment that maintains an insulin sensitive state.

There is a short list of published work addressing the role of eosinophils in AT inflammation thus far, however it is interesting to consider and compare the metabolic phenotypes seen in their models (metabolic improvements (73)) with that of our previous report (no metabolic improvements (43)) (Figure 3.12). There are two primary differences between the studies: the systemic tissue distribution of eosinophils and localization of eosinophils to specific regions within AT. First, the studies by Wu *et al.* used IL-5-overexpressing mice, which have systemic elevations in eosinophils (73, 74). While one of the major metabolic phenotypes seen in their model was in the AT and attributed to AT eosinophils, a role for eosinophils in other tissues cannot be ruled out. It is also important to note that the IL-5 transgenic mice had reduced body weight compared to controls, which could account for the improved insulin sensitivity. In the current study, we demonstrate that the CCR2$^{-/-}$ mouse is a model of peritoneal and AT-specific eosinophil accumulation, as excess eosinophils were not detected in the bone marrow, blood or other tissues examined (Fig. 3.2 & 3.7). Systemic versus AT-specific eosinophil accumulation may therefore be a cause of the different metabolic phenotypes in the two studies. Of note, not all sites prone to eosinophil accumulation were assessed, including the GI tract, lung, and thymus; several of these tissues were examined in subsequent studies using different models, and will be discussed in Chapters 4 & 5.

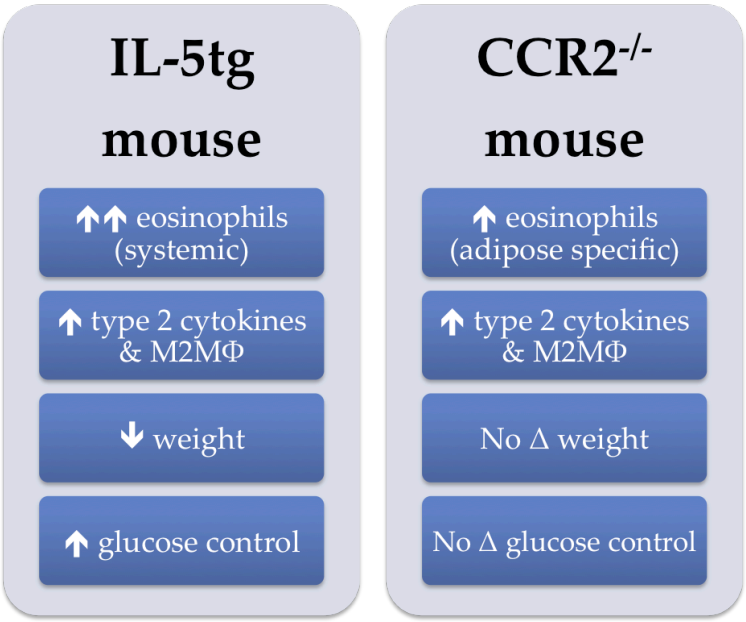

Figure 3.12. Comparison of the IL5tg hypereosinophilic mouse with the CCR2$^{-/-}$ mouse. While IL5tg mice have massive systemic hypereosinophilia, CCR2$^{-/-}$ have moderate eosinophilia that is at least partially specific to AT. CCR2$^{-/-}$ eosinophilia was not observed in other tissues examined (i.e. bone marrow, blood, spleen, or liver). In contrast to IL5tg mice, CCR2$^{-/-}$ mice on a HFD have no difference in body weight or glucose tolerance compared to wildtype controls.

Second, differential localization of eosinophils within the AT could be an important indication of their function. Our data showed that while in WT mice eosinophils were only seen in interstitial spaces, in CCR2$^{-/-}$ mice eosinophils localized both interstitially and to CLSs. In fact, in obese CCR2$^{-/-}$ mice ~8% of the CLS cell milieu were eosinophils. It is established that AT macrophages in CLSs are M1-like, pro-inflammatory, and induce insulin resistance (42, 87); while AT macrophages in interstitial spaces are M2-like, anti-inflammatory, and protect from insulin resistance (42, 87). It would be intriguing for future studies to determine whether AT eosinophil function also varies depending upon localization within the tissue. It is important to note that the novel and surprising finding of eosinophils in CLSs of CCR2$^{-/-}$ mice correlated with a reduction in both the absolute number and percent of macrophages in CLS. This reduction in CLS macrophages could be due to the absence of CCL2-mediated recruitment in

CCR2$^{-/-}$ mice. An alternative explanation could be that CLS-eosinophils reduce accumulation of macrophages. Also unknown is whether interstitially spaced eosinophils produce basal levels of mediators beneficial to AT homeostasis, while CLS eosinophils may release some of their more potent inflammatory agents *i.e.* MBP, EPO, TNF-α, etc. Implications of AT eosinophil localization were further discussed in a commentary written by editors of the *Journal of Leukocyte Biology*, in response to (and paired with) our publication (96).

Findings from our current study, integrated with recently published work, now suggest that AT eosinophil number alone is not sufficient to determine the effect on insulin resistance. Context dependent eosinophil function will need to be more critically examined in future studies, in acknowledgment of the newly forming dogma that eosinophils are multi-functional cells that can impart either destructive or restorative effects (71, 72, 97). In addition, this comparison elicits further investigation to separate a potential therapeutic effect of increased levels of IL-5 and/or eosinophils outside of the AT on metabolism and glucose tolerance.

Our data point to at least two mechanisms for altered eosinophil content in AT of CCR2$^{-/-}$ mice. First, we demonstrate that genes such as *Epx*, *Prg2*, and *Il5ra* were increased during the differentiation process in bone marrow cells lacking intrinsic CCR2 expression, although numerical yield of eosinophils did not differ. Eosinophils express CCL2 and eotaxin, both of which can interact with the CCR2 receptor (45, 98, 99). Thus a lack of the receptor in CCR2$^{-/-}$ bone marrow progenitors may inhibit auto-regulation of differentiation, accounting for the

greater expression of certain eosinophil genes. Second, we found a strong positive correlation between expression of *Il5* in AT and levels of eosinophils in both genotypes. ILC2s were recently shown to produce *Il5* in AT that then modulated the accumulation of eosinophils (74). If the same mechanism is at play, our data suggest that CCR2 deficiency increases production of IL-5 by ILC2s and/or the numbers of these cells, leading to increased recruitment of eosinophils. This hypothesis remains to be tested but could provide interesting insights into the biology of the newly discovered ILC2s.

In addition to AT, a role for resident eosinophils in homeostasis has been reported in a variety of tissues. Eosinophils have been shown to regulate tissue damage in the lung (46) and liver (100), epidermal wound healing (48), the onset and duration of estrus in the uterus (49), mammary gland development (50), and GI tract remodeling (51). Each of these processes involves angiogenesis, fibrin/collagen deposition, and/or cell turnover; all of which can be specifically regulated by eosinophils and are also key processes in AT homeostasis. These environments also possess a unique milieu of local stimuli that likely generate specific eosinophil phenotypes. This notion is supported by the LIAR hypothesis, mentioned in Chapter 1, that suggests "eosinophils are actually regulators of *L*ocal *I*mmunity *A*nd*/*or *R*emodeling*/R*epair in both health and disease…(and)...accumulation occurs as part of a strategy(ies) to maintain tissue homeostasis." (72). It is plausible that resident eosinophils assist in maintaining AT function based on local environmental signals, which ultimately affects the state of insulin resistance both locally and systemically.

Our data show that AT eosinophil accumulation in CCR2$^{-/-}$ mice occurs concomitantly with elevated expression of the classical type-2 cytokines, *Il4*, *Il5*, and *Il13*, and macrophage M2-like polarization (Fig. 3.2, 3.9, & 3.11). Our results regarding AT macrophage polarization in CCR2$^{-/-}$ mice are similar to previous reports. For instance, studies utilizing CCR2 inhibitors have shown decreased M1 and increased M2 polarization of AT macrophages (101). In contrast, Weisberg *et al.* also demonstrated increased inflammatory genes, but did not report whether there were changes in M2 markers (36). Likewise Ito *et al*. also reported an increase in expression of *Itgax* and *Tlr4*, but did not see any changes in the M2 markers, *Mrc1* or *CD163* (102). Thus there are multiple bodies of work reporting altered macrophage polarization associated with the modulation of CCR2. However the mechanism for this polarization has yet to be defined. We are the first to demonstrate increased AT eosinophil number in CCR2$^{-/-}$ mice, and thus we suggest eosinophils may account for the previously unexplained mechanism of macrophage polarization in CCR2$^{-/-}$ mice. Future studies may now test whether the maintained M2-like phenotype of AT macrophages in CCR2$^{-/-}$ mice is due to the increased eosinophils or to the systemic absence of CCR2 signaling.

Several studies have demonstrated that CCR2$^{-/-}$ mice have a pronounced type-2 polarization (84, 86); however to date, the function of CCR2 in this context has not been fully delineated. Furthermore, to our knowledge there is no previous evidence that has linked CCR2 deficiency to eosinophilia or to any hypereosinophilic diseases. Thus, because of the advanced stages in the

development of several CCR2 antagonists as drugs against atherosclerosis, arthritis and autoimmune disease (103), it is worthwhile to consider eosinophilic hyperplasia and tissue accumulation as a likely side effect of these therapies that could be beneficial or detrimental depending upon the context in which the drugs are administered. Eosinophilia has several clinical implications including the response against helminthic parasite infections (104), in which an over-active type-2 response would promote resistance towards infection. In fact, $CCR2^{-/-}$ mice were recently found to be resistant to infection by the helminthic parasite *Trichuris muris* (105), suggesting a therapeutic potential for the inhibition of CCR2 in fighting parasitic infections. Conversely, deficiency of CCR2 was shown to promote infection in the lung by the dimorphic fungus *Histoplasma capsulatum* due to increased IL-4 levels and an increased type-2 response (86). Thus, depending on the pathogen and/or the clinical condition of the affected patient, CCR2 inhibition may improve or worsen the infection. It is also important to note that a hypereosinophilic state has been shown to either promote or arrest several tumors and cancers (106, 107). Clearly, altered eosinophil content can impart a plurality of effects for a diverse range of diseases, which demands further study to understand the nuances of eosinophil function.

In summary, in this study we demonstrate that CCR2 deficiency leads to increased eosinophil number, alternative macrophage activation, and type-2 cytokine expression in white AT. CCR2 and its ligand CCL2 have been heavily studied in the context of AT inflammation during obesity, leading to conflicting results and conclusions. Several studies have shown CCR2 deficiency or

antagonism to have a protective effect on AT inflammation and insulin resistance (36, 42, 43, 87, 101, 102, 108), but have focused on decreased number of recruited macrophages to AT as the explanation. Additionally, many of these studies have shown “M2” macrophage polarization as a result of CCR2 deficiency or inhibition, without a corresponding mechanism for this observation. The current study provides a link between the newly discovered role of eosinophils in sustaining alternative macrophage activation (73, 74) and the enigmatic consequences of CCR2 deficiency/inhibition on AT macrophages and inflammation. Additionally, we now present a model of localized increases in AT eosinophils that could be utilized in future studies to distinguish the effects of AT-specific eosinophil accumulation versus systemically elevated eosinophils on metabolism.

CHAPTER IV

RESTORING OBESE ADIPOSE EOSINOPHILS TO LEAN ADIPOSE LEVELS VIA RIL5 ADMINISTRATION IS NOT SUFFICIENT TO REGAIN METABOLIC FITNESS

(Adapted from Bolus, *et al.*, to be submitted to *Molecular Metabolism*, 2017)

Introduction

Eosinophils are fascinating immune cells classically associated with clearing parasitic infections and mediating immune reactions such as allergy and asthma. The characteristic appearance of an eosinophil is marked by its multi-lobular nucleus and granule-rich cytoplasm. Like many leukocytes, eosinophils develop in the bone marrow and migrate through the blood to infiltrate tissues in response to potent cytokines and chemokines such as eotaxin 1, 2, & 3; IL-5; GM-CSF; and RANTES (45). Eosinophils can synthesize an array of chemokines, cytokines, and lipid mediators; aiding in their ability to regulate tissue damage (46, 47), wound healing (48), the onset of estrus (49), mammary gland development (50), GI tract remodeling (51), and T-cell proliferation, polarization, and apoptosis (52, 53). Thus, eosinophils are versatile immune cells that contribute to their local environment in a tissue-specific manner.

Perhaps one of the most intriguing new roles identified for eosinophils is their influence on whole-body metabolic fitness by regulating AT health. The presence of eosinophils in AT was first discovered in 2011 by Wu *et al* (73). In this seminal paper, an eosinophil-deficient mouse model (ΔdblGATA) was more

susceptible to weight gain on a high fat diet, had impaired systemic glucose tolerance, greater AT insulin resistance, and less M2-like anti-inflammatory macrophages; all potentially signs of AT dysfunction. In contrast, hypereosinophilic IL-5tg mice had reduced weight and improved glucose tolerance. Since this striking finding, a series of papers have further elucidated the role of eosinophils in AT (74, 75, 109-111). It has been shown that eosinophils accumulate in AT in response to IL5 produced by ILC2 cells when activated by IL33 and/or IL25. AT eosinophils can then produce IL4 and/or IL13 to yield a more M2-like polarization of the macrophage pool, which is typically associated with better AT health.

To date, interventional studies have targeted eosinophils via non-specific means (e.g. helminth infection, IL25/IL33 injections, cold-exposure) (73-75, 109-111), which do increase eosinophils but also alter a cascade of upstream or off target immune reactions. Thus, making it difficult to definitively conclude eosinophils are responsible for the improved metabolic fitness observed. Studies that directly targeted eosinophils were genetic mouse models that exhibit altered eosinophil content throughout gestational and post-natal development, and thus it is difficult to determine if metabolic improvements were developmental in origin. Our current study aimed to determine whether directly normalizing AT eosinophils via rIL5 injections in obese mice, after normal development has occurred, would have a similar effect (i.e. improved metabolic fitness) as seen in previous models that did not control for these factors. AT eosinophils of obese mice were successfully restored to levels of lean mice with rIL5 treatment, but

none of the metabolic improvements seen in other hypereosinophilic models were observed. Thus, we conclude that emerging paradigms suggesting eosinophils improve AT function, and thus systemic metabolic health, will need further study to fully understand the role of eosinophils in metabolic disease.

Results

Eosinophil levels in AT and various other tissues of rIL5 injected mice.

Male C57BL/6J mice were fed either chow or HFD for 8 weeks and simultaneously injected twice weekly with rIL5 protein as depicted in Fig. 4.1A. AT eosinophils were identified as $CD45^{+}$, $F4/80^{lo}$, $CD11b^{lo}$, $SiglecF^{+}$ (Fig 1B), as previously reported (44, 73). Replicating the literature, we report the percent eosinophils in AT declines with increased body weight; slope = -0.96, R^2 = 0.75 (Fig. 4.1C). Despite the decline in AT eosinophils with weight gain on HFD (Fig. 4.1D), eosinophils of obese mice injected with rIL5 are increased compared to vehicle injected controls, representing a physiological restoration to AT eosinophil percentages and numbers observed in lean mice (Fig 1D & E). In both circulating blood and at the site of eosinophil origin in the bone marrow, eosinophils are not increased with rIL5 (Fig. 4.1F). In the liver, another metabolically relevant tissue to obesity, there was no change in the amount of eosinophils (Fig. 4.1F). However, another eosinophil-prone tissue, the intestine, showed 3x-fold increased eosinophils from rIL5 injection; P = 0.0298 (Fig. 4.1F). Slight changes in some other immune cell populations were observed in blood and liver, but not bone marrow or intestine (Fig. 4.2).

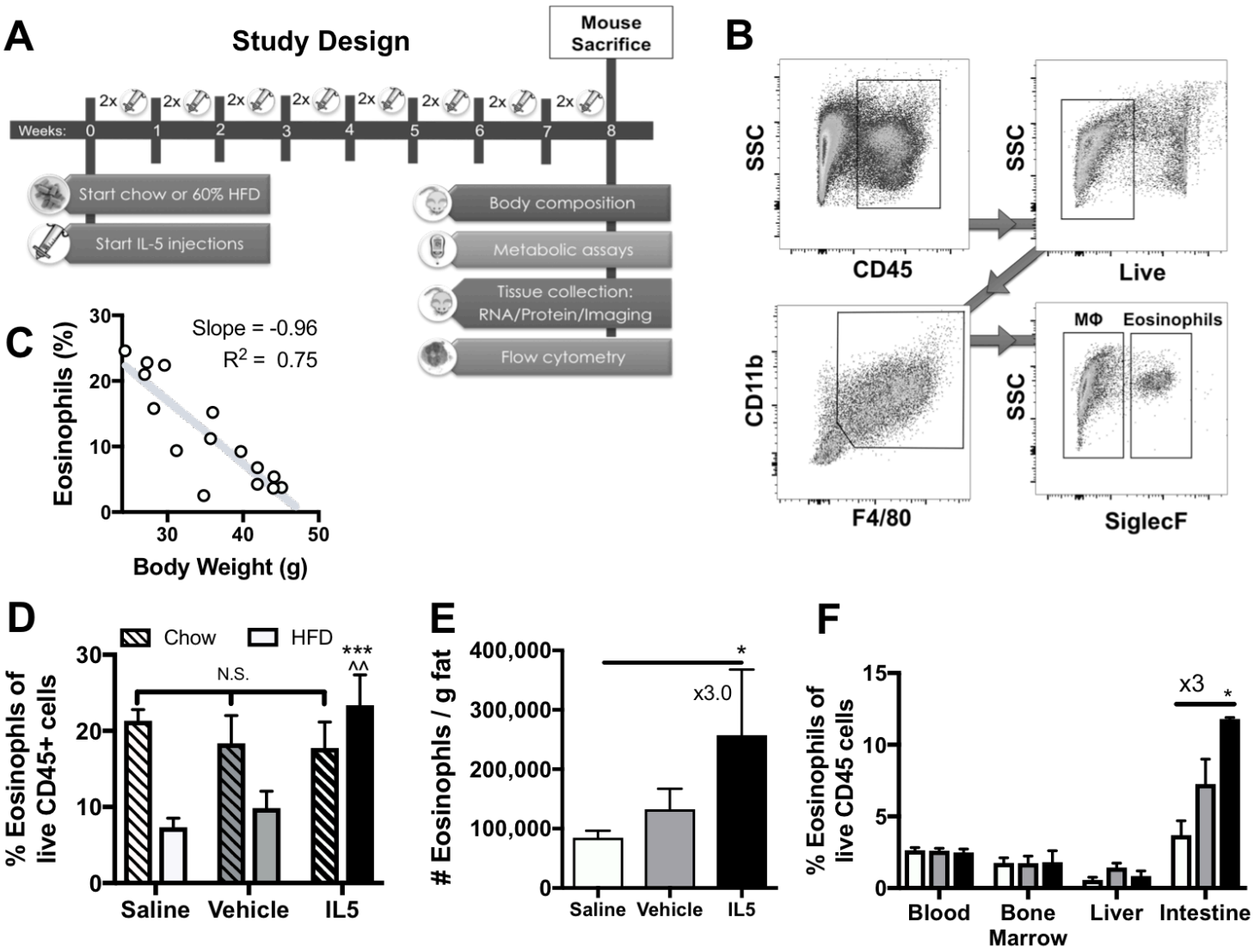

Figure 4.1 Eosinophil levels in AT and various other tissues of rIL5 injected mice.

(A) Male C57BL/6J mice were fed either chow or HFD for 8 weeks and simultaneously injected twice weekly with rIL5 protein. **(B)** Flow cytometry gating strategy for eosinophils (CD45+, live, F4/80^{lo}, CD11b^{lo}, SiglecF^{+}) and macrophages (CD45+, live, F4/80^{hi}, CD11b^{hi}, SiglecF^{-}). **(C)** Percent AT eosinophils negatively correlate with body weight (slope = -0.96, R^2 = 0.75). **(D)** Treatment with rIL5 elevates AT eosinophils in HFD-fed mice, compared to saline and vehicle controls, back to chow-fed levels [n=4-11]. **(E)** Number eosinophils per gram AT are increased in rIL5 treated mice compared to control [n=3-7]. **(F)** No difference in percent eosinophils in blood, bone marrow, or liver of rIL5 treated mice, but intestine does show an increase [n=2-8].

Data are shown as means ± SEM.

AT = adipose tissue; HFD = high fat diet.

Key: chow = hashed bars; HFD = open bars; saline = white; vehicle = grey; rIL5 = black

*P < 0.05, compared to saline; ***P < 0.0005, compared to saline; ^^P < 0.005, compared to vehicle.

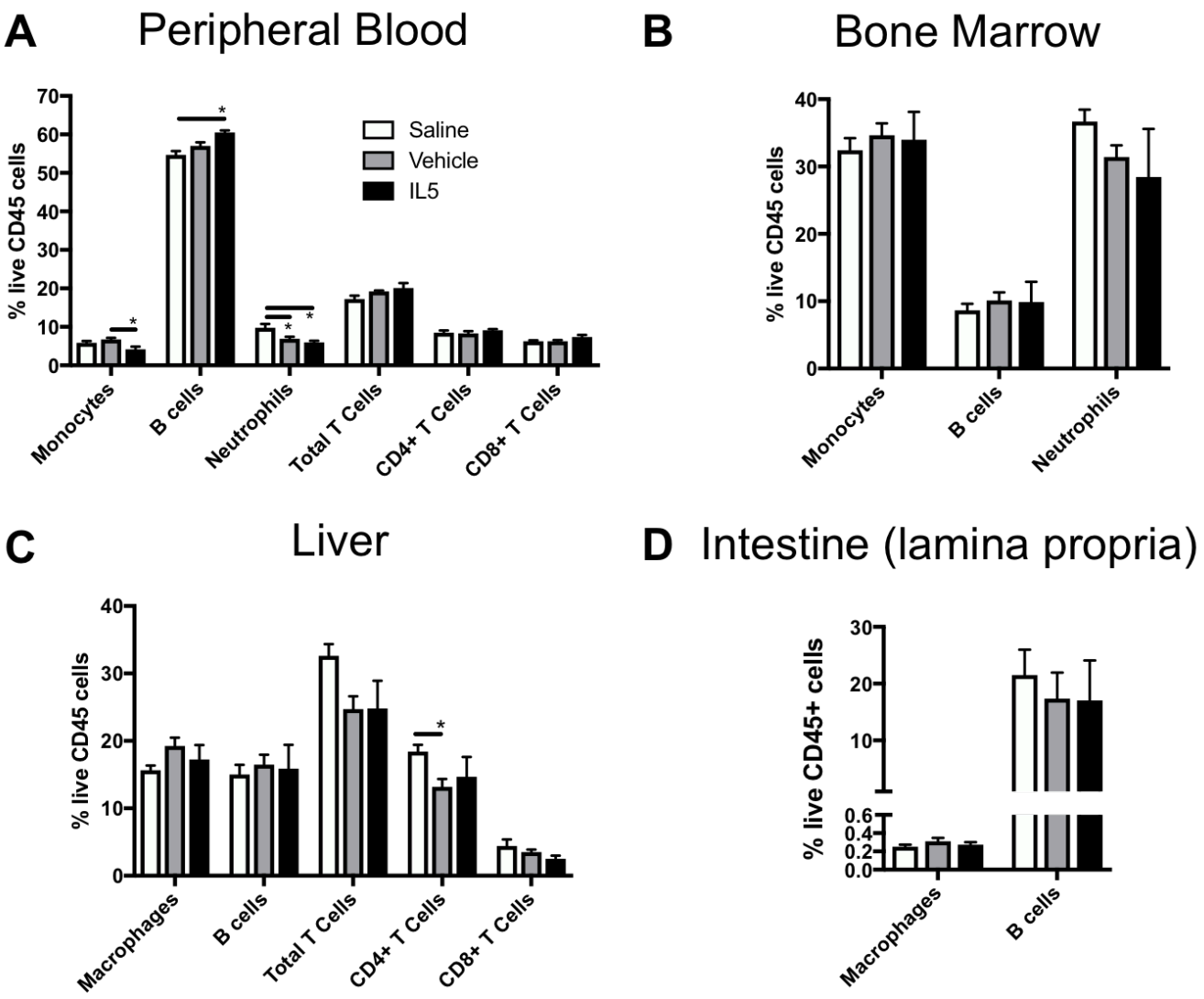

Figure 4.2 Leukocyte levels in systemic and metabolic tissues of rIL5 injected mice.

Male C57BL/6J mice were fed HFD for 8 weeks and simultaneously injected twice weekly with rIL5 protein. Percent monocytes, macrophages, B cells, neutrophils, Total T cells, CD4 T cells, and/or CD8 T cells were measured in **(A)** peripheral blood, **(B)** bone marrow, **(C)** liver, and **(D)** intestine.

Data are shown as means ± SEM.

HFD = high fat diet.

Key: saline = white; vehicle = grey; rIL5 = black

*$P < 0.05$

Inflammatory profile of obese AT with elevated eosinophils.

The typical eAT inflammation associated with moderate obesity was seen in both Saline and Vehicle controls, with classic crown-like structures of macrophages encompassing dead or dying adipocytes (Fig. 4.3A). AT of rIL5 treated mice retain macrophages, but now eosinophils are much more visually apparent throughout the tissue (Fig. 4.3A). In addition to cell surface markers (F4/80+ macrophages, SiglecF+ eosinophils), these cell types can be further verified via nuclear morphology with a spherical nucleus in macrophages and a donut-shaped or multi-lobed nucleus in eosinophils. There was no significant difference in the percent macrophages (Fig. 4.3B) or protein expression of proinflammatory M1-like marker, MHCII (Fig. 4.3C), in the eAT stromal vascular fraction as assessed by flow cytometry. Likewise, whole eAT gene expression analysis of macrophage marker, *Adgre1* (F4/80), was not statistically different between groups (Fig. 4.3D). An assortment of macrophage polarization genes, including proinflammatory M1-like markers (*Tnf, Il1β*), metabolically active Mme markers (*Tnf, Il1β, Plin2, Abca1*), and anti-inflammatory M2-like markers (*Clec10a, Arg1, Retnla, Chil3*) showed no difference with vehicle- or rIL5-treatment (Fig. 4.3D).

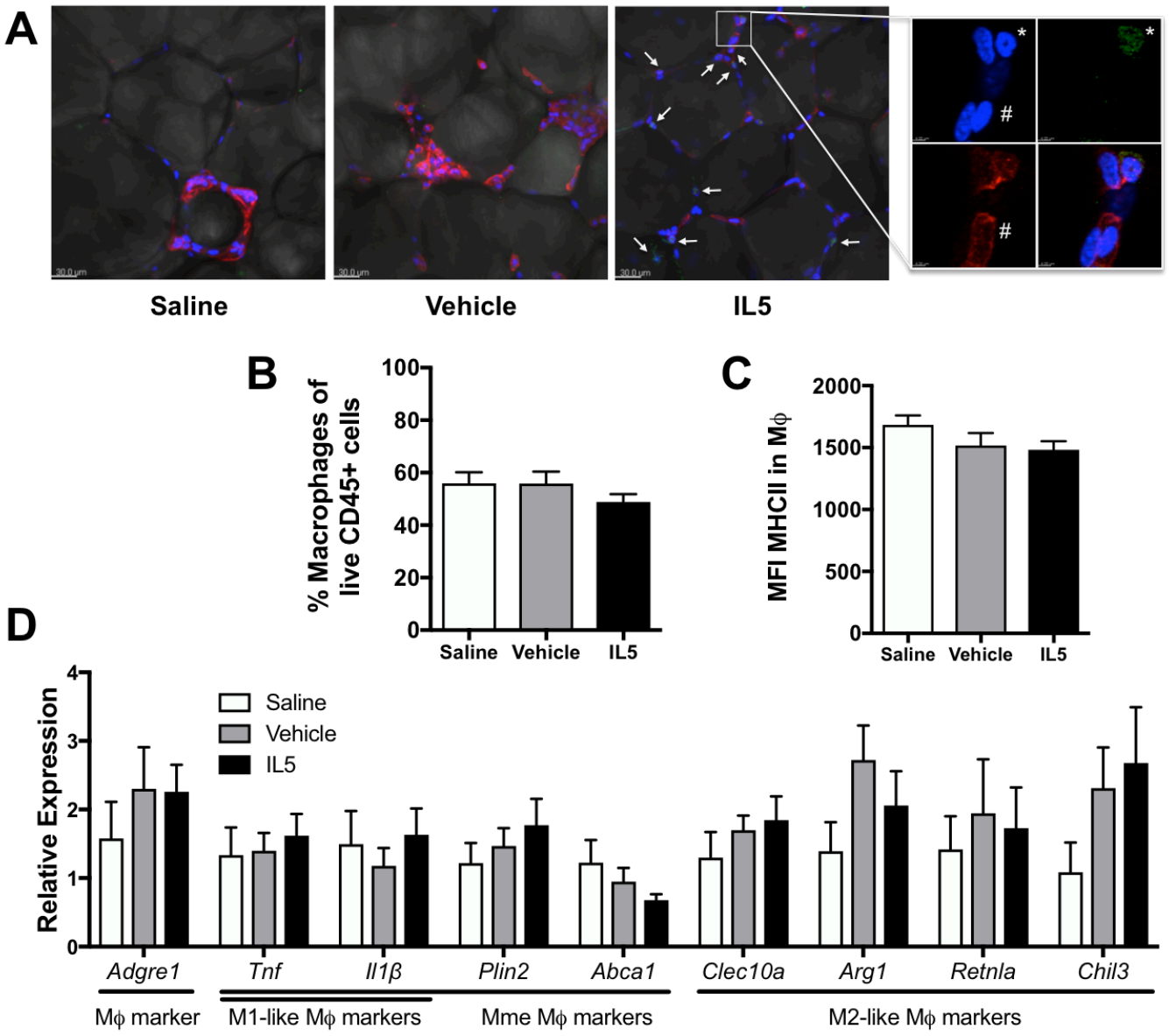

Figure 4.3 Inflammatory profile of obese AT with elevated eosinophils.
(A) Representative 40x images of eAT from HFD-fed obese mice treated with saline, vehicle, or rIL5. Macrophages (red, F4/80) are seen in abundance in all groups, whereas eosinophils (green, SiglecF) are increased in rIL5 treated mice. Magnified view shows the donut-shaped nucleus (*) of eosinophils juxtaposed to the spherical nucleus (#) of macrophages [n=3]. **(B)** Treatment with rIL5 does not alter percent eAT macrophages or **(C)** protein expression of proinflammatory marker MHCII [n=6-11]. **(D)** Gene expression analysis of macrophage marker, *Adgre1* (F4/80), and an array of macrophage polarization genes were not statistically different between groups in eAT [n=6-8].
Data are shown as means ± SEM.
AT = adipose tissue, HFD = high fat diet.
Key: saline = white; vehicle = grey; rIL5 = black

Weight gain, body composition, and glucose tolerance in mice with elevated AT eosinophils.

Mice were challenged with HFD and simultaneously given rIL5 injections to determine if restored adipose eosinophils would reduce weight gain, modulate body composition, and/or improve glucose tolerance. Typical of diet-induced obesity, vehicle HFD-fed mice gained more weight (~7 g) than their vehicle chow-fed counterparts (Fig. 4.4A-B). However, rIL5 did not reduce the total weight gain in mice on HFD (Fig. 4.4B). Likewise, vehicle-treated mice gained proportionally more fat mass while on HFD than chow-fed, but rIL5 did not blunt this effect (Fig. 4.4C-D). Specifically, epididymal AT (eAT) and subcutaneous AT (sAT) expanded in mass equally vehicle- and rIL5-treated mice while on HFD, with no difference in liver weight at this duration of diet (Fig. 4.4E). Glucose tolerance tests showed an expected impairment of both fasting blood glucose and systemic glucose tolerance in HFD-fed mice compared to chow-fed mice, but the increased AT eosinophils from 8 weeks of rIL5 injections did not improve glucose tolerance (Fig. 4.4F).

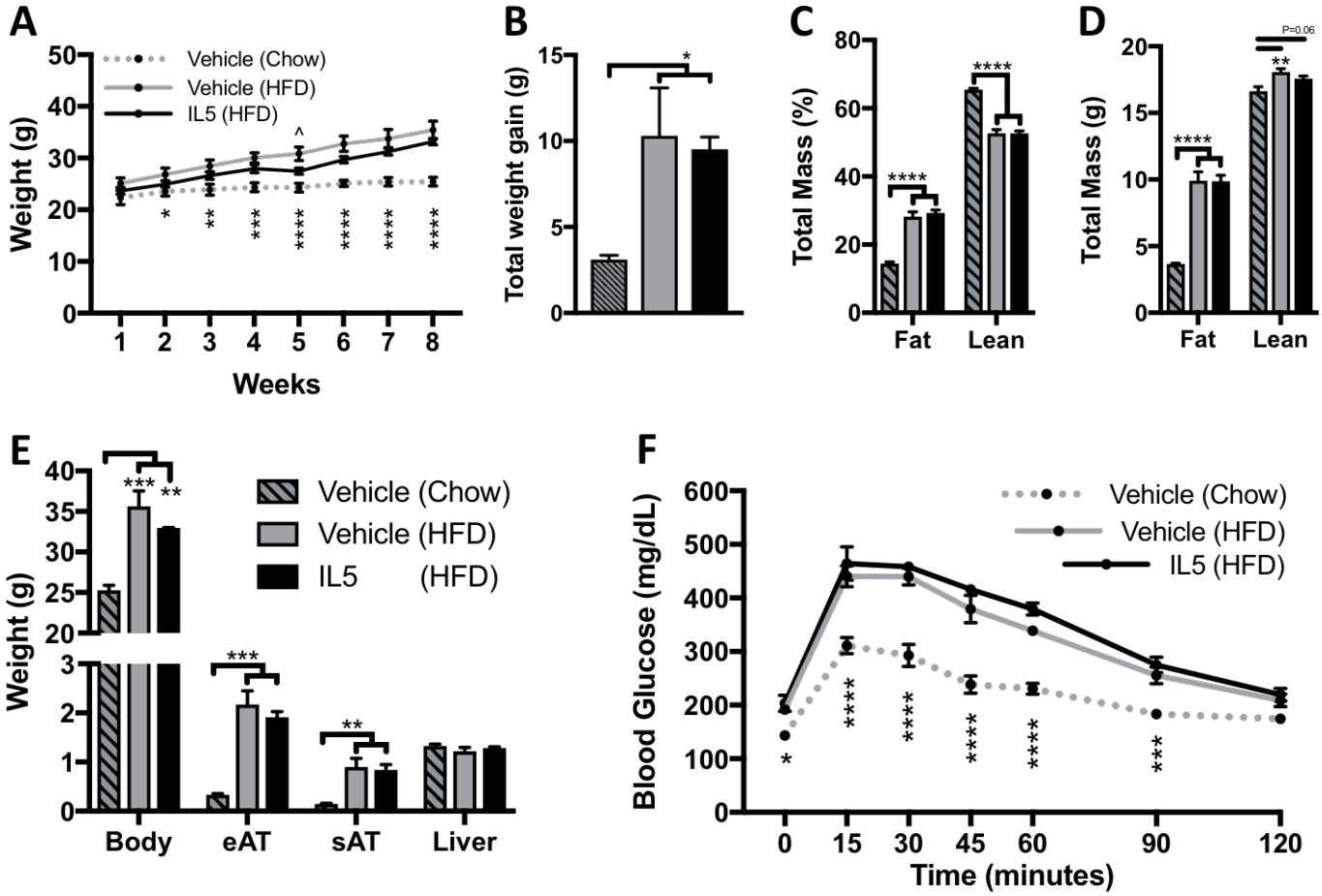

Figure 4.4 Weight gain, body composition, and glucose tolerance in mice with elevated AT eosinophils.

(A) HFD-fed mice gained more weight over 8 weeks compared to chow, with no difference in **(B)** total weight gained between vehicle or rIL5 treated mice [n=4]. HFD-fed vehicle and rIL5 treated mice have equally altered total fat and lean mass by **(C)** percent or **(D)** grams at study completion [n=4-12]. **(E)** HFD-fed mice have increased body, eAT, and sAT weight, but no further difference with rIL5 [n=4]. **(F)** Glucose tolerance is impaired by HFD-feeding, but not rescued by rIL5 treatment [n=4].

Data are shown as means ± SEM.

AT = adipose tissue; HFD = high fat diet; eAT = epididymal AT; sAT = subcutaneous AT.

Key: chow = hashed bars, dotted lines; HFD = open bars, solid lines; vehicle = grey; rIL5 = black

*P < 0.05, compared to chow; **P < 0.005, compared to chow; ***P < 0.0005, compared to chow; ****P < 0.0001, compared to chow; ^P < 0.005, compared to vehicle.

Triglyceride tolerance in mice with elevated AT eosinophils.

Fasted mice were challenged with an oral gavage of fats (i.e. olive oil) to determine whether increased eosinophils impact AT function by changing uptake of dietary fats. Following fat gavage, plasma TG peaked between 2-3 h in both vehicle- and rIL5-treated mice, with a slight non-significant trend towards rIL5 mice peaking and clearing quicker (Fig. 4.5A). Plasma FFAs also peaked at ~2 h in both groups (Fig. 4.5B). There was no difference in blood glucose (Fig. 4.5C) or plasma cholesterol (Fig. 4.5D) between groups.

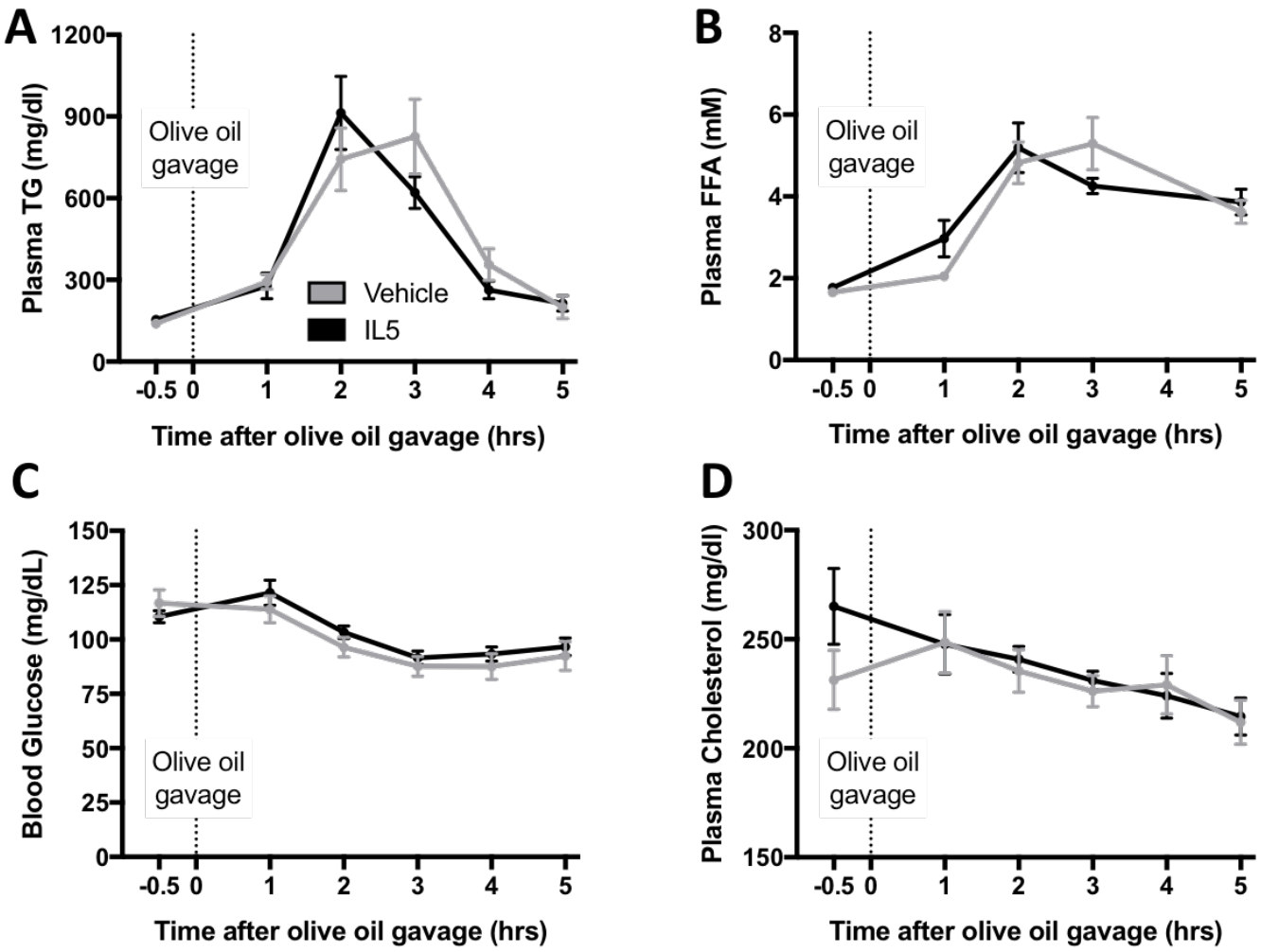

Figure 4.5 Triglyceride tolerance in mice with elevated AT eosinophils.
Fasted HFD-fed mice treated with vehicle or rIL5 for 8 weeks were given a bolus of triglycerides (i.e. olive oil) and showed no difference between groups in **(A)** plasma (TG) [n=8] **(B)** plasma FFA [n=4] **(C)** blood glucose [n=8] **(D)** or plasma cholesterol [n=8] over the course of 5 h.
Data are shown as means ± SEM.
HFD = high fat diet; TG = triglycerides; FFA = free fatty acids.
Key: vehicle = grey; rIL5 = black

Metabolic parameters of rIL5 treated mice during a mixed-meal test.

Fasted mice were given access to HFD *ad libitum* for 3 h to determine any differences in food consumption or metabolic parameters in response to elevated AT eosinophils. Both groups consumed the same amount of food, ~0.65 g, during the first 3 h of refeeding (Fig. 4.6A). Upon refeeding, blood glucose levels increased and peaked at 0.5 h with a slow decline thereafter, but with no difference in mice with increased AT eosinophils compared to control (Fig. 4.6B). Correspondingly, insulin levels increased alongside glucose levels (Fig. 4.6C). Similar to the TG tolerance test (Fig. 4.5), both TGs (Fig. 4.6D) and FFAs (Fig. 4.6E) took several hours to peak and then returned to baseline by the last time point (3 h), but with no difference in groups. Plasma cholesterol did not vary between groups (Fig. 4.6F). There were no differences in basal fasting levels of any of the metabolic parameters measured (Fig. 4.6).

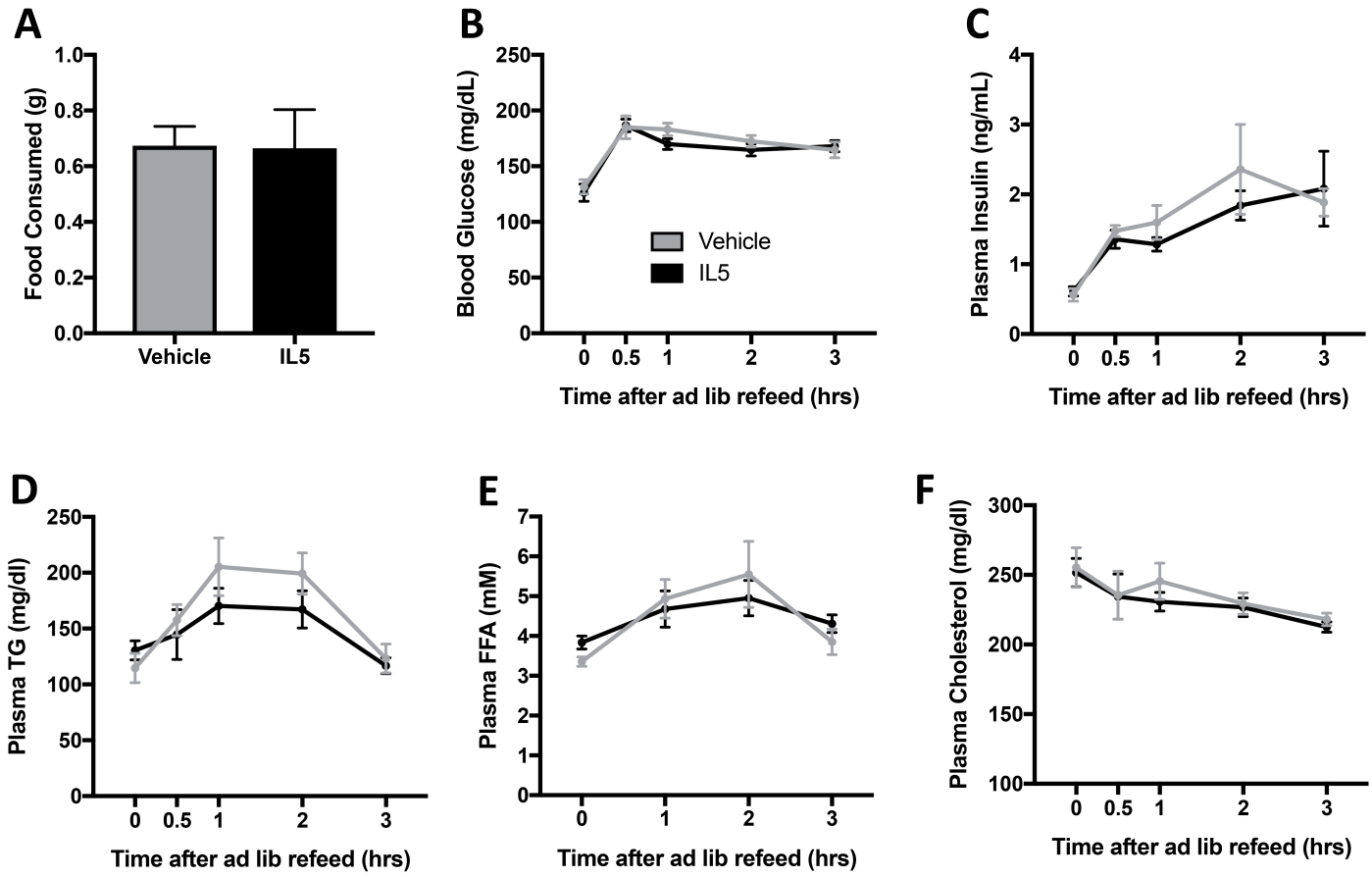

Figure 4.6 Metabolic parameters of rIL5 treated mice during a mixed-meal test.

HFD-fed mice treated with vehicle or rIL5 for 8 weeks were fasted and then allowed access to HFD *ad libitum* for 3 h. **(A)** Both groups consumed the same amount of food [n=6-7]. **(B)** A spike in blood glucose occurred at 0.5 h following refeeding with no difference between groups [n=6-7]. **(C)** Insulin also spiked at 0.5 h and then held relatively steady in both groups [n=6-7]. Plasma **(D)** TG [n=6-7], **(E)** FFA [n=4], and **(F)** cholesterol [n=5-7] do not vary between groups upon refeeding.

Data are shown as means ± SEM.

HFD = high fat diet; TG = triglycerides; FFA = free fatty acids

Key: vehicle = grey; rIL5 = black

****$P < 0.0001$, compared to vehicle.

Insulin signaling in AT with elevated eosinophils.

The ratio of phosphorylated AKT (pAKT) to total AKT was assessed as a readout of tissue-specific insulin sensitivity. As expected, the ratio of pAKT/AKT from AT was increased in vehicle-treated mice upon insulin stimulation (Fig. 4.7A-B). Though the AT pAKT/AKT ratio from rIL5-treated mice also increased with insulin stimulation, there was no difference compared to control (Fig. 4.7A-B).

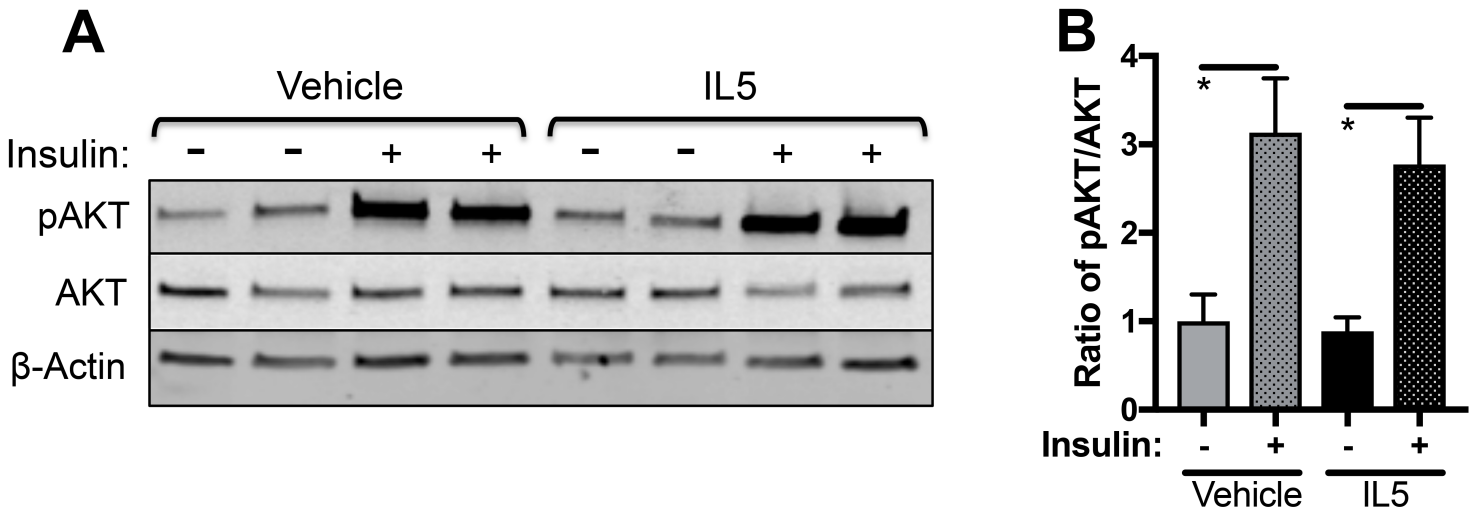

Figure 4.7 Insulin signaling in AT with elevated eosinophils.
(A) Representative western blots of eAT showed an increase in the ratio pAKT/AKT upon insulin stimulation in HFD-fed mice that received vehicle or rIL5 for 8 weeks. **(B)** Quantification of western blots revealed no difference in the eAT insulin signaling response via pAKT/AKT between vehicle and rIL5 treated mice.
Data are shown as means ± SEM.
eAT = epididymal adipose tissue; HFD = high fat diet.
Key: vehicle = grey; rIL5 = black; insulin injected = dotted bars; no-insulin saline control injection = open bars
*$P < 0.05$, compared to no insulin stimulation.

Cold challenge: energy balance in mice with elevated eosinophils.

Mice were individually housed in metabolic cages to measure an array of sensitive physiological parameters for 4 days. The second half was spent in 4^{o}C to determine any differences in energy balance while under a demanding stress on AT function. The average daily body weight was similar between vehicle- and rIL5-treated mice (Fig. 4.8A). Average daily food intake (Fig. 4.8B) and movement (Fig. 4.8C) was increased in the dark cycle compared to the light cycle as expected, but with no difference between groups. Even before cold induction, the respiratory quotient for both groups is closer to 0.7 than 1.0, indicative of the high fat content from the HFD being used as a primary energy source (Fig. 4.8D). Upon cold exposure, both groups continue to modulate their ratio of carbs/fats as a fuel source in the same manner with no significant differences at any time point (Fig. 4.8D). Energy expenditure fluxes were higher during the dark cycle than the light cycle for both groups equally, at both RT and cold (Fig. 4.8E). Upon cold exposure, rIL5-treated mice increase their energy expenditure to maintain body heat at the same rate as control mice (Fig. 4.8E). The amount of total body mass (Fig. 4.8F), fat mass (Fig. 4.8G), and lean mass (Fig. 4.8H) lost during cold exposure was not significantly different between groups.

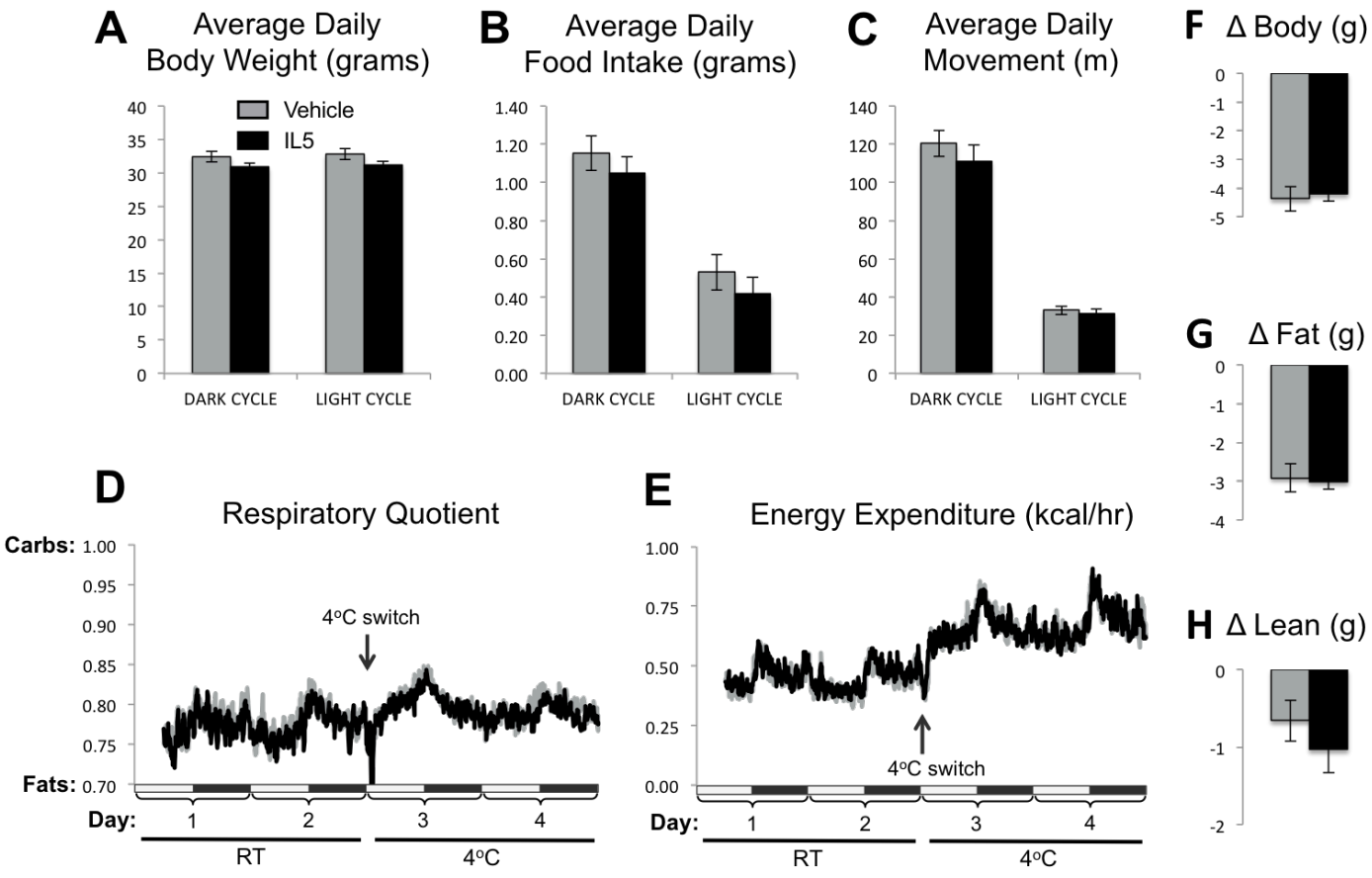

Figure 4.8 Cold challenge: energy balance in mice with elevated eosinophils.

HFD-fed mice that previously received vehicle or rIL5 for 8 weeks were individually housed in metabolic cages to measure an array of physiological parameters for 2 days at RT and 2 days at 4°C [n=8]. **(A)** Average daily body weight did not vary between vehicle and rIL5 treated mice. **(B)** Average daily food intake and **(C)** average daily movement were increased in the dark cycle compared to light cycle, but with no difference between vehicle and rIL5. **(D)** The respiratory quotient oscillated between light and dark cycles to equal degrees in vehicle and rIL5 treated mice, both during RT and the 4°C cold challenge; indicating both groups had the same energy substrate utilization. **(E)** Energy expenditure increased upon 4°C cold challenge to maintain body heat, but did not vary between vehicle and rIL5 treated mice. Both treatment groups lost the same amount of **(F)** body mass, **(G)** fat mass, and **(H)** lean mass.

Data are shown as means ± SEM.

RT = room temperature, set at 21°C; HFD = high fat diet.

Key: vehicle = grey bars/lines; rIL5 = black bars/lines.

Cold challenge: beiging capacity of white AT with elevated eosinophils.

AT of mice subjected to 48 h 4^{o}C cold exposure was examined for indicators of beiging, the process of white AT assimilating the energy burning phenotype of brown AT. In agreement with the lost fat mass during cold exposure (Fig. 4.8G), adipocytes of both sAT and eAT were visibly smaller in cold compared to RT conditions with no obvious difference between vehicle and rIL5 treated mice (Fig. 4.9A). Eosinophil levels were examined after cold exposure because published work has shown a correlation between cold-exposure & the amount of AT eosinophils (109, 111). Indeed, sAT eosinophils increased with cold exposure (Fig. 4.9B), with a further increase in sAT eosinophils in rIL5-treated mice. Indicative of an initiated beiging response, sAT *Ucp1* gene expression was significantly increased ~307-fold in cold-exposed mice compared to RT (Fig. 4.9C); however, there was no further increase in *Ucp1* despite the increased eosinophils from rIL5. The eAT eosinophils did not increase upon cold exposure, but did respond to rIL5 with ~3.2-fold increased eosinophils (Fig 4.9B). Gene expression of *Ucp1* in eAT trended towards an increase with cold exposure but displayed no additive effect with rIL5 treatment (Fig. 4.9C).

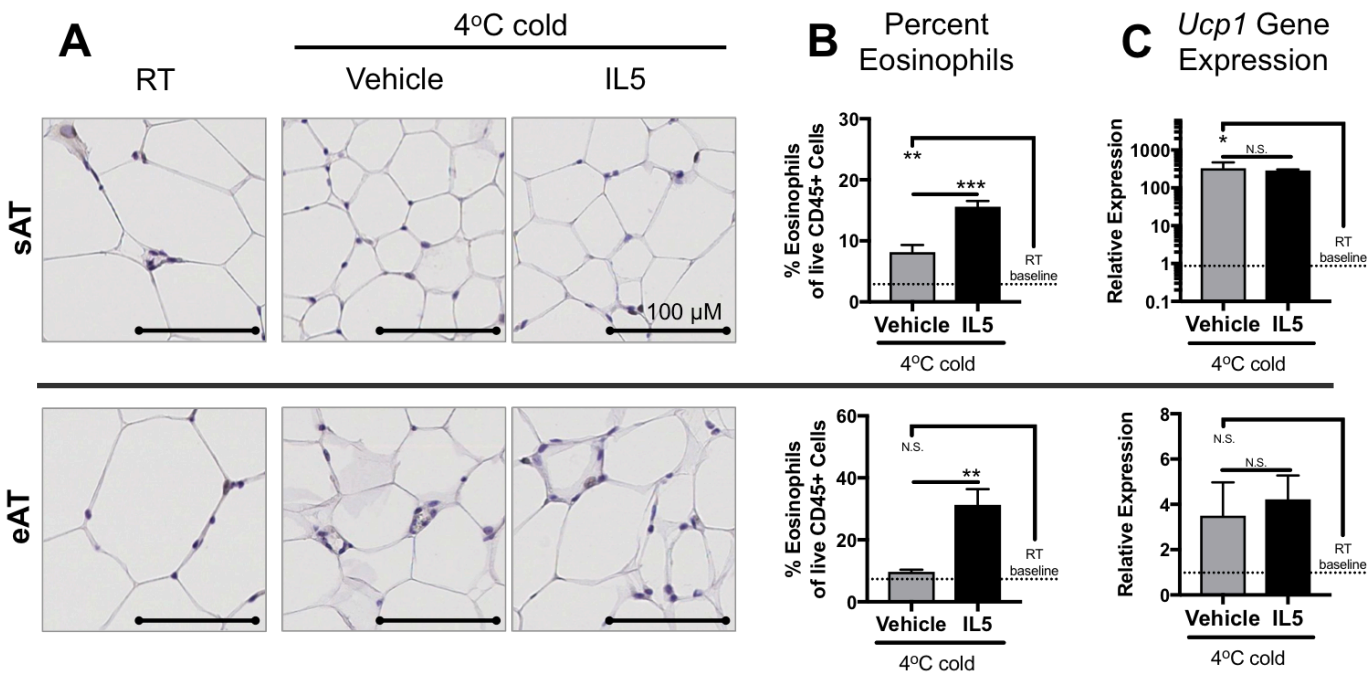

Figure 4.9 Cold challenge: beiging capacity of white AT with elevated eosinophils.

AT of HFD-fed mice that received vehicle or rIL5 for 8 weeks was examined after 2 days of RT or 4°C cold exposure. **(A)** H&E: Adipocytes from sAT and eAT were smaller in 4°C cold compared to RT conditions, with no apparent difference in vehicle versus rIL5 treated mice [n=3]. **(B)** After cold exposure, the presence of increased eosinophils was verified in sAT and eAT of rIL5 treated mice compared to vehicle controls [n=5-7]. Cold exposure alone was able to increase eosinophils in sAT but not eAT. **(C)** *Ucp1* gene expression in sAT was increased ~307-fold in the cold compared to RT, with no further increase in rIL5 treated mice [n=4-5]. *Ucp1* gene expression in eAT trended towards an increase under cold conditions, but no difference was observed between vehicle and rIL5 treated mice [n=5-7].

Data are shown as means ± SEM.

RT = room temperature, set at 21°C; HFD = high fat diet; *Ucp1* = uncoupling protein 1

Key: vehicle = grey bars; rIL5 = black bars.

Discussion

The major finding from this study was that restoring naturally occurring eosinophil numbers in AT, otherwise compromised by diet-induced obesity, is not sufficient to reestablish metabolic fitness. Administration of rIL5 was effectively used to elevate AT eosinophils during 8 weeks of HFD feeding and yet had no effect on AT inflammation, weight gain, glucose or lipid tolerance, insulin sensitivity, energy substrate utilization, energy expenditure, or AT beiging capacity. Though this set of metabolic parameters of AT health is not exhaustive, it is quite comprehensive. Thus it is unlikely an effect of restoring AT eosinophils in obese mice on metabolic output was overlooked.

These findings are perplexing in light of multiple other studies that used hypereosinophilic models to improve metabolic health (Fig. 4.10). While the studies summarized in the Introduction are supportive of AT being positively affected by eosinophils, some publications have revealed that the initial mechanism may be more dynamic or complex than originally appreciated. For instance, Qiu *et al.* argued that AT eosinophils secrete IL4/IL13 to induce macrophage expression of tyrosine hydroxylase required for catecholamine production that then beiges subcutaneous white AT (109). Beiging is typically favorable because it reduces weight and inflammation, while increasing metabolic functions such as glucose tolerance and insulin sensitivity (112). This mechanism was challenged in a multi-laboratory paper providing strong evidence that macrophages are incapable of expressing tyrosine hydroxylase and therefore can't produce catecholamines to beige white AT (113), hereby also

calling into question the upstream role of eosinophils in beiging. Separately, Brestoff *et al.* showed that while ILC2s can be stimulated with IL33 to induce AT beiging, their model was not dependent on eosinophils or IL4 signaling (114). Instead, their evidence suggested ILC2s could act directly on the adipocytes to increase UCP1 via methionine-enkephalin peptides. In our previously published work, we showed $CCR2^{-/-}$ mice have increased AT eosinophils but no reduction in fat mass or improved glucose tolerance (43, 44). Lastly, while previous studies have shown increased eosinophils correlated with M2-like macrophage polarization, an intriguing new study by Qin *et al.* demonstrates that eosinophils treated first with oxidized-LDL elicit M1-like macrophages (115); suggesting that eosinophils are capable of polarizing either M1- or M2-like macrophages depending on environmental cues.

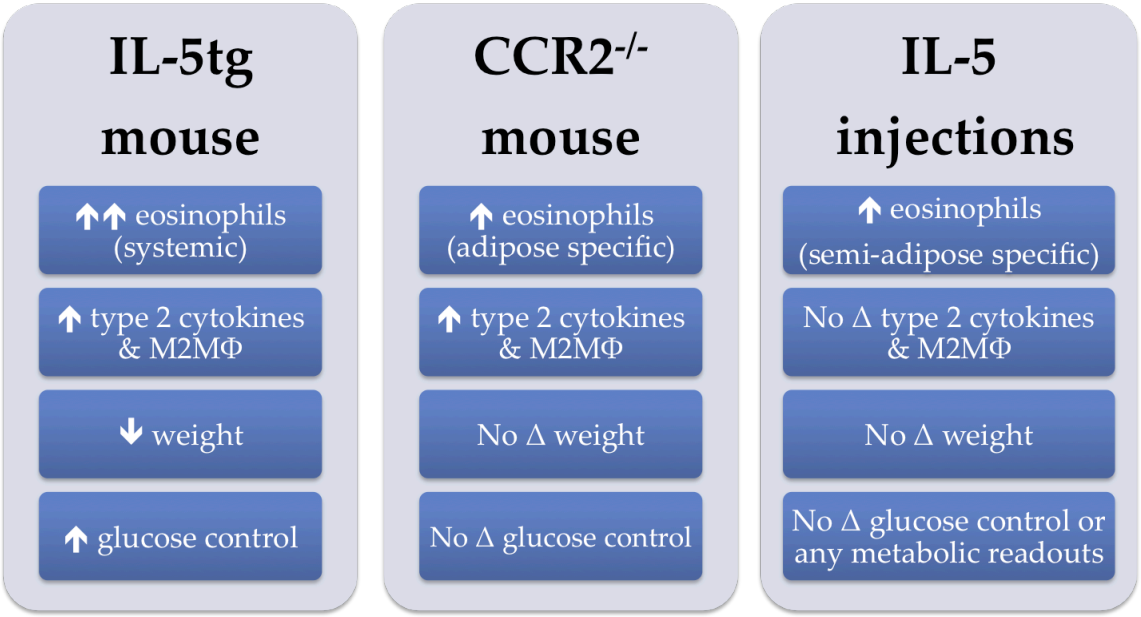

Figure 4.10. Comparison of exogenous rIL5 administration model of hypereosinophilic AT models with previous models.
Similar to the obese CCR2$^{-/-}$ mouse, injection of rIL5 increased eosinophils in AT but not bone marrow, blood, or liver. However, intestinal eosinophils were increased with rIL5 injections, which were not examined in the CCR2$^{-/--}$ mouse or the IL5tg mouse. Injections of rIL5 were associated with no change in AT type 2 cytokines, AT M2-like macrophage polarization, adipose or body weight, or glucose homeostasis, compared to control. This was now the second model to show that moderate increases in AT eosinophils was associated with no improvements in obesity or glucose homeostasis while on a HFD, which was in contrast to the first model of hypereosinophilic AT (i.e. IL5tg mouse).

While these studies do not outright undermine a role for eosinophils to positively regulate AT function and thus metabolic fitness, they do call into question the currently proposed mechanisms. Our study shows that restoring AT eosinophils in obese mice to the higher levels seen in lean mice, does not improve any of a wide range of metabolic parameters, either at the local AT level or systemically. It is our conclusion that if eosinophils are capable of improving metabolic health via AT tissue, increasing the number of eosinophils alone is not sufficient to drive such changes. Rather, the eosinophil phenotype and level of activation may also be playing a critically necessary role.

CHAPTER V

INDUCTION OF HYPEREOSINOPHILIC ADIPOSE TISSUE BY REPEATED EXPOSURE TO A FOREIGN SUBSTANCE: A ROLE FOR ALLERGY IN ADIPOSE?

Preface

Out of this dissertation work on AT eosinophils in metabolism, discussed in Chapters III and IV, has emerged an intriguing new project implicating that AT eosinophils may have a link to allergic diseases. Preliminary data for this new project was developed within the later stages of my PhD and will be discussed here in Chapter V, along with the future directions of the project that will be pursued in post-doctoral studies.

Introduction

The disease of allergy can take many forms, but a mutual characteristic is the overreaction or hypersensitivity of the immune system to what the body detects as a foreign antigen. A common form of airway allergy is asthma, which affects at least 235 million people worldwide and is the most common chronic disease among children (116). According to the World Health Organization (WHO), there were 383,000 deaths due to asthma in 2015 alone (116). The WHO states, “the strongest risk factors for developing asthma are inhaled substances and particles that may provoke allergic reactions or irritate the airways.”

Interestingly, obese individuals have a staggering 92% increased risk of asthma, displaying enhancement of asthmatic symptoms, airway hyper-responsiveness, and atopy (117). Studies have even found that reducing weight can improve asthma. Indeed, weight loss from bariatric surgery and dietary restriction in obese patients with asthma improved bronchial hyper-responsiveness, airway inflammation, and clinical outcomes (118). Because of these clinical correlations between obesity and asthma, scientific endeavors have tried to understand the causal link. It has been shown that leptin, an adipokine secreted by adipose at higher rates with increasing obesity, has pro-inflammatory activity in the lungs (119). Conversely, the adipokine adiponectin has anti-inflammatory effects in the lungs but is decreased during obesity (120). Diet-induced obesity increases migration of eosinophils from their origin in the bone marrow to the lung, as well as delays exit from the airway epithelium to the lumen (120). Furthermore, BMI has been correlated with increased respiratory sputum IL-5 concentrations and submucosal eosinophil levels in individuals with severe obesity (121).

These and other studies have solidified a strong correlation between asthma and obesity, but have yet to yield a direct mechanism. Curiously, investigators have been trying to understand the clinical link between obesity and asthma, without looking at the fat tissue itself. Our preliminary data shows that AT mounts a hypereosinophilic state (i.e. a hallmark of allergy and asthma in lung) after repeated exposure to a foreign substance (bovine serum album). Our continued studies will elucidate whether AT and lung act within a detrimental feedback loop during obesity that results in greater incidence and severity of allergy and asthma.

Results

Chronic exposure to BSA leads to hypereosinophilic AT

It is well established that exposure to foreign substances can induce eosinophilic inflammation in the lungs and airways of challenged mice. Furthermore, obesity has been shown to increase the severity of allergic conditions, but with little insight to the mechanism(s) responsible. There has been no thorough investigation of atypical secondary sites of eosinophilic inflammation upon exposure to foreign substances, and how such reactions may feedback to lung inflammation and distress. Thus, in the current study, male C57BL/6J mice were fed either chow or HFD for 4 or 8 weeks and simultaneously IP injected twice weekly with varying concentrations of BSA (0.001%, 0.01%, 0.1%).

The highest concentration of 0.1% BSA, though admittedly still a dilute solution, was able to elicit a potent increase in the percent of eAT eosinophils at both 4 and 8 weeks of exposure, and on either chow or HFD (Fig. 5.1A-D). Interestingly, the middle concentration of 0.01% BSA only increased AT eosinophils after 8 weeks of exposure (Fig. 5.1C&D), but not 4 weeks (Fig. 5.1A&B). However, in the mice exposed for 8 weeks to the 0.01% BSA, the elevation in AT eosinophils was more stable and reached significance in HFD (Fig. 5.1D), while only trended towards an increase with greater variability in chow-fed mice (Fig. 5.1C). This finding suggests HFD-fed obesity may create an inflammatory environment that is more conducive to foreign substances (e.g. BSA) eliciting an eosinophilic response. The lowest concentration of 0.001% BSA used did not increase eosinophils at any time point tested under either chow or HFD-fed conditions. Alterations in percent AT eosinophils were further verified by changes in absolute number of AT eosinophils, with less than 100,000 eosinophils in eAT of saline injected mice but upwards of several million eosinophils upon repeated exposure to 0.1% BSA (data not shown).

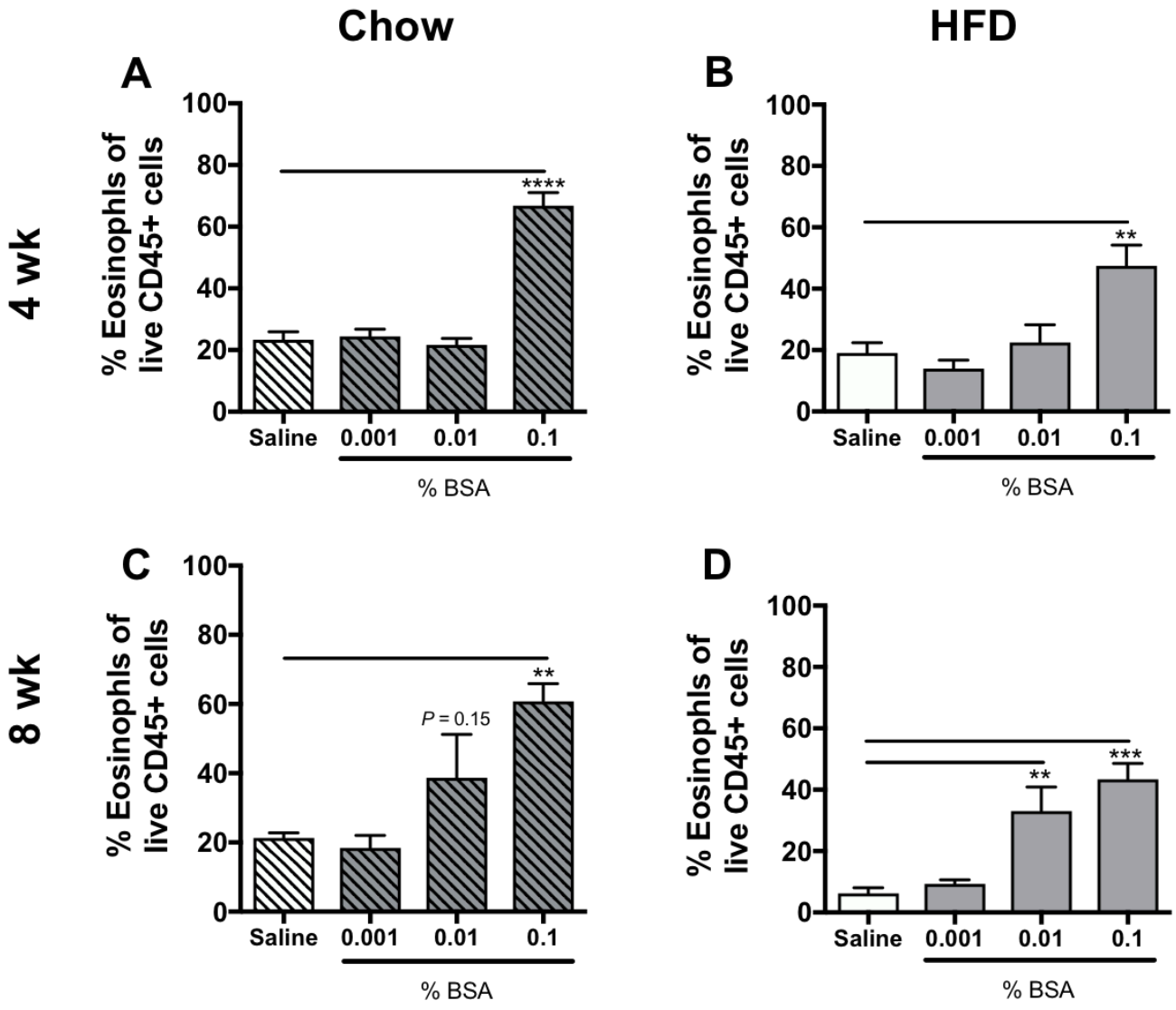

Figure 5.1 Chronic exposure to BSA leads to hypereosinophilic AT.
Male C57BL/6J mice were fed either chow or HFD for 4 or 8 weeks and simultaneously injected twice weekly with varying concentrations of BSA (0.001%, 0.01%, 0.1%). BSA exposure for 4 weeks on either **(A)** chow [n=4-10] or **(B)** HFD [n=8] increased eAT eosinophils only at highest concentration, 0.1% BSA. BSA exposure for 8 weeks on **(C)** chow trends towards an increase in eAT eosinophils even at mid-grade 0.01% BSA concentration [n=4-5], but reaches statistical significance in **(D)** HFD-fed mice [n=4].
Data are shown as means ± SEM.
BSA = bovine serum albumin; AT = adipose tissue; eAT = epididymal AT; HFD = high fat diet.
Key: chow = hashed bars; HFD = open bars; saline = white; vehicle = BSA.
*P < 0.05, compared to saline; **P < 0.01, compared to saline; ***P < 0.001, compared to saline; ****P < 0.0001, compared to saline.

Chronic BSA exposure prevents reduction in M2-like polarization of AT macrophages during HFD-feeding

A shift in polarization of the AT macrophage pool from an M2-like state to an M1-like state is a hallmark of obesity, and correlates with impaired AT function. Furthermore, eosinophils have been shown to influence AT macrophage polarization. Thus we evaluated the effect of BSA-induced hypereosinophilic AT on macrophage polarization. Male C57BL/6J mice were fed either chow or HFD for 8 weeks and simultaneously injected twice weekly with 0.1% BSA. The expected decrease in M2-like polarization of the eAT macrophage pool occurred with HFD-feeding compared to chow in saline treated mice (Fig. 5.2). However, the decrease in M2-like macrophage polarization from HFD was inhibited with BSA exposure (Fig. 5.2).

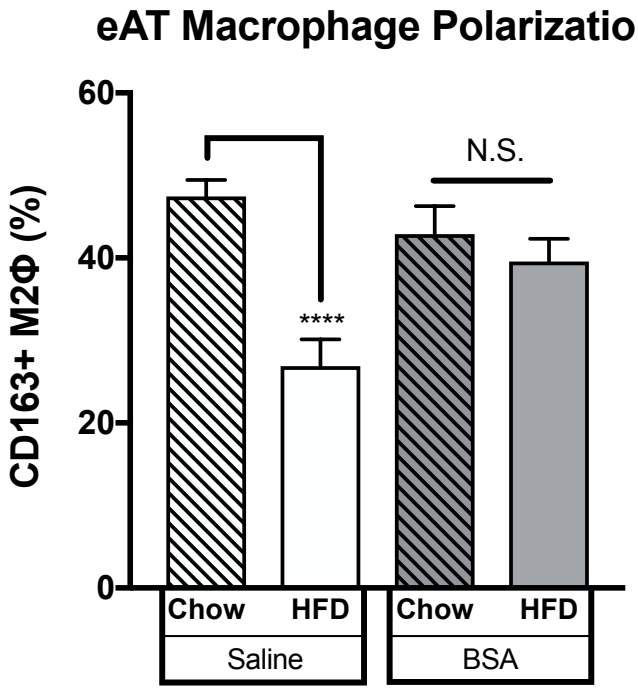

Figure 5.2 Chronic BSA exposure prevents reduction in M2-like polarization of AT macrophages during HFD-feeding.
Male C57BL/6J mice were fed either chow or HFD for 8 weeks and simultaneously injected twice weekly with 0.1% BSA. Typical decrease in M2-like polarization of eAT macrophage pool occurred with HFD-feeding compared to chow in saline treated mice [n=]. Decrease in M2-like macrophage polarization from HFD was inhibited with 8 weeks 0.1% BSA exposure [n=6-7].
Data are shown as means ± SEM.

BSA = bovine serum albumin; AT = adipose tissue; eAT = epididymal AT; HFD = high fat diet; N.S. = not significant. ****$P < 0.0001$, compared to saline.

Chronic BSA exposure does not affect weight gain in chow- or HFD-fed mice

An increase in AT eosinophils along with a reduction in AT inflammation often correlates with reduced body weight. Therefore, we evaluated weight gain in male C57BL/6J mice fed either chow or HFD for 8 weeks and simultaneously injected twice weekly with varying concentrations of BSA (0.001%, 0.01%, 0.1%). Mice fed HFD weighed more than chow fed mice, but there were no significant differences in weight within diet groups between varying BSA doses (Fig. 5.3).

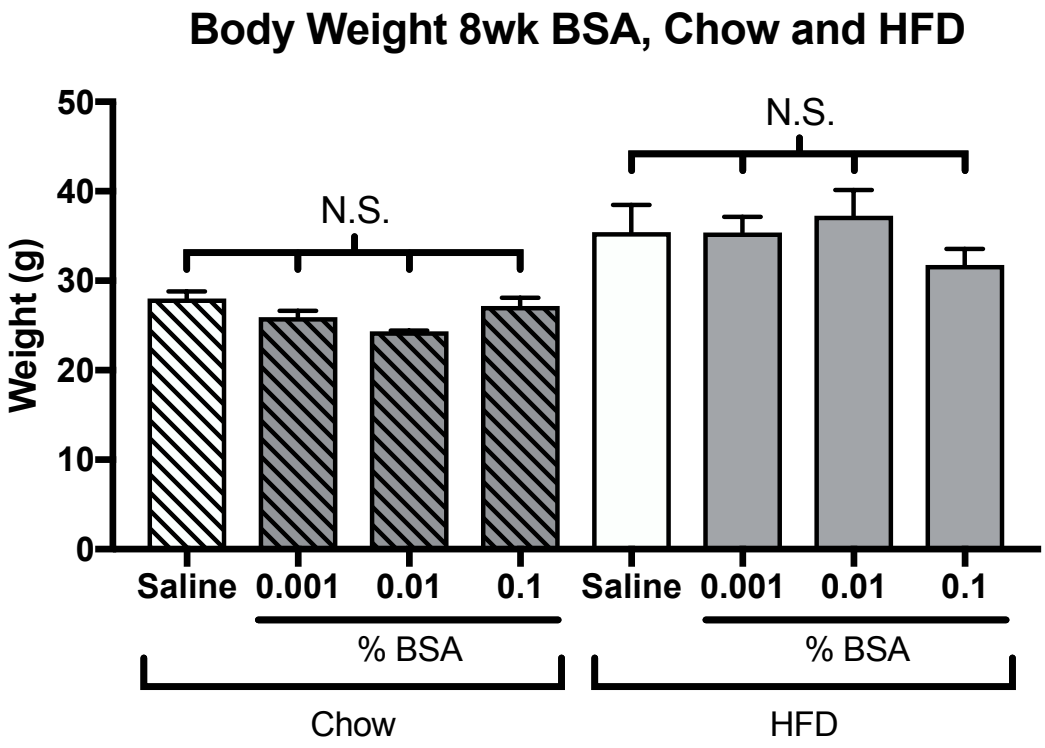

Figure 5.3 Chronic BSA exposure does not affect weight gain in chow- or HFD-fed mice.
Male C57BL/6J mice were fed either chow or HFD for 8 weeks and simultaneously injected twice weekly with varying concentrations of BSA (0.001%, 0.01%, 0.1%). Mice on HFD weighed more than chow fed mice, but with no significant differences in weight within diet groups between varying BSA doses [n=3-5].
Data are shown as means ± SEM.
BSA = bovine serum albumin; HFD = high fat diet; N.S. = not significant.
Key: chow = hashed bars; HFD = open bars; saline = white; vehicle = BSA.

Chronic BSA exposure does not affect glucose tolerance in chow- or HFD-fed mice

Typically glucose tolerance negatively correlates with body weight, but has been shown to deviate from this trend in the presence of improved AT inflammation and AT eosinophilia. In our model, though there was no difference in body weight in mice chronically exposed to BSA, there was an increase in eosinophils and preservation of anti-inflammatory M2-like macrophages. Therefore, we tested if the BSA-induced AT inflammatory improvements altered glucose tolerance. Male C57BL/6J mice were fed either chow or HFD for 8 weeks and simultaneously injected twice weekly with varying concentrations of BSA (0.001%, 0.01%, 0.1%). As expected, saline-treated HFD-fed mice had impaired glucose tolerance compared to chow-fed controls (Fig. 5.4; $p<0.0001$). However, there was no difference in glucose tolerance (AUC) within each diet group, even with the highest concentration of 0.1% BSA (Fig. 5.4).

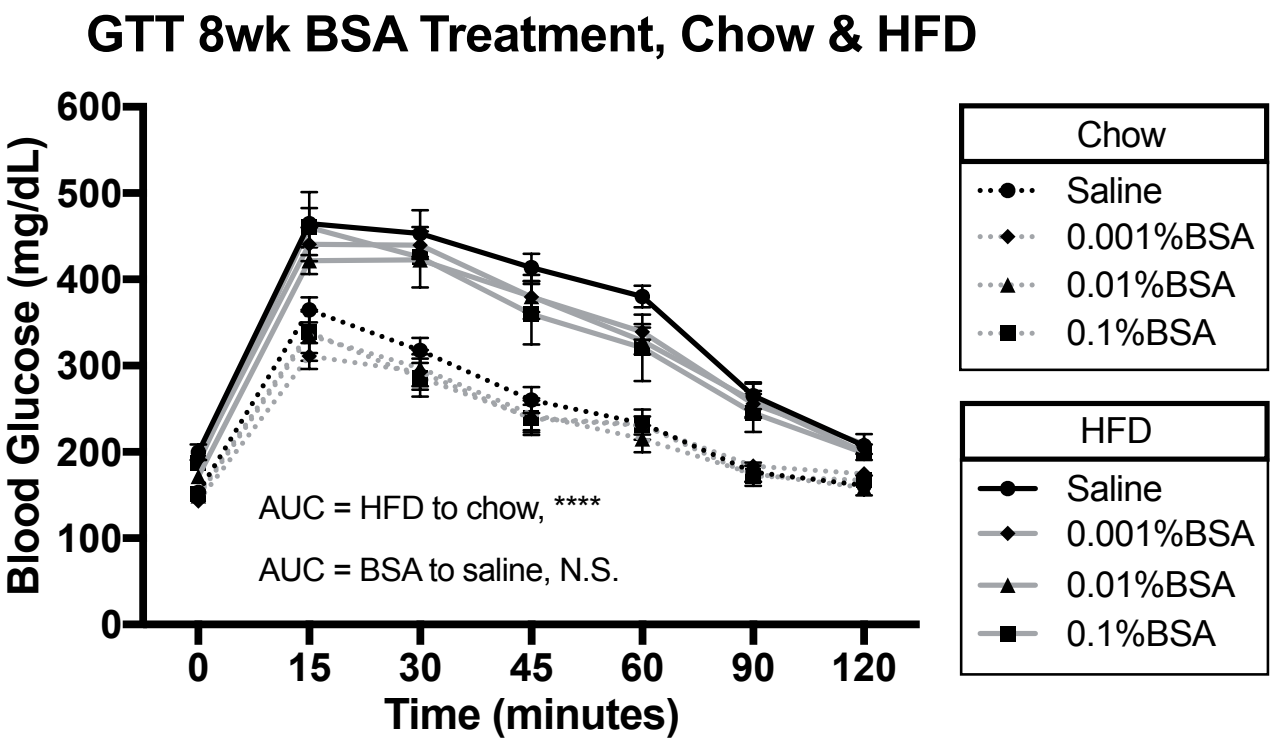

Figure 5.4 Chronic BSA exposure does not affect glucose tolerance in chow- or HFD-fed mice.
Male C57BL/6J mice were fed either chow or HFD for 8 weeks and simultaneously injected twice weekly with varying concentrations of BSA (0.001%, 0.01%, 0.1%). Glucose tolerance is not altered by 8 weeks of BSA exposure in chow-fed mice, as assessed by AUC. Glucose tolerance is impaired with HFD-feeding compared to chow-fed mice in saline control. Glucose tolerance is not altered by 8 weeks of BSA exposure in HFD-fed mice, as assessed by AUC. [n=4]
Data are shown as means ± SEM.
HFD = high fat diet; AUC = area under the curve; N.S. = not significant.
Key: chow = dotted lines; HFD = solid lines; saline = black; BSA = grey.
****$P < 0.0001$, compared to chow.

Effect of chronic BSA-induced AT eosinophilia conserved in BALB/c mouse strain

Observing no evidence of a metabolic phenotype (i.e. changes in body weight or glucose tolerance) in BSA-exposed mice, we next focused on whether the relationship between the BSA and hypereosinophilic AT was allergic in origin. Many models of allergy are tested in BALB/cJ mice because they are more prone to allergic reactions, and thus many genetic models and tools utilize the BALB/cJ strain. As such, we tested whether the BSA-induced hypereosinophilic AT observed in C57BL/6J mice was conserved in BALB/cJ mice. Male BALB/cJ mice were fed either chow or HFD for 4 weeks and simultaneously injected twice weekly with 0.1% BSA. Indeed there was a large increase in the percent eAT eosinophils after 4 weeks of 0.1% BSA in both chow- and HFD-fed BALB/cJ mice (Fig. 5.5). Of note, the percent eAT eosinophils of chow-fed saline-treated BALB/cJ mice (Fig. 5.5, 4.68%) were ~5-fold lower at baseline than C57BL/6J mice (Fig. 5.1, 23.35%).

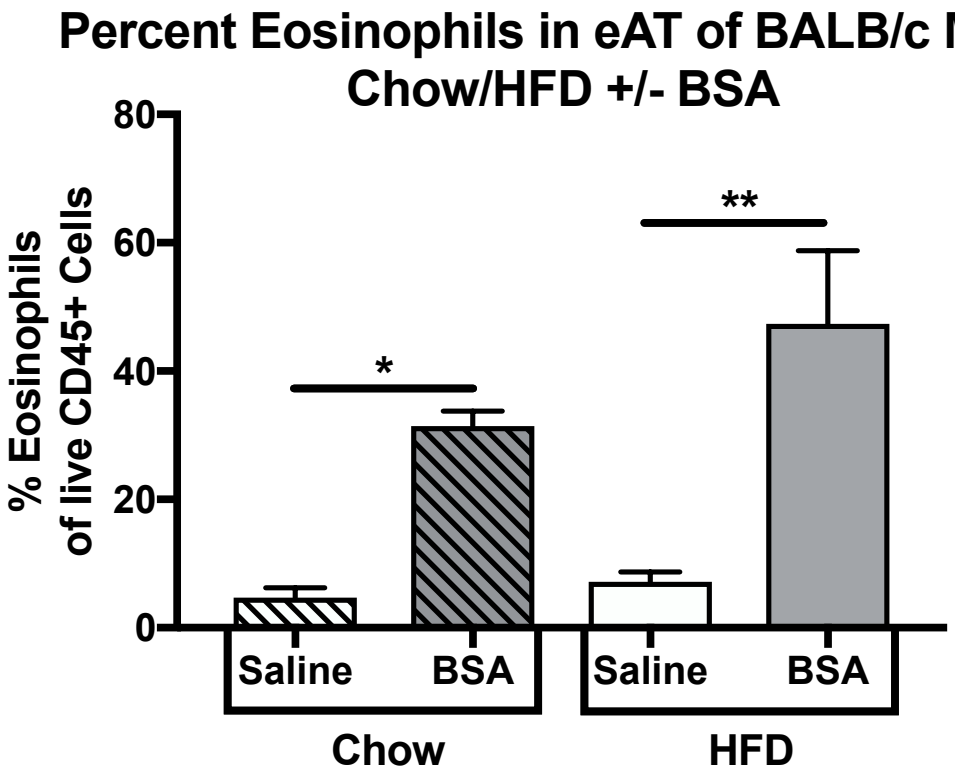

Figure 5.5 Effect of chronic BSA-induced AT eosinophilia conserved in BALB/c mouse strain.
Male BALB/cJ mice were fed either chow or HFD for 4 weeks and simultaneously injected twice weekly with 0.1% BSA. Chronic BSA exposure induced eAT hypereosinophilia in both chow- and HFD-fed BALB/cJ mice. [n=4-5].
Data are shown as means ± SEM.
BSA = bovine serum albumin; AT = adipose tissue; eAT = epididymal AT; HFD = high fat diet.
Key: chow = hashed bars; HFD = open bars; saline = white; vehicle = BSA.
*$P < 0.05$, compared to saline; **$P < 0.005$, compared to saline.

AT eosinophilia from chronic BSA exposure is partially dependent on an IL33 mechanism

Interleukin-33 is upstream of eosinophilic airway inflammation, and has been shown to influence AT eosinophil number and function (122-124). We determined whether the increase in AT eosinophils from chronic BSA exposure was dependent on IL33. Male WT BALB/cJ and IL-33 KO mice were exposed to 0.1% BSA for 4 weeks. Once again, chronic exposure to BSA induced a substantial increase in the percent eAT eosinophils in WT BALB/cJ mice (Fig. 5.6A); however, this effect was blunted in IL-33 KO mice. The reduction of BSA-induced AT hypereosinophilia in IL-33 KO mice is even more evident when comparing the absolute cell number, which shows a drastic disparity between WT BALB/cJ and IL-33 KO mice (Fig. 5.6B). Interestingly, the dependency on IL33 for BSA-induced eosinophilia was conserved in the lung (Fig. 5.6C&D).

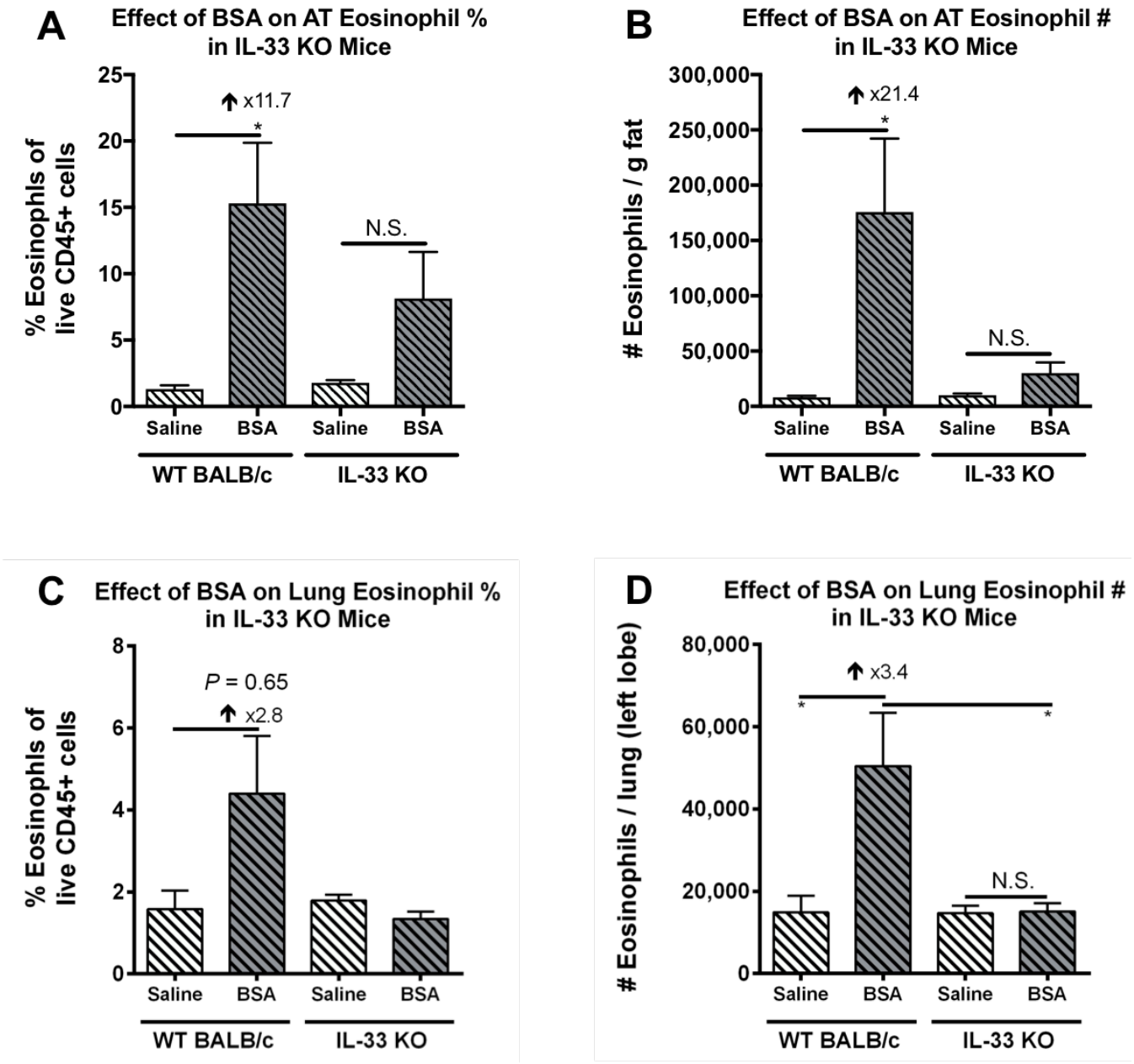

Figure 5.6 AT eosinophilia from chronic BSA exposure is partially dependent on an IL33 mechanism.

Male WT BALB/cJ and IL-33 KO mice were exposed to 0.1% BSA for 4 weeks. **(A)** BSA exposure increased the percent of eosinophils in eAT of WT BALB/cJ mice ~12 fold, but the effect was blunted in IL-33 KO mice [n=5-6]. **(B)** Likewise, BSA exposure increased the number of eosinophils in eAT of WT BALB/cJ mice ~21 fold, but was the effect was severely blunted in IL-33 KO mice [n=4-6]. Similar effects were seen in lung for **(C)** eosinophil percents and **(D)** eosinophil number.

Data are shown as means ± SEM.

BSA = bovine serum albumin; AT = adipose tissue; eAT = epididymal AT; N.S. = not significant.

Key: chow = hashed bars; saline = white; vehicle = BSA.

*$P < 0.05$, compared to saline.

Discussion

The primary finding from this study was that AT is capable of mounting a hypereosinophilic response to repeated exposure of a foreign substance (i.e. BSA); a reaction typically associated with the lung or skin during an allergic reaction. This hypereosinophilic state affects the inflammatory state of the AT macrophages, an immune cell population that has been shown to greatly influence AT function and inflammation. Despite data in the literature showing that increased AT eosinophils reduce body weight and improve glucose tolerance, there was no change in these measures in the BSA model; a lack of metabolic phenotype associated with hypereosinophilic AT is consistent with our two previous models, the CCR2$^{-/-}$ mouse and IL5 treatment (Fig. 5.7).

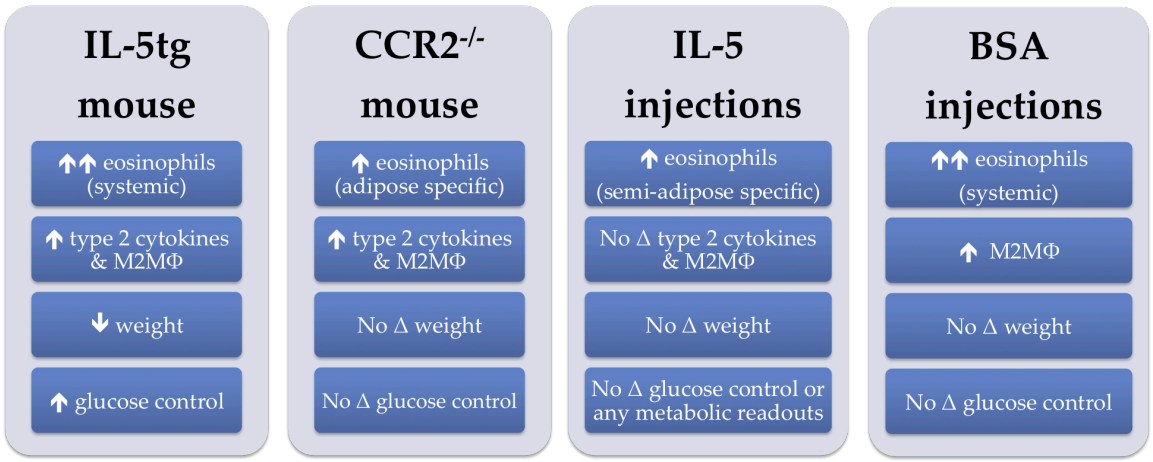

Figure 5.7. Comparison of BSA-exposure model of hypereosinophilic AT models with previous models.
Mice were exposed to bovine serum albumin (BSA) twice-weekly for 4-8 weeks. This resulted in systemic hypereosinophilia and increased AT M2-like polarization. In contrast to the systemic hypereosinophilia in the IL5tg mouse, BSA exposure was associated with no difference in body weight, AT mass, or glucose tolerance compared to control. The BSA exposure model was the third model in which we have increased AT eosinophils but seen no improvements in AT or systemic metabolic function reported by other models in the literature. It is our belief that eosinophils in other non-AT tissues of the models in the literature were responsible for metabolic improvements or that there are differences in eosinophil phenotype between models.

The finding that chronically administered BSA induces such a massive accumulation of eosinophils in AT is quite novel. This reaction appears to be an adaptive response because the reaction is more sensitive based upon the number of repeated exposure, i.e 4 week data vs. 8 week data (Fig. 5.1). This suggests there may be a classic allergic reaction that requires repeated exposure, agitation of the endothelium/epithelium to produce IL33, presentation of antigen, activation of naïve T cells, and Th2 mediated production of IL5 that then recruits eosinophils. Alternatively, BSA could be inducing an innate immune response: production of IL33 from macrophages, NKT cells, and/or the endothelium which activates ILC2 cells to produce IL5 that can then recruit eosinophils. An innate response is less likely because a single exposure of BSA did not induce any reaction (data not shown).

We have shown the BSA-induced eosinophil accumulation is at least partially dependent on IL33, and have thus identified the most upstream step of the mechanism. A dependency on IL33 could apply to either an allergic or non-allergic mediated response, thus future experiments will specifically test the role of T-cells (adaptive) and ILC2 cells (innate). ILC2 number and production of IL5 can be tested by flow cytometry, and similarly with T cells. In addition, we will remove AT T-cells both from mice that have been repeatedly challenged with BSA and a saline control; these T-cells will then be exposed to BSA *in vitro* and activation (i.e. cytokine production) will be assessed as a readout of antigen specificity. If T-cells from chronically exposed mice react with higher production

of cytokines to BSA *in vitro* than their non-exposed controls, then there will be evidence of previous *in* vivo naïve T-cell activation via antigen presentation.

Future experiments will also focus on the respiratory physiology of mice using our chronic BSA model. We have not yet tested airway hyperresponsiveness or mucus production but have developed collaborations with labs that have expertise in these analyses. There is reason to believe the chronically BSA-challenged mice will show an asthmatic phenotype because we have shown an eosinophilic response in the lung (Fig. 5.6C&D). We also plan to transplant AT from a BSA-exposed mouse to a naïve mouse to determine if the AT can influence AT/lung inflammation and AT/lung function of the naïve mouse.

These future experiments will determine a mechanism of the hypereosinophilic response in AT upon repeated exposure to a foreign substance. Secondly, these proposed experiments will determine the contribution of AT inflammation on lung function, and thus shed light on the link between obesity and asthma.

CHAPTER VI

FINAL DISCUSSION AND FUTURE DIRECTIONS

Progress in understanding obesity and T2D

Obesity and T2D are highly prevalent diseases that lead to increased comorbidities, reduced life expectancy, and significantly higher medical costs. While there may be no instant cure for obesity or T2D, there has been significant progress in the therapies available to treat symptoms or prevent progression. Exercise and dietary intervention remain two effective means to lose weight, without having to resort to pharmacological solutions. When diet and exercise are not enough, or in order to supplement further control over obesity and/or T2D, several medications are available. Typically the first medication prescribed is Metformin, which improves insulin sensitivity in the body and helps lower glucose production by the liver (125). Other drug options include: Sulfonylureas, which help the body secrete more insulin; Thiazolidinediones, which allow for greater insulin sensitivity; DPP-4 inhibitors, which reduce blood sugar levels; SGLT2 inhibitors, which prevent sugar reabsorption by the kidneys and therefore the sugar is excreted in the urine; and lastly, exogenous insulin may be required for severe T2D patients (125). A more drastic, but highly effective method for treating T2D is bariatric surgery. Bariatric surgery improves glucose homeostasis and results in weight loss, but comes at the cost of drastic lifestyle change. Nevertheless, until obesity, its comorbidities, and associated massive health

costs are eliminated from society, it is imperative to better understand the molecular mechanisms underlying these diseases.

Decades of research have led to a better understanding of the progression of obesity, its associated inflammation, and the propensity for obesity to increase the risk for T2D. To this end, it is now known that during obesity a proinflammatory immune cell milieu manifests in various AT depots of the body. The increased inflammation contributes to AT insulin resistance, unregulated lipolysis, and ultimately ectopic lipid storage in organs and tissues ill-equiped to deal with the high lipid content. A host of metabolic dysfunctions ensues, resulting in many of the symptoms and comorbidities that present clinically.

One attractive avenue to treat obesity and T2D is to reduce AT inflammation and restore its functional capability to properly store fat. One of the key players in AT inflammation is the macrophage; much research has focused on how to deplete or modify AT macrophages to improve metabolic health during obesity (126). During the pursuits investigating AT macrophages, it was discovered that nearly every other known immune cell type also exists in lean and obese AT (Fig. 1.4). More recent work has focused on the contribution of these other immune cell populations to AT homeostasis, including the role of eosinophils.

An unexpected role for CCR2 in AT eosinophil homeostasis

In the same year that eosinophils were first discovered in AT, our lab was working with CCR2$^{-/-}$ mice to study macrophage recruitment to AT.

Serendipitously, we discovered that while there was no difference in macrophage recruitment, we did observe an increased population of AT eosinophils in lean CCR2$^{-/-}$ mice that was exacerbated in obesity (Chapter III). However, in contrast to the first and only publication at the time showing eosinophils improved AT and whole-body metabolic health, we saw no such improvements in our model of hypereosinophilic AT in CCR2$^{-/-}$ mice. There were a few differences in the two studies that might explain the conflicting results. First the AT eosinophil levels in CCR2$^{-/-}$ mice were ~3-4-fold higher than WT controls, but not nearly as high as the super-physiological levels reported in IL5tg mice (73). Second, the tissue eosinophilia of CCR2$^{-/-}$ was somewhat tissue-specific, found in multiple AT depots and the peritoneal cavity, but not in the bone marrow, blood, spleen, or liver. In contrast, IL5tg mice have high levels of eosinophils in virtually every tissue and organ of the mouse. Thus, the simplest explanation is that to achieve beneficial effects on metabolism, one needs to 1) massively elevate eosinophil levels, 2) elevate eosinophils in a tissue other than AT, or 3) CCR2 deficiency itself somehow inhibits the beneficial effects of AT eosinophils on metabolic fitness.

Caveats with previous hypereosinophilic AT models

Within less than a decade, studies have revealed the presence of eosinophils in AT, showed that AT eosinophils naturally decline with weight gain, and provided evidence that eosinophils contribute to M2 macrophage polarization. Furthermore, these published studies suggest eosinophils may

induce weight loss, improve glucose tolerance, and restore insulin sensitivity. The newly evolving idea that eosinophils appear to play such a substantial role in AT metabolic health was met with much enthusiasm by the field, but also with due skepticism. With a multitude of studies on AT eosinophils now published we can compare and contrast the results across a range of models, as shown in Table 1. This table summarizes the evidence that is or is not able to support a definitive role of eosinophils in AT homeostasis and/or whole body metabolic fitness.

For example, we can breakdown how differing studies looked at one parameter, glucose tolerance. One of the most common readouts in examining the role of AT eosinophils has been whole body glucose tolerance, tested in at least 7 different studies (73-75, 127-130). The first study to show improvements in glucose tolerance from increased AT eosinophils used the IL5tg mouse. The primary caveat of this model is that this mouse line is known to be somewhat sickly, even at baseline before any experimental manipulation. It is not surprising that the IL5tg mouse did not gain as much weight as it's wildtype counterpart when placed on a HFD (73). This is an issue because weight differences, often regardless of mechanism, can impart improved glucose tolerance. Therefore it is difficult to know if the increased AT eosinophils were responsible for the reduced weight and improved glucose tolerance or if the weight of the mouse was influenced by the systemic increases in eosinophils that occur throughout the rest of the IL5tg mouse, which then accounted for improved glucose homeostasis. Several studies have used alternative ways to increase AT eosinophils, such as

the parasitic infection model. Yet again, however the question must be asked whether weight loss simply occurs due to the mouse being energetically taxed while clearing an infection. One study even used a honeybee extract, propolis, to increase AT eosinophils and reported improved glucose tolerance (128). It must be acknowledged however, that a parasitic infection most certainly modulates a number of other immune cells, and it is unknown how propolis influences other immune processes; for this reason, it is not possible to say the increased eosinophils are definitively responsible for the improved glucose tolerance in such models. In contrast, the models that do suggest eosinophils influence glucose tolerance are the ΔdblGATA and $IL5^{-/-}$ transgenic mouse lines, which have a near complete absence of eosinophils. In these eosinophil deficient mice, glucose tolerance is impaired while on a HFD compared to wildtype mice. Thus, while it is difficult to be confident increasing eosinophils over baseline can improve glucose tolerance, it does appear that depleting eosinophils negatively impacts glucose tolerance.

These same caveats of testing the effect of AT eosinophils on glucose tolerance, are shared with testing lipid and mixed-meal tolerance, insulin sensitivity, weight gain, white AT beiging, metabolic rate, food intake & locomotion, and general inflammation, all of which are summarized in Table 1.

In conclusion, the studies implicating a protective role for eosinophils in AT each had at least one of the following caveats: 1) had correlative, not casual data, 2) targeted eosinophils systemically but attributed improvements in whole-body metabolism to AT eosinophils, 3) used genetically modified mice that may

have had developmental differences, 4) induced eosinophilia with a parasite, making it difficult to distinguish the effects of weight loss from infection vs. an increase in AT eosinophils, or 5) targeted upstream pathways that change more than only eosinophils. In summary, it had not been shown that *directly* targeting eosinophils *post normal development* at the *onset of obesity* could effectively reduce weight loss and improve metabolic outputs. Our studies have addressed these caveats and shown that increasing mouse AT eosinophils in adulthood during obesity does not improve metabolic fitness. This remains an important finding if treatments targeting eosinophils are to be translationally applied to the clinic for obese patients based on previous literature.

So how might some of these caveats be avoided? How might it be more explicitly known if eosinophils do or do not play a role in AT homeostasis and whole body metabolic fitness?

Directly and specifically modulate eosinophils:

Much of the published data generated from manipulating AT eosinophils came from altering eosinophils in a non-specific fashion, as outlined above and as described in Table 1. To circumvent this caveat, future studies could employ more *in vitro* methods that allow for specialized control of exactly what cell types are interacting. For instance, only pairing eosinophils with macrophages or adipocytes and then applying an experimental challenge, such as high/low glucose or saturated vs. unsaturated FAs. When working *in vivo*, methodology should directly modulate eosinophils. For example, powerful experimental questions can be asked about AT eosinophils by employing antibody depletion

methods (anti-SiglecF, anti-IL5). In fact, there is already an FDA approved drug against IL5 used to treat asthma, called Mepolizumab; thus there is immediate clinical relevance to how depletion of eosinophils may effect adipose function in humans taking the drug Mepolizumab. Inversely, non-genetic approaches for specifically increasing eosinophils could be employed. Now that eosinophils can be cultured *in vitro* in large quantities from bone marrow (78), simple addback methods could introduce varying amounts of eosinophils to nearly any existing disease model. In this way, eosinophils could be given to obese mice without introducing any of the off target effects of other methods such as the helminth infection. Whether decreasing or increasing eosinophils with these approaches, they offer the distinct advantage of altering eosinophils at any given time, compared to genetic models that have life long altered eosinophils. Direct manipulation of eosinophils also offers a better approach to proving causality instead of relying on correlative data. Another recent advancement in this field is the first ever eosinophil specific Cre-recombinase mouse line, designed under the control of the eosinophil peroxidase (*Epx*) promoter (eoCre, (131)). Previous models used global knockouts, like the IL4/IL13 double knockout mouse to infer that eosinophil-derived IL4/IL13 was responsible for improvements in metabolic fitness in cases where eosinophils were increased. However this has been a major caveat of such studies because other cells, most prominently CD4+ T cells and ILC2 cells, also express IL4 and IL13, respectively. With the eoCre mouse, eosinophil deletion or overexpression of IL4 and/or IL13 could be used to more

confidently prove or disprove the role of these eosinophil-derived interleukins in AT health.

Table 1. Comprehensive summary of all evidence that can and cannot support a definitive role of eosinophils in AT homeostasis and/or whole body metabolic fitness.

Metabolic parameter:	Experiment:	Study Author (citation):	Definitive role of eosinophils:	Rationale:
Glucose tolerance	• Glucose tolerance test (GTT)	1) Wu, 2011 (73)	1) Yes	1) ΔdblGATA (eosinophil$^{-/-}$) mice → impaired GTT on HFD
		2) Wu, 2011 (73)	2) No	2) Sickly nature of IL5tg mice may explain impaired weight gain → thus improved GTT
		3) Molofsky, 2013 (74)	3) Yes	3) IL5$^{-/-}$ (eosinophil$^{-/-}$) mice → impaired GTT on HFD
		4) Zhu, 2013 (127)	4) No	4) Eosinophils correlated with better GTT, but no causation
		5) Hams, 2013 (75)	5) No	5) Glucose tolerance was not proportional to eosinophil #
		6) Kitamura, 2013 (128)	6) No	6) Propolis → could target cells other than eosinophils
		7) Berbudi, 2016 (129)	7) No	7) *L. sigmodontis* → also targets cells other than eosinophils
		8) Bolus, 2017, *in revision*	8) No	8) Increasing eosinophils via rIL5 did not alter GTT
Lipid tolerance	• Lipid tolerance test (LTT)	9) Bolus, 2017, *in revision*	9) No	9) Increasing eosinophils via rIL5 did not alter LTT
Mixed-meal tolerance	• Mixed meal tolerance test (MTT)	10) Bolus, 2017, *in revision*	10) No	10) Increasing eosinophils via rIL5 did not alter MMT
Insulin sensitivity	• AKT signaling (pAKT) • ITT • HOMA-IR	11) Wu, 2011 (73)	11) Yes	11) ΔdblGATA (Eos$^{-/-}$) mice → reduced pAKT on HFD
		12) Molofsky, 2013 (74)	12) Yes	12) IL5$^{-/-}$ (eosinophil$^{-/-}$) mice → impaired ITT on HFD
		13) Zhu, 2013 (127)	13) No	13) Eosinophils correlated with better HOMA-IR, but no causation was shown
		14) Kitamura, 2013 (128)	14) No	14) Propolis → not a specific regulator of eosinophils
		15) Bolus, 2017, *in revision*	15) No	15) Increasing eosinophils via rIL5 did not alter pAKT
Weight gain	• Fat mass • Body mass	16) Wu, 2011 (73)	16) Yes	16) ΔdblGATA (Eos$^{-/-}$) mice → increased fat mass on HFD
		17) Wu, 2011 (73)	17) No	17) Sickly nature of IL5tg mice may explain impaired weight gain
		18) Molofsky, 2013 (74)	18) Yes	18) IL5$^{-/-}$ mice → increased fat mass on HFD
		19) Hams, 2013 (75)	19) No	19) Weight loss was not proportional to eosinophil #

		20) Kitamura, 2013 (128)	20) No	20) Despite increase eosinophils → no Δ in weight
		21) Satoh, 2013 (132)	21) No	21) Reduced weight in Trib1$^{-/-}$ mice correlates with low eosinophils → but no causation is shown
		22) Berbudi, 2016 (129)	22) No	2) *L. sigmodontis* → can target cells other than eosinophils
		23) Fabbiano, 2016 (110)	23) No	23) Reduced weight from caloric restriction correlates with increased eosinophils → but no causation is shown
		24) Bolus, 2017 *in revision*	24) No	24) Increasing eosinophils via rIL5 did not alter fat mass
Beiging	• UCP1 expression	25) Qiu, 2014 (109)	25) Yes	25) 4get-ΔdblGATA (Eos$^{-/-}$) mice → reduced expression of AT UCP1 during cold
		26) Brestoff, 2015 (114)	26) No	26) Increased UCP1 expression was not dependent on eosinophils → occurred with ILC2 alone
		27) Rao, 2014 (133)	27) Yes	27) ΔdblGATA (Eos$^{-/-}$) mice → reduced UPCP1 when induced by Metrnl
		28) Suarez-Zamorano, 2015 (134)	28) No	28) Increased eosinophils from microbiota depletion correlate with UCP1 → no causation
		29) Lee, 2015 (135)	29) No	29) A) ΔdblGATA (eosinophil$^{-/-}$) mice still elicited beige progenitors upon IL33 stimulation B) ΔdblGATA (eosinophil$^{-/-}$) mice have lower baseline beige progenitors
		30) Fabbiano, 2016 (110)	30) No	30) Increased UCP1 from caloric restriction correlates with increased eosinophils → but no causation is shown
		31) Ding, 2016 (111)	31) No	31) A) Increased eosinophils from rIL33 correlate with UCP1 → no causation B) ILC2s were also increased with eosinophils → ILC2s can increase UCP1 so unclear which is responsible
		32) Bolus, 2017 *in revision*	32) No	32) Increasing eosinophils via rIL5 did not alter UCP1
Metabolic rate	• Energy expenditure (EE)	33) Molofsky, 2013 (74)	33) Yes	33) ΔdblGATA (eosinophil$^{-/-}$) mice → reduced EE on HFD
		34) Bolus, 2017 *in revision*	34) No	34) Increasing eosinophils via rIL5 did not alter EE
Food intake/ locomotion	• Mass consumed • Line-break detection	35) Bolus, 2017 *in revision*	35) No	35) Increasing eosinophils via rIL5 did not alter food intake or movement

Inflammation	• Type 2 cytokines • M2-like MΦ polarization	36) Wu, 2011 (73)	36) No	36) Sickly nature of IL5tg mice may explain impaired weight gain → thus more M2MΦ
		37) Wu, 2011 (73)	37) No	37) IL-4/13$^{-/-}$ mouse model is not specific to eosinophils
		38) Molofsky, 2013 (74)	38) No	38) Rag2$^{-/-}$ x γ_C mice lack AT eosinophils and ILC2s → ILC2s can directly impact MΦ
		39) Hams, 2013 (75)	39) No	39) M2MΦ was not proportional to eosinophil #
		40) Kitamura, 2013 (128)	40) No	40) A) Propolis → not a specific regulator of eosinophils B) M2MΦ → some genes increase and some decrease
		41) Satoh, 2013 (132)	41) No	41) Lack of M2MΦ in Trib1$^{-/-}$ mice correlates with low eosinophils → but no causation is shown
		42) Bolus, 2015 (44)	42) No	42) Increased eosinophils in CCR2-/- mice correlate with M2MΦ → no causation
		43) Suarez-Zamorano, 2015 (134)	43) No	43) Increased eosinophils from microbiota depletion correlate with M2MΦ → no causation
		44) Berbudi, 2016 (129)	44) No	44) *L. sigmodontis* → also targets cells other than eosinophils
		45) Fabbiano, 2016 (110)	45) No	45) Increased type 2 cytokines and M2MΦ from caloric restriction correlates with increased eosinophils → but no causation is shown
		46) Ding, 2016 (111)	46) No	46) Loss of eosinophils did not reduce M2MΦ, and is some cases, increased M2MΦ
		47) Qin, 2017 (115)	47) No	47) Eosinophils preincubated with oxidized-LDL polarize M2MΦ to M1MΦ
		48) Bolus 2017 *in revision*	48) No	48) Increasing eosinophils via rIL5 did not alter M2MΦ
Adipose architecture	• Perivascular • Mammary gland • FAP muscle regeneration	49) Gouon-Evans, 2000 (136)	49) Yes	49) Eotaxin$^{-/-}$ mice → poor mammary branch formation
		50) Heredia, 2013 (137)	50) Yes	50) ΔdblGATA (eosinophil$^{-/-}$) mice → impaired FAP proliferation and muscle regeneration
		51) Withers, 2017 (138)	51) Yes	51) A) ΔdblGATA (eosinophil$^{-/-}$) mice → impaired anti-contractile perivascular function B) Reconstitution of eosinophils restored anti-contractile perivascular function

Transitioning models of hypereosinophilic AT to better understand metabolic consequences

Given that CCR2$^{-/-}$ was influencing the amount of AT eosinophils and that it altered gene expression of eosinophil markers during *in vitro* differentiation, we could not rule out that CCR2$^{-/-}$ was also altering eosinophil function within AT. For this reason, we moved away from the CCR2$^{-/-}$ model and chose to develop a new model of hypereosinophilic AT that might more closely mimic the protective role against obesity seen in IL5tg mice. Our new model utilized rIL5 that could be administered after mice developed normally, which would directly target eosinophils to level of our choosing (Chapter IV).

Evolving complexity of the eosinophil's beneficial effects on health

Our studies using rIL5 successfully increased AT eosinophils during obesity in a semi-tissue-specific manner; eosinophils were not changed in bone marrow, blood, or liver, but were elevated in the intestine, another naturally eosinophil-prone tissue. More importantly, eosinophils were not modulated until mice had undergone normal development and reached adulthood. Equally important, eosinophils of obese AT were restored with rIL5 to physiologically relevant levels observed in lean AT, not the super-physiological levels seen in previous models. Despite returning obese AT eosinophils to levels in lean mice, we saw no improvements in a wide variety of metabolic assays (Fig. 6.1). There was no change in body weight, fat mass, AT inflammation, glucose-, triglyceride-,

or mixed meal- tolerance, AT insulin signaling, energy expenditure, or white AT beiging capacity.

It was unexpected that the rIL5-driven increase in AT eosinophils did not improve metabolic fitness, given the growing literature on a positive role for eosinophils on AT function. However, alongside the publications supporting a role for eosinophils in AT homeostasis, several more recent publications suggest the mechanisms at play may be more dynamic or complex than originally appreciated (Fig. 6.1). There has been a great deal of discussion within the immunometabolism field around a paper that argued IL4/IL13 secreted by AT eosinophils induces macrophage expression of tyrosine hydroxylase (TH). The paper went on to suggest macrophage TH was required for catecholamine production that results in beiging of subcutaneous white AT (109). Beiging is favorable because it decreases weight and inflammation, while improving metabolic functions such as insulin sensitivity and glucose tolerance (112). These findings were disputed in a multi-laboratory paper providing strong evidence that macrophages cannot express TH and therefore can't produce catecholamines to beige white AT (113), which called into question the upstream role of eosinophils in beiging as well. A separate publication by Brestoff *et al.* showed that while IL33 can stimulate ILC2s to induce AT beiging, their model was independent of eosinophils (114). Instead, their evidence showed ILC2s act directly on adipocytes via methionine-enkephalin peptides to increase UCP1. Lastly, while studies have shown eosinophils correlated with M2-like macrophage polarization, a fascinating new study demonstrates that eosinophils treated first

with oxidized-LDL elicit M1-like macrophages (115); revealing eosinophils are capable of polarizing macrophages to either M1- or M2-like states depending on environmental stimuli. As more varied eosinophilic models have been employed, studies are introducing results that require reassessment of the direct impact of AT eosinophils on AT and whole-body health (Fig. 6.1).

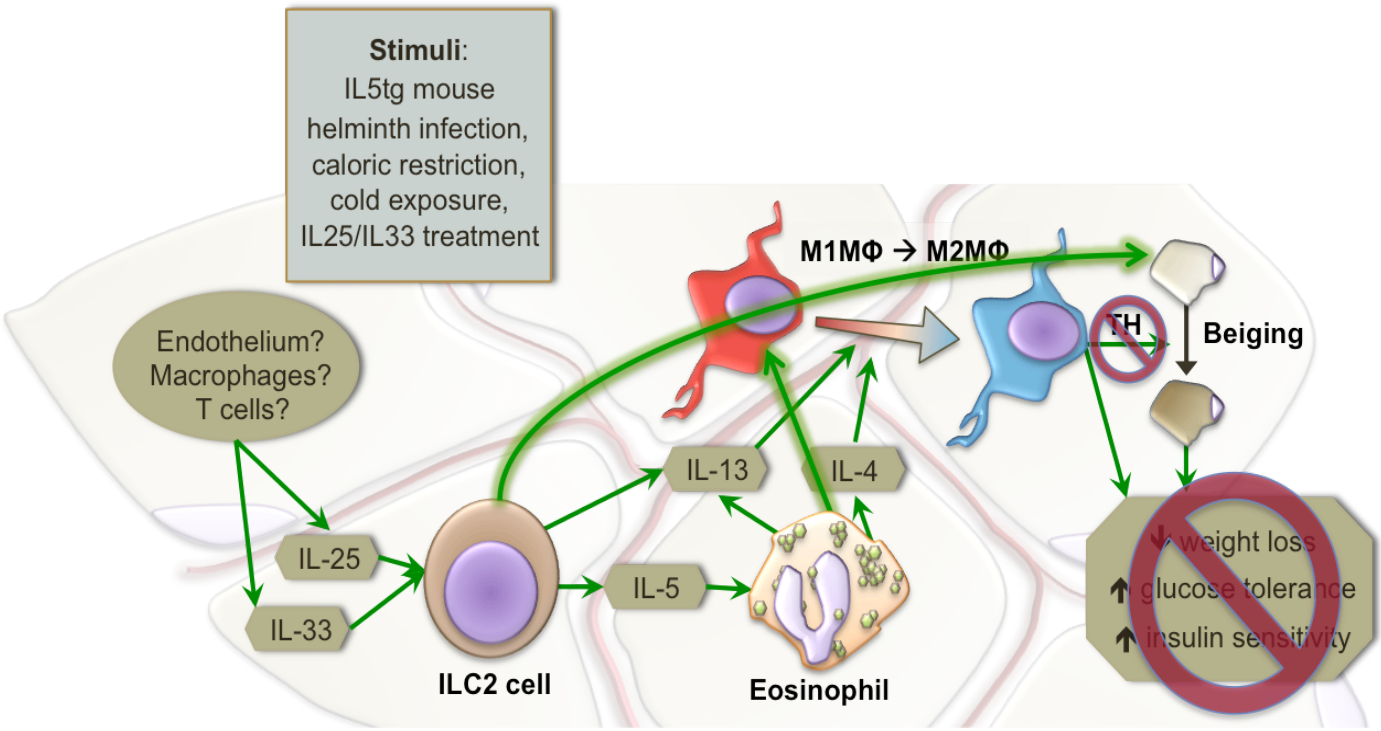

Figure 6.1. Revised understanding of the role of eosinophils in AT function based on this dissertation work and the most recent immunometabolism literature.

A number of stimuli can produce IL33/IL25 that activates ILC2 cells in AT which then produce IL13 and IL5. Eosinophils accumulate in AT in response to the IL5, and produce IL4 and IL13. IL4/IL13 polarize macrophages from an M1- to an M2-like state, which can induce weight loss, decrease inflammation, and improve glucose tolerance and insulin sensitivity. However, ILC2 cells have been shown to secrete IL13 to yield M2-like macrophages and to directly beige adipocytes, independent of eosinophils. Furthermore, eosinophils are now known to be able to also polarize macrophages to an M1-like state, when eosinophils are first exposed to oxidized-LDL. Lastly, studies have provided substantial evidence that macrophages do not express the tyrosine hydroxylase required to synthesize catecholamines to beige white AT; rather macrophages regulate beiging by absorbing and degrading local AT supplies of catecholamines released by sympathetic nerves innervating the AT depot. Ultimately we found in our studies that restoring eosinophils during obesity did not impart metabolic improvements, such as weight loss, glucose tolerance, or insulin sensitivity, as had been reported in other models in the literature.

Massive AT eosinophil accumulation from chronic BSA exposure

The argument could be made that the modest increase in AT eosinophils in our CCR2$^{-/-}$ and rIL5 injection model was simply not substantial enough to impart improvements in AT homeostasis during obesity. After all, the positive effects on metabolic health of IL5tg mice had very high numbers of AT eosinophils. Our model of hypereosinophilic AT from chronic BSA exposure allows us to address this issue (Chapter V).

We serendipitously discovered during the rIL5 studies that BSA could elicit an eosinophillic response when used at higher concentrations. BSA was used as a carrier protein for the rIL5. At a low enough concentration of 0.001% BSA, there was no eosinophilic response above saline treatment, and thus 0.001% BSA was used for the rIL5 studies as a vehicle control for the studies in Chapter IV. However, upon titrating the BSA up to 0.1% we observed a massive accumulation of AT eosinophils. The number of eosinophils went from less than 100,000 per gram AT in saline controls, up to several million per gram AT upon 0.1% BSA exposure; sometimes upwards of 90% of the AT immune cell population! These levels were comparable to those reported in IL5tg mice. Despite the incredible rise in AT eosinophils, we still observed no reduction in weight gain or improvement in glucose tolerance. This data suggests that modulating AT eosinophil number alone is not sufficient to bestow metabolic benefits in either the lean or obese state. It is possible the activation state of the eosinophils is as important as the quantity, which will be testing in current ongoing studies. It is also possible that eosinophils in AT simply do not influence

whole body metabolism as previous studies have suggested, but rather eosinophils in other tissues are responsible. Yet another possibility is that inherent characteristics of previous study designs (e.g. infection with a parasite) induced weight loss with subsequent improvements in metabolic measures, and that while AT eosinophil numbers were higher, they had nothing to do with the metabolic changes.

Does BSA act as an antigen to elicit hypereosinophilic AT?

Regardless of a lack of a metabolic phenotype in the mice chronically exposed to BSA, it is very interesting that AT responds to BSA by increasing eosinophil numbers. In a generalized inflammatory response, one might expect to see macrophages or neutrophils increased, but not eosinophils. Perhaps it shouldn't have been so unexpected since chicken egg ovalbumin (OVA) is commonly used to induce eosinophilic inflammation in the lung, as a model of allergy-mediated asthma (139). However, this logic would suggest that the AT is responding to the BSA with an allergic mediated reaction. This would be an entirely novel idea as we have found no studies implicating a type 2 mediated allergic response in AT against a foreign antigen. There was a single study that looked at AT following a food allergy model, but they only noted a slight increase in macrophages (140). These studies aside, there is cause to study the AT environment during allergic conditions. There is a clinical link between obesity and asthma that has yet to be properly understood. Research performed thus far has not been able to define a mechanism as to why obesity increases the risk

and severity of asthma. The answer may lie in the tissue most significantly expanded in obesity, the adipose tissue itself.

Determining how obesity promotes allergy

Our data described in Chapter V show that upon repeated exposures, BSA can induce massive eosinophil accumulation in both lean and obese mice, that this response is more stable in obese mice, that M2 macrophage polarization is maintained despite obesity, and that this process is at least partially dependent on IL33. As described in Chapter V Discussion, we plan to further elucidate whether the observed increase in AT eosinophils from BSA exposure is due to the innate or adaptive immune response. Furthermore, we will determine if the increased eosinophilic inflammation in AT feeds back to worsen lung inflammation characteristic of allergic asthma. These studies will broaden our understanding of how obesity promotes allergic conditions such as asthma and potentially provide targets to clinically intervene.

Future Directions

In addition to the future experiments proposed earlier within this Final Discussion on ways to address the caveats of previous studies, there are many other topics regarding AT eosinophils that have yet to be explored.

Do eosinophils aid in AT remodeling during weight loss?

While studies have begun to elucidate the role of AT eosinophils during weight gain, very little work has determined how eosinophils function in the setting of

physiologically normal weight loss. We could delineate the functional role, if any, of eosinophils in returning AT to a healthy state during negative energy balance. Weight loss could be induced in a number of ways, such as, caloric restriction, forced exercise, or a dietary switch from HFD to chow diet after a prolonged HFD feeding. After determining the role of eosinophils in the physiological response of AT during weight loss, we could increase and decrease eosinophil numbers to study any acceleration or delay in the rate of weight loss. Any insight into the processes that govern a return to AT homeostasis during weight loss offers the potential to make weight loss a more manageable goal for third of Americans struggling with obesity. Based on the combined data from the field, I hypothesize a minimum number of eosinophils would be required for appropriate weight loss (as has been shown to be the case for muscle regeneration (137)), but that excess eosinophils will likely have diminishing returns in accelerating the weight loss and AT resolution.

Do eosinophils regulate AT vascularization?

One of the primary reasons AT becomes dysfunctional in obesity is due to insufficient angiogenesis, leading to increased hypoxia that initiates an inflammatory response (141-143). Eosinophils can secrete an assortment of resolving and remodeling mediators: TGF-β, protectin D1, IL-4, IL-8, IL-10, IL-13, VEGF, and stem cell factor (76). Such a cell type would be critical to an environment such as AT where remodeling occurs on a daily basis. In fact, eosinophil sonicates can induce angiogenesis in an *in vitro* model dependent on VEGF (144). Under hypoxic conditions eosinophils display increased survival and

secrete pro-angiogenic VEGF and IL-8 (145). Angiogenesis can even be inhibited by reducing eosinophil count with Siglec-F antibody in an *in vivo* model of eosinophilic esophagitis (146). No study to date has addressed whether these angiogenic properties of eosinophils also apply in AT, and thus there are several questions that could be addressed. Will adding back eosinophils that have been pre-activated with hypoxic stimuli could improve AT vascularization during obesity? Furthermore, is it a compromised vascular network that is responsible for impaired metabolic fitness in eosinophil deficient mouse models of previous studies? If so, do eosinophils act directly on AT blood vessels or act in coordination with other cells in the AT environment? Do eosinophils undergo a phenotypic switch during obesity that prevents proper regulation of AT vasculature? None of these questions have been addressed in the AT field, but could offer new insights into the pathology of a compromised vascular network during obesity.

Summary

In summary, the completion of my dissertation work has shown that $CCR2^{-/-}$ regulates chemotactic factors that upregulate AT eosinophil accumulation. Interventional treatment used to restore obese AT eosinophils to higher levels of lean AT by injection of rIL5 does not reduce obesity and its comorbidities. Lastly, we discovered that repeated exposure to a foreign substance such as BSA greatly increased AT eosinophils. While there were no metabolic improvements in mice chronically exposed to BSA, we have evidence

to believe AT is capable of mounting a type 2 allergic response to antigens similar to the lung of an asthmatic, resulting in the large increase in AT eosinophils observed. Future studies will determine whether the AT eosinophilia following BSA exposure feeds back to the lung in allergic models, increasing both incidence and severity. In conclusion, we have found that restoring AT eosinophils to either physiological levels or super-physiological levels during obesity is not able to improve metabolic fitness (e.g. weight gain, glucose intolerance). Furthermore, we have potentially discovered a novel site of allergy that could offer insights and treatment opportunities for obese subjects that have increased difficulty with allergic disease.

REFERENCES

1. CDC. 2016. Behavioral Risk Factor Surveillance System.
2. Flegal, K.M., Carroll, M.D., Kit, B.K., and Ogden, C.L. 2012. Prevalence of obesity and trends in the distribution of body mass index among US adults, 1999-2010. *JAMA* 307:491-497.
3. Ogden, C.L., Carroll, M.D., Fryar, C.D., and Flegal, K.M. 2015. Prevalence of Obesity Among Adults and Youth: United States, 2011-2014. *NCHS Data Brief*:1-8.
4. Shoelson, S.E., Herrero, L., and Naaz, A. 2007. Obesity, inflammation, and insulin resistance. *Gastroenterology* 132:2169-2180.
5. Prospective Studies, C., Whitlock, G., Lewington, S., Sherliker, P., Clarke, R., Emberson, J., Halsey, J., Qizilbash, N., Collins, R., and Peto, R. 2009. Body-mass index and cause-specific mortality in 900 000 adults: collaborative analyses of 57 prospective studies. *Lancet* 373:1083-1096.
6. Finkelstein, E.A., Trogdon, J.G., Cohen, J.W., and Dietz, W. 2009. Annual medical spending attributable to obesity: payer-and service-specific estimates. *Health Aff (Millwood)* 28:w822-831.
7. American Diabetes Association. 2015. Statistics About Diabetes.
8. American Diabetes Association. 2017. Diagnosing Diabetes and Learning About Prediabetes.
9. van Belle, T.L., Coppieters, K.T., and von Herrath, M.G. 2011. Type 1 diabetes: etiology, immunology, and therapeutic strategies. *Physiol Rev* 91:79-118.
10. Klinke, D.J., 2nd. 2008. Extent of beta cell destruction is important but insufficient to predict the onset of type 1 diabetes mellitus. *PLoS One* 3:e1374.
11. Bacha, F., Lee, S., Gungor, N., and Arslanian, S.A. 2010. From pre-diabetes to type 2 diabetes in obese youth: pathophysiological characteristics along the spectrum of glucose dysregulation. *Diabetes Care* 33:2225-2231.
12. Stumvoll, M., Goldstein, B.J., and van Haeften, T.W. 2005. Type 2 diabetes: principles of pathogenesis and therapy. *Lancet* 365:1333-1346.
13. Hotamisligil, G.S., Budavari, A., Murray, D., and Spiegelman, B.M. 1994. Reduced tyrosine kinase activity of the insulin receptor in obesity-diabetes. Central role of tumor necrosis factor-alpha. *J Clin Invest* 94:1543-1549.
14. Hotamisligil, G.S., Murray, D.L., Choy, L.N., and Spiegelman, B.M. 1994. Tumor necrosis factor alpha inhibits signaling from the insulin receptor. *Proc Natl Acad Sci U S A* 91:4854-4858.
15. Chang-Chen, K.J., Mullur, R., and Bernal-Mizrachi, E. 2008. Beta-cell failure as a complication of diabetes. *Rev Endocr Metab Disord* 9:329-343.
16. Billings, L.K., and Florez, J.C. 2010. The genetics of type 2 diabetes: what have we learned from GWAS? *Ann N Y Acad Sci* 1212:59-77.

17. Karaderi, T., Drong, A.W., and Lindgren, C.M. 2015. Insights into the Genetic Susceptibility to Type 2 Diabetes from Genome-Wide Association Studies of Obesity-Related Traits. *Curr Diab Rep* 15:83.
18. Boden, G., Ruiz, J., Urbain, J.L., and Chen, X. 1996. Evidence for a circadian rhythm of insulin secretion. *Am J Physiol* 271:E246-252.
19. Van Cauter, E. 1998. Putative roles of melatonin in glucose regulation. *Therapie* 53:467-472.
20. Peschke, E., Frese, T., Chankiewitz, E., Peschke, D., Preiss, U., Schneyer, U., Spessert, R., and Muhlbauer, E. 2006. Diabetic Goto Kakizaki rats as well as type 2 diabetic patients show a decreased diurnal serum melatonin level and an increased pancreatic melatonin-receptor status. *J Pineal Res* 40:135-143.
21. Chen, W.M., Erdos, M.R., Jackson, A.U., Saxena, R., Sanna, S., Silver, K.D., Timpson, N.J., Hansen, T., Orru, M., Grazia Piras, M., et al. 2008. Variations in the G6PC2/ABCB11 genomic region are associated with fasting glucose levels. *J Clin Invest* 118:2620-2628.
22. Bouatia-Naji, N., Bonnefond, A., Cavalcanti-Proenca, C., Sparso, T., Holmkvist, J., Marchand, M., Delplanque, J., Lobbens, S., Rocheleau, G., Durand, E., et al. 2009. A variant near MTNR1B is associated with increased fasting plasma glucose levels and type 2 diabetes risk. *Nat Genet* 41:89-94.
23. Johnson, A.R., Milner, J.J., and Makowski, L. 2012. The inflammation highway: metabolism accelerates inflammatory traffic in obesity. *Immunol Rev* 249:218-238.
24. Hirosumi, J., Tuncman, G., Chang, L., Gorgun, C.Z., Uysal, K.T., Maeda, K., Karin, M., and Hotamisligil, G.S. 2002. A central role for JNK in obesity and insulin resistance. *Nature* 420:333-336.
25. Bandyopadhyay, G.K., Yu, J.G., Ofrecio, J., and Olefsky, J.M. 2005. Increased p85/55/50 expression and decreased phosphotidylinositol 3-kinase activity in insulin-resistant human skeletal muscle. *Diabetes* 54:2351-2359.
26. Sun, K., Kusminski, C.M., and Scherer, P.E. 2011. Adipose tissue remodeling and obesity. *J Clin Invest* 121:2094-2101.
27. Hotamisligil, G.S., Shargill, N.S., and Spiegelman, B.M. 1993. Adipose expression of tumor necrosis factor-alpha: direct role in obesity-linked insulin resistance. *Science* 259:87-91.
28. Hotamisligil, G.S., Arner, P., Caro, J.F., Atkinson, R.L., and Spiegelman, B.M. 1995. Increased adipose tissue expression of tumor necrosis factor-alpha in human obesity and insulin resistance. *J Clin Invest* 95:2409-2415.
29. Hotamisligil, G.S., and Spiegelman, B.M. 1994. Tumor necrosis factor alpha: a key component of the obesity-diabetes link. *Diabetes* 43:1271-1278.
30. Xu, H., Barnes, G.T., Yang, Q., Tan, G., Yang, D., Chou, C.J., Sole, J., Nichols, A., Ross, J.S., Tartaglia, L.A., et al. 2003. Chronic inflammation in fat plays a crucial role in the development of obesity-related insulin resistance. *J Clin Invest* 112:1821-1830.

31. Weisberg, S.P., McCann, D., Desai, M., Rosenbaum, M., Leibel, R.L., and Ferrante, A.W., Jr. 2003. Obesity is associated with macrophage accumulation in adipose tissue. *J Clin Invest* 112:1796-1808.
32. Winer, S., and Winer, D.A. 2012. The adaptive immune system as a fundamental regulator of adipose tissue inflammation and insulin resistance. *Immunol Cell Biol* 90:755-762.
33. Huber, J., Kiefer, F.W., Zeyda, M., Ludvik, B., Silberhumer, G.R., Prager, G., Zlabinger, G.J., and Stulnig, T.M. 2008. CC chemokine and CC chemokine receptor profiles in visceral and subcutaneous adipose tissue are altered in human obesity. *J Clin Endocrinol Metab* 93:3215-3221.
34. Horuk, R. 2001. Chemokine receptors. *Cytokine Growth Factor Rev* 12:313-335.
35. Dunzendorfer, S., Kaneider, N.C., Kaser, A., Woell, E., Frade, J.M., Mellado, M., Martinez-Alonso, C., and Wiedermann, C.J. 2001. Functional expression of chemokine receptor 2 by normal human eosinophils. *J Allergy Clin Immunol* 108:581-587.
36. Weisberg, S.P., Hunter, D., Huber, R., Lemieux, J., Slaymaker, S., Vaddi, K., Charo, I., Leibel, R.L., and Ferrante, A.W., Jr. 2006. CCR2 modulates inflammatory and metabolic effects of high-fat feeding. *J Clin Invest* 116:115-124.
37. Kanda, H., Tateya, S., Tamori, Y., Kotani, K., Hiasa, K., Kitazawa, R., Kitazawa, S., Miyachi, H., Maeda, S., Egashira, K., et al. 2006. MCP-1 contributes to macrophage infiltration into adipose tissue, insulin resistance, and hepatic steatosis in obesity. *J Clin Invest* 116:1494-1505.
38. Inouye, K.E., Shi, H., Howard, J.K., Daly, C.H., Lord, G.M., Rollins, B.J., and Flier, J.S. 2007. Absence of CC chemokine ligand 2 does not limit obesity-associated infiltration of macrophages into adipose tissue. *Diabetes* 56:2242-2250.
39. Kirk, E.A., Sagawa, Z.K., McDonald, T.O., O'Brien, K.D., and Heinecke, J.W. 2008. Monocyte chemoattractant protein deficiency fails to restrain macrophage infiltration into adipose tissue [corrected]. *Diabetes* 57:1254-1261.
40. Tsou, C.L., Peters, W., Si, Y., Slaymaker, S., Aslanian, A.M., Weisberg, S.P., Mack, M., and Charo, I.F. 2007. Critical roles for CCR2 and MCP-3 in monocyte mobilization from bone marrow and recruitment to inflammatory sites. *J Clin Invest* 117:902-909.
41. Sullivan, T.J., Miao, Z., Zhao, B.N., Ertl, L.S., Wang, Y., Krasinski, A., Walters, M.J., Powers, J.P., Dairaghi, D.J., Baumgart, T., et al. 2013. Experimental evidence for the use of CCR2 antagonists in the treatment of type 2 diabetes. *Metabolism* 62:1623-1632.
42. Lumeng, C.N., DelProposto, J.B., Westcott, D.J., and Saltiel, A.R. 2008. Phenotypic switching of adipose tissue macrophages with obesity is generated by spatiotemporal differences in macrophage subtypes. *Diabetes* 57:3239-3246.
43. Gutierrez, D.A., Kennedy, A., Orr, J.S., Anderson, E.K., Webb, C.D., Gerrald, W.K., and Hasty, A.H. 2011. Aberrant accumulation of

undifferentiated myeloid cells in the adipose tissue of CCR2-deficient mice delays improvements in insulin sensitivity. *Diabetes* 60:2820-2829.
44. Bolus, W.R., Gutierrez, D.A., Kennedy, A.J., Anderson-Baucum, E.K., and Hasty, A.H. 2015. CCR2 deficiency leads to increased eosinophils, alternative macrophage activation, and type 2 cytokine expression in adipose tissue. *J Leukoc Biol* 98:467-477.
45. Rothenberg, M.E., and Hogan, S.P. 2006. The eosinophil. *Annu Rev Immunol* 24:147-174.
46. Hogan, S.P., Koskinen, A., and Foster, P.S. 1997. Interleukin-5 and eosinophils induce airway damage and bronchial hyperreactivity during allergic airway inflammation in BALB/c mice. *Immunol Cell Biol* 75:284-288.
47. Proctor, W.R., Chakraborty, M., Chea, L.S., Morrison, J.C., Berkson, J.D., Semple, K., Bourdi, M., and Pohl, L.R. 2012. Eosinophils mediate the pathogenesis of halothane-induced liver injury in mice. *Hepatology*.
48. Leitch, V.D., Strudwick, X.L., Matthaei, K.I., Dent, L.A., and Cowin, A.J. 2009. IL-5-overexpressing mice exhibit eosinophilia and altered wound healing through mechanisms involving prolonged inflammation. *Immunol Cell Biol* 87:131-140.
49. Robertson, S.A., Mau, V.J., Young, I.G., and Matthaei, K.I. 2000. Uterine eosinophils and reproductive performance in interleukin 5-deficient mice. *J Reprod Fertil* 120:423-432.
50. Gouon-Evans, V., Lin, E.Y., and Pollard, J.W. 2002. Requirement of macrophages and eosinophils and their cytokines/chemokines for mammary gland development. *Breast Cancer Res* 4:155-164.
51. Jordan, H.E., and Speidel, C.C. 1923. Blood Cell Formation and Distribution in Relation to the Mechanism of Thyroid-Accelerated Metamorphosis in the Larval Frog. *J Exp Med* 38:529-541.
52. MacKenzie, J.R., Mattes, J., Dent, L.A., and Foster, P.S. 2001. Eosinophils promote allergic disease of the lung by regulating CD4(+) Th2 lymphocyte function. *J Immunol* 167:3146-3155.
53. Odemuyiwa, S.O., Ghahary, A., Li, Y., Puttagunta, L., Lee, J.E., Musat-Marcu, S., and Moqbel, R. 2004. Cutting edge: human eosinophils regulate T cell subset selection through indoleamine 2,3-dioxygenase. *J Immunol* 173:5909-5913.
54. David, J.R., Butterworth, A.E., and Vadas, M.A. 1980. Mechanism of the interaction mediating killing of Schistosoma mansoni by human eosinophils. *Am J Trop Med Hyg* 29:842-848.
55. Haque, A., Ouaissi, A., Joseph, M., Capron, M., and Capron, A. 1981. IgE antibody in eosinophil- and macrophage-mediated in vitro killing of Dipetalonema viteae microfilariae. *J Immunol* 127:716-725.
56. Kazura, J.W., and Grove, D.I. 1978. Stage-specific antibody-dependent eosinophil-mediated destruction of Trichinella spiralis. *Nature* 274:588-589.

57. Hamann, K.J., Gleich, G.J., Checkel, J.L., Loegering, D.A., McCall, J.W., and Barker, R.L. 1990. In vitro killing of microfilariae of Brugia pahangi and Brugia malayi by eosinophil granule proteins. *J Immunol* 144:3166-3173.
58. Butterworth, A.E., Wassom, D.L., Gleich, G.J., Loegering, D.A., and David, J.R. 1979. Damage to schistosomula of Schistosoma mansoni induced directly by eosinophil major basic protein. *J Immunol* 122:221-229.
59. Shi, H.Z. 2004. Eosinophils function as antigen-presenting cells. *J Leukoc Biol* 76:520-527.
60. Behm, C.A., and Ovington, K.S. 2000. The role of eosinophils in parasitic helminth infections: insights from genetically modified mice. *Parasitol Today* 16:202-209.
61. de Groot, J.C., Ten Brinke, A., and Bel, E.H. 2015. Management of the patient with eosinophilic asthma: a new era begins. *ERJ Open Res* 1.
62. Korsgren, M., Erjefalt, J.S., Korsgren, O., Sundler, F., and Persson, C.G. 1997. Allergic eosinophil-rich inflammation develops in lungs and airways of B cell-deficient mice. *J Exp Med* 185:885-892.
63. Hogan, S.P., Mishra, A., Brandt, E.B., Royalty, M.P., Pope, S.M., Zimmermann, N., Foster, P.S., and Rothenberg, M.E. 2001. A pathological function for eotaxin and eosinophils in eosinophilic gastrointestinal inflammation. *Nat Immunol* 2:353-360.
64. Mishra, A., Hogan, S.P., Brandt, E.B., and Rothenberg, M.E. 2000. Peyer's patch eosinophils: identification, characterization, and regulation by mucosal allergen exposure, interleukin-5, and eotaxin. *Blood* 96:1538-1544.
65. Flood-Page, P.T., Menzies-Gow, A.N., Kay, A.B., and Robinson, D.S. 2003. Eosinophil's role remains uncertain as anti-interleukin-5 only partially depletes numbers in asthmatic airway. *Am J Respir Crit Care Med* 167:199-204.
66. Foster, P.S., Hogan, S.P., Ramsay, A.J., Matthaei, K.I., and Young, I.G. 1996. Interleukin 5 deficiency abolishes eosinophilia, airways hyperreactivity, and lung damage in a mouse asthma model. *J Exp Med* 183:195-201.
67. Garrett, J.K., Jameson, S.C., Thomson, B., Collins, M.H., Wagoner, L.E., Freese, D.K., Beck, L.A., Boyce, J.A., Filipovich, A.H., Villanueva, J.M., et al. 2004. Anti-interleukin-5 (mepolizumab) therapy for hypereosinophilic syndromes. *J Allergy Clin Immunol* 113:115-119.
68. Humbles, A.A., Lu, B., Friend, D.S., Okinaga, S., Lora, J., Al-Garawi, A., Martin, T.R., Gerard, N.P., and Gerard, C. 2002. The murine CCR3 receptor regulates both the role of eosinophils and mast cells in allergen-induced airway inflammation and hyperresponsiveness. *Proc Natl Acad Sci U S A* 99:1479-1484.
69. Gonzalo, J.A., Lloyd, C.M., Wen, D., Albar, J.P., Wells, T.N., Proudfoot, A., Martinez, A.C., Dorf, M., Bjerke, T., Coyle, A.J., et al. 1998. The coordinated action of CC chemokines in the lung orchestrates allergic inflammation and airway hyperresponsiveness. *J Exp Med* 188:157-167.

70. Ma, W., Bryce, P.J., Humbles, A.A., Laouini, D., Yalcindag, A., Alenius, H., Friend, D.S., Oettgen, H.C., Gerard, C., and Geha, R.S. 2002. CCR3 is essential for skin eosinophilia and airway hyperresponsiveness in a murine model of allergic skin inflammation. *J Clin Invest* 109:621-628.
71. Rosenberg, H.F., Dyer, K.D., and Foster, P.S. 2013. Eosinophils: changing perspectives in health and disease. *Nat Rev Immunol* 13:9-22.
72. Lee, J.J., Jacobsen, E.A., McGarry, M.P., Schleimer, R.P., and Lee, N.A. 2010. Eosinophils in health and disease: the LIAR hypothesis. *Clin Exp Allergy* 40:563-575.
73. Wu, D., Molofsky, A.B., Liang, H.E., Ricardo-Gonzalez, R.R., Jouihan, H.A., Bando, J.K., Chawla, A., and Locksley, R.M. 2011. Eosinophils sustain adipose alternatively activated macrophages associated with glucose homeostasis. *Science* 332:243-247.
74. Molofsky, A.B., Nussbaum, J.C., Liang, H.E., Van Dyken, S.J., Cheng, L.E., Mohapatra, A., Chawla, A., and Locksley, R.M. 2013. Innate lymphoid type 2 cells sustain visceral adipose tissue eosinophils and alternatively activated macrophages. *J Exp Med* 210:535-549.
75. Hams, E., Locksley, R.M., McKenzie, A.N., and Fallon, P.G. 2013. Cutting edge: IL-25 elicits innate lymphoid type 2 and type II NKT cells that regulate obesity in mice. *J Immunol* 191:5349-5353.
76. Yamada, T., Tani, Y., Nakanishi, H., Taguchi, R., Arita, M., and Arai, H. 2011. Eosinophils promote resolution of acute peritonitis by producing proresolving mediators in mice. *FASEB J* 25:561-568.
77. Pfaffl, M.W. 2001. A new mathematical model for relative quantification in real-time RT-PCR. *Nucleic Acids Res* 29:e45.
78. Dyer, K.D., Moser, J.M., Czapiga, M., Siegel, S.J., Percopo, C.M., and Rosenberg, H.F. 2008. Functionally competent eosinophils differentiated ex vivo in high purity from normal mouse bone marrow. *J Immunol* 181:4004-4009.
79. Boring, L., Gosling, J., Monteclaro, F.S., Lusis, A.J., Tsou, C.L., and Charo, I.F. 1996. Molecular cloning and functional expression of murine JE (monocyte chemoattractant protein 1) and murine macrophage inflammatory protein 1alpha receptors: evidence for two closely linked C-C chemokine receptors on chromosome 9. *J Biol Chem* 271:7551-7558.
80. Kurihara, T., and Bravo, R. 1996. Cloning and functional expression of mCCR2, a murine receptor for the C-C chemokines JE and FIC. *J Biol Chem* 271:11603-11607.
81. Charo, I.F., and Ransohoff, R.M. 2006. The many roles of chemokines and chemokine receptors in inflammation. *N Engl J Med* 354:610-621.
82. Loetscher, P., Seitz, M., Baggiolini, M., and Moser, B. 1996. Interleukin-2 regulates CC chemokine receptor expression and chemotactic responsiveness in T lymphocytes. *J Exp Med* 184:569-577.
83. Kuziel, W.A., Morgan, S.J., Dawson, T.C., Griffin, S., Smithies, O., Ley, K., and Maeda, N. 1997. Severe reduction in leukocyte adhesion and monocyte extravasation in mice deficient in CC chemokine receptor 2. *Proc Natl Acad Sci U S A* 94:12053-12058.

84. Boring, L., Gosling, J., Chensue, S.W., Kunkel, S.L., Farese, R.V., Jr., Broxmeyer, H.E., and Charo, I.F. 1997. Impaired monocyte migration and reduced type 1 (Th1) cytokine responses in C-C chemokine receptor 2 knockout mice. *J Clin Invest* 100:2552-2561.
85. Shu, C.J., Benoist, C., and Mathis, D. 2012. The immune system's involvement in obesity-driven type 2 diabetes. *Semin Immunol* 24:436-442.
86. Szymczak, W.A., and Deepe, G.S., Jr. 2009. The CCL7-CCL2-CCR2 axis regulates IL-4 production in lungs and fungal immunity. *J Immunol* 183:1964-1974.
87. Lumeng, C.N., Bodzin, J.L., and Saltiel, A.R. 2007. Obesity induces a phenotypic switch in adipose tissue macrophage polarization. *J Clin Invest* 117:175-184.
88. Cinti, S., Mitchell, G., Barbatelli, G., Murano, I., Ceresi, E., Faloia, E., Wang, S., Fortier, M., Greenberg, A.S., and Obin, M.S. 2005. Adipocyte death defines macrophage localization and function in adipose tissue of obese mice and humans. *J Lipid Res* 46:2347-2355.
89. Broughton, S.E., Dhagat, U., Hercus, T.R., Nero, T.L., Grimbaldeston, M.A., Bonder, C.S., Lopez, A.F., and Parker, M.W. 2012. The GM-CSF/IL-3/IL-5 cytokine receptor family: from ligand recognition to initiation of signaling. *Immunol Rev* 250:277-302.
90. Yamaguchi, Y., Suda, T., Ohta, S., Tominaga, K., Miura, Y., and Kasahara, T. 1991. Analysis of the survival of mature human eosinophils: interleukin-5 prevents apoptosis in mature human eosinophils. *Blood* 78:2542-2547.
91. Sabroe, I., Hartnell, A., Jopling, L.A., Bel, S., Ponath, P.D., Pease, J.E., Collins, P.D., and Williams, T.J. 1999. Differential regulation of eosinophil chemokine signaling via CCR3 and non-CCR3 pathways. *J Immunol* 162:2946-2955.
92. Feuerer, M., Herrero, L., Cipolletta, D., Naaz, A., Wong, J., Nayer, A., Lee, J., Goldfine, A.B., Benoist, C., Shoelson, S., et al. 2009. Lean, but not obese, fat is enriched for a unique population of regulatory T cells that affect metabolic parameters. *Nat Med* 15:930-939.
93. Benoist, C., and Mathis, D. 2012. Treg cells, life history, and diversity. *Cold Spring Harb Perspect Biol* 4:a007021.
94. Cipolletta, D., Feuerer, M., Li, A., Kamei, N., Lee, J., Shoelson, S.E., Benoist, C., and Mathis, D. 2012. PPAR-gamma is a major driver of the accumulation and phenotype of adipose tissue Treg cells. *Nature* 486:549-553.
95. Nishimura, S., Manabe, I., Nagasaki, M., Eto, K., Yamashita, H., Ohsugi, M., Otsu, M., Hara, K., Ueki, K., Sugiura, S., et al. 2009. CD8+ effector T cells contribute to macrophage recruitment and adipose tissue inflammation in obesity. *Nat Med* 15:914-920.
96. Goldberg, E.L., and Dixit, V.D. 2015. Editorial: "Crowning" eosinophils in adipose tissue: does location matter? *J Leukoc Biol* 98:451-452.

97. Jacobsen, E.A., Helmers, R.A., Lee, J.J., and Lee, N.A. 2012. The expanding role(s) of eosinophils in health and disease. *Blood* 120:3882-3890.
98. Ogilvie, P., Bardi, G., Clark-Lewis, I., Baggiolini, M., and Uguccioni, M. 2001. Eotaxin is a natural antagonist for CCR2 and an agonist for CCR5. *Blood* 97:1920-1924.
99. Izumi, S., Hirai, K., Miyamasu, M., Takahashi, Y., Misaki, Y., Takaishi, T., Morita, Y., Matsushima, K., Ida, N., Nakamura, H., et al. 1997. Expression and regulation of monocyte chemoattractant protein-1 by human eosinophils. *Eur J Immunol* 27:816-824.
100. Proctor, W.R., Chakraborty, M., Chea, L.S., Morrison, J.C., Berkson, J.D., Semple, K., Bourdi, M., and Pohl, L.R. 2013. Eosinophils mediate the pathogenesis of halothane-induced liver injury in mice. *Hepatology* 57:2026-2036.
101. Tamura, Y., Sugimoto, M., Murayama, T., Minami, M., Nishikaze, Y., Ariyasu, H., Akamizu, T., Kita, T., Yokode, M., and Arai, H. 2010. C-C chemokine receptor 2 inhibitor improves diet-induced development of insulin resistance and hepatic steatosis in mice. *J Atheroscler Thromb* 17:219-228.
102. Ito, A., Suganami, T., Yamauchi, A., Degawa-Yamauchi, M., Tanaka, M., Kouyama, R., Kobayashi, Y., Nitta, N., Yasuda, K., Hirata, Y., et al. 2008. Role of CC chemokine receptor 2 in bone marrow cells in the recruitment of macrophages into obese adipose tissue. *J Biol Chem* 283:35715-35723.
103. Struthers, M., and Pasternak, A. 2010. CCR2 antagonists. *Curr Top Med Chem* 10:1278-1298.
104. Shin, M.H., Lee, Y.A., and Min, D.Y. 2009. Eosinophil-mediated tissue inflammatory responses in helminth infection. *Korean J Parasitol* 47 Suppl:S125-131.
105. Mullaly, S.C., Oudhoff, M.J., Min, P.H., Burrows, K., Antignano, F., Rattray, D.G., Chenery, A., McNagny, K.M., Ziltener, H.J., and Zaph, C. 2013. Requirement for core 2 o-glycans for optimal resistance to helminth infection. *PLoS One* 8:e60124.
106. Gatault, S., Legrand, F., Delbeke, M., Loiseau, S., and Capron, M. 2012. Involvement of eosinophils in the anti-tumor response. *Cancer Immunol Immunother* 61:1527-1534.
107. Podjasek, J.C., and Butterfield, J.H. 2013. Mortality in hypereosinophilic syndrome: 19 years of experience at Mayo Clinic with a review of the literature. *Leuk Res* 37:392-395.
108. Kang, Y.S., Lee, M.H., Song, H.K., Ko, G.J., Kwon, O.S., Lim, T.K., Kim, S.H., Han, S.Y., Han, K.H., Lee, J.E., et al. 2010. CCR2 antagonism improves insulin resistance, lipid metabolism, and diabetic nephropathy in type 2 diabetic mice. *Kidney Int* 78:883-894.
109. Qiu, Y., Nguyen, K.D., Odegaard, J.I., Cui, X., Tian, X., Locksley, R.M., Palmiter, R.D., and Chawla, A. 2014. Eosinophils and type 2 cytokine

signaling in macrophages orchestrate development of functional beige fat. *Cell* 157:1292-1308.
110. Fabbiano, S., Suarez-Zamorano, N., Rigo, D., Veyrat-Durebex, C., Stevanovic Dokic, A., Colin, D.J., and Trajkovski, M. 2016. Caloric Restriction Leads to Browning of White Adipose Tissue through Type 2 Immune Signaling. *Cell Metab* 24:434-446.
111. Ding, X., Luo, Y., Zhang, X., Zheng, H., Yang, X., Yang, X., and Liu, M. 2016. IL-33-driven ILC2/eosinophil axis in fat is induced by sympathetic tone and suppressed by obesity. *J Endocrinol* 231:35-48.
112. Harms, M., and Seale, P. 2013. Brown and beige fat: development, function and therapeutic potential. *Nat Med* 19:1252-1263.
113. Fischer, K., Ruiz, H.H., Jhun, K., Finan, B., Oberlin, D.J., van der Heide, V., Kalinovich, A.V., Petrovic, N., Wolf, Y., Clemmensen, C., et al. 2017. Alternatively activated macrophages do not synthesize catecholamines or contribute to adipose tissue adaptive thermogenesis. *Nat Med* 23:623-630.
114. Brestoff, J.R., Kim, B.S., Saenz, S.A., Stine, R.R., Monticelli, L.A., Sonnenberg, G.F., Thome, J.J., Farber, D.L., Lutfy, K., Seale, P., et al. 2015. Group 2 innate lymphoid cells promote beiging of white adipose tissue and limit obesity. *Nature* 519:242-246.
115. Qin, M., Wang, L., Li, F., Yang, M., Song, L., Tian, F., Yukht, A., Shah, P.K., Rothenberg, M.E., and Sharifi, B.G. 2017. Oxidized LDL activated eosinophil polarize macrophage phenotype from M2 to M1 through activation of CD36 scavenger receptor. *Atherosclerosis* 263:82-91.
116. World Health Organization. 2017. Chronic respiratory diseases: Asthma.
117. Beuther, D.A., and Sutherland, E.R. 2007. Overweight, obesity, and incident asthma: a meta-analysis of prospective epidemiologic studies. *Am J Respir Crit Care Med* 175:661-666.
118. Dixon, A.E., Pratley, R.E., Forgione, P.M., Kaminsky, D.A., Whittaker-Leclair, L.A., Griffes, L.A., Garudathri, J., Raymond, D., Poynter, M.E., Bunn, J.Y., et al. 2011. Effects of obesity and bariatric surgery on airway hyperresponsiveness, asthma control, and inflammation. *J Allergy Clin Immunol* 128:508-515 e501-502.
119. Shore, S.A., Schwartzman, I.N., Mellema, M.S., Flynt, L., Imrich, A., and Johnston, R.A. 2005. Effect of leptin on allergic airway responses in mice. *J Allergy Clin Immunol* 115:103-109.
120. Shore, S.A., Terry, R.D., Flynt, L., Xu, A., and Hug, C. 2006. Adiponectin attenuates allergen-induced airway inflammation and hyperresponsiveness in mice. *J Allergy Clin Immunol* 118:389-395.
121. Desai, D., Newby, C., Symon, F.A., Haldar, P., Shah, S., Gupta, S., Bafadhel, M., Singapuri, A., Siddiqui, S., Woods, J., et al. 2013. Elevated sputum interleukin-5 and submucosal eosinophilia in obese individuals with severe asthma. *Am J Respir Crit Care Med* 188:657-663.
122. Hu, Z.Q., and Zhao, W.H. 2015. The IL-33/ST2 axis is specifically required for development of adipose tissue-resident regulatory T cells. *Cell Mol Immunol* 12:521-524.

123. Hashiguchi, M., Kashiwakura, Y., Kojima, H., Kobayashi, A., Kanno, Y., and Kobata, T. 2015. IL-33 activates eosinophils of visceral adipose tissue both directly and via innate lymphoid cells. *Eur J Immunol* 45:876-885.
124. Han, J.M., Wu, D., Denroche, H.C., Yao, Y., Verchere, C.B., and Levings, M.K. 2015. IL-33 Reverses an Obesity-Induced Deficit in Visceral Adipose Tissue ST2+ T Regulatory Cells and Ameliorates Adipose Tissue Inflammation and Insulin Resistance. *J Immunol* 194:4777-4783.
125. Clinic, M. 2017. Diabetes medications and insulin therapy.
126. Hill, A.A., Reid Bolus, W., and Hasty, A.H. 2014. A decade of progress in adipose tissue macrophage biology. *Immunol Rev* 262:134-152.
127. Zhu, L., Su, T., Xu, M., Xu, Y., Li, M., Wang, T., Sun, J., Zhang, J., Xu, B., Lu, J., et al. 2013. Eosinophil inversely associates with type 2 diabetes and insulin resistance in Chinese adults. *PLoS One* 8:e67613.
128. Kitamura, H., Naoe, Y., Kimura, S., Miyamoto, T., Okamoto, S., Toda, C., Shimamoto, Y., Iwanaga, T., and Miyoshi, I. 2013. Beneficial effects of Brazilian propolis on type 2 diabetes in ob/ob mice: Possible involvement of immune cells in mesenteric adipose tissue. *Adipocyte* 2:227-236.
129. Berbudi, A., Surendar, J., Ajendra, J., Gondorf, F., Schmidt, D., Neumann, A.L., Wardani, A.P., Layland, L.E., Hoffmann, L.S., Pfeifer, A., et al. 2016. Filarial Infection or Antigen Administration Improves Glucose Tolerance in Diet-Induced Obese Mice. *J Innate Immun* 8:601-616.
130. Bolus, W.R., Kristin Peterson, Merla Hubler, Arion J. Kennedy, Marnie Gruen, Alyssa Hasty. 2017. Elevating adipose eosinophils in obese mice to physiologically normal levels does not rescue metabolic impairments. *Molecular Metabolism, In Revision*.
131. Doyle, A.D., Jacobsen, E.A., Ochkur, S.I., Willetts, L., Shim, K., Neely, J., Kloeber, J., Lesuer, W.E., Pero, R.S., Lacy, P., et al. 2013. Homologous recombination into the eosinophil peroxidase locus generates a strain of mice expressing Cre recombinase exclusively in eosinophils. *J Leukoc Biol* 94:17-24.
132. Satoh, T., Kidoya, H., Naito, H., Yamamoto, M., Takemura, N., Nakagawa, K., Yoshioka, Y., Morii, E., Takakura, N., Takeuchi, O., et al. 2013. Critical role of Trib1 in differentiation of tissue-resident M2-like macrophages. *Nature* 495:524-528.
133. Rao, R.R., Long, J.Z., White, J.P., Svensson, K.J., Lou, J., Lokurkar, I., Jedrychowski, M.P., Ruas, J.L., Wrann, C.D., Lo, J.C., et al. 2014. Meteorin-like is a hormone that regulates immune-adipose interactions to increase beige fat thermogenesis. *Cell* 157:1279-1291.
134. Suarez-Zamorano, N., Fabbiano, S., Chevalier, C., Stojanovic, O., Colin, D.J., Stevanovic, A., Veyrat-Durebex, C., Tarallo, V., Rigo, D., Germain, S., et al. 2015. Microbiota depletion promotes browning of white adipose tissue and reduces obesity. *Nat Med* 21:1497-1501.
135. Lee, M.W., Odegaard, J.I., Mukundan, L., Qiu, Y., Molofsky, A.B., Nussbaum, J.C., Yun, K., Locksley, R.M., and Chawla, A. 2015. Activated type 2 innate lymphoid cells regulate beige fat biogenesis. *Cell* 160:74-87.

136. Gouon-Evans, V., Rothenberg, M.E., and Pollard, J.W. 2000. Postnatal mammary gland development requires macrophages and eosinophils. *Development* 127:2269-2282.
137. Heredia, J.E., Mukundan, L., Chen, F.M., Mueller, A.A., Deo, R.C., Locksley, R.M., Rando, T.A., and Chawla, A. 2013. Type 2 innate signals stimulate fibro/adipogenic progenitors to facilitate muscle regeneration. *Cell* 153:376-388.
138. Withers, S.B., Forman, R., Meza-Perez, S., Sorobetea, D., Sitnik, K., Hopwood, T., Lawrence, C.B., Agace, W.W., Else, K.J., Heagerty, A.M., et al. 2017. Eosinophils are key regulators of perivascular adipose tissue and vascular functionality. *Sci Rep* 7:44571.
139. Nials, A.T., and Uddin, S. 2008. Mouse models of allergic asthma: acute and chronic allergen challenge. *Dis Model Mech* 1:213-220.
140. Dourado, L.P., Noviello Mde, L., Alvarenga, D.M., Menezes, Z., Perez, D.A., Batista, N.V., Menezes, G.B., Ferreira, A.V., de Souza Dda, G., and Cara, D.C. 2011. Experimental food allergy leads to adipose tissue inflammation, systemic metabolic alterations and weight loss in mice. *Cell Immunol* 270:198-206.
141. Spencer, M., Unal, R., Zhu, B., Rasouli, N., McGehee, R.E., Jr., Peterson, C.A., and Kern, P.A. 2011. Adipose tissue extracellular matrix and vascular abnormalities in obesity and insulin resistance. *J Clin Endocrinol Metab* 96:E1990-1998.
142. Pasarica, M., Sereda, O.R., Redman, L.M., Albarado, D.C., Hymel, D.T., Roan, L.E., Rood, J.C., Burk, D.H., and Smith, S.R. 2009. Reduced adipose tissue oxygenation in human obesity: evidence for rarefaction, macrophage chemotaxis, and inflammation without an angiogenic response. *Diabetes* 58:718-725.
143. Trayhurn, P. 2013. Hypoxia and adipose tissue function and dysfunction in obesity. *Physiol Rev* 93:1-21.
144. Puxeddu, I., Alian, A., Piliponsky, A.M., Ribatti, D., Panet, A., and Levi-Schaffer, F. 2005. Human peripheral blood eosinophils induce angiogenesis. *Int J Biochem Cell Biol* 37:628-636.
145. Nissim Ben Efraim, A.H., Eliashar, R., and Levi-Schaffer, F. 2010. Hypoxia modulates human eosinophil function. *Clin Mol Allergy* 8:10.
146. Rubinstein, E., Cho, J.Y., Rosenthal, P., Chao, J., Miller, M., Pham, A., Aceves, S.S., Varki, A., and Broide, D.H. 2011. Siglec-F inhibition reduces esophageal eosinophilia and angiogenesis in a mouse model of eosinophilic esophagitis. *J Pediatr Gastroenterol Nutr* 53:409-416.